Analysis of the impact of climate change on the global risk of dam failure due to overtopping

Nathalia Silva Cancino

MSc Thesis Identifier WSE-HERBD.20-10
March 2020

Updated version, April 2020

Cover photo: Itaipu dam on the Paraná River in Brazil/Paraguay. Source: https://www.dutchwatersector.com/news/witteveenbos-to-do-feasibility-study-into-bypass-itaipu-dam-brazil

Analysis of the impact of climate change on the global risk of dam failure due to overtopping

Master of Science Thesis
by

Nathalia Silva Cancino

Supervisors
Dr. Micha Werner

Mentors
Dr. Daniel Valero Huerta

Examination Committee
Dr. Micha Werner
Dr, Daniel Valero Huerta
MSc. Javier Fluixá Sanmartín

This research is done for the partial fulfilment of requirements for the Master of Science degree at the IHE Delft Institute for Water Education, Delft, the Netherlands.

Delft
March, 2020

Abstract

The most recent report of the Intergovernmental Panel on Climate Change (IPPC) presented medium confidence in projected increases of precipitation and run-off in some regions, while in others these are projected to decrease. However, the intensification of the climate is more generally projected to increase, which may lead to larger floods. Other studies have assessed the projected precipitation and have agreed with the IPPC assessment. These changes in climate present a concern about the risk of failure of large dams, given that most of these structures were built during the second half of the 20th century with different methods and often with limited hydrological data, resulting in uncertainty on how the design discharge capacity of the spillways can provide sufficient safety levels against overtopping in both the current and future climate. This study analyses the impacts of climate change on the failure of dams due to overtopping at a global scale The analysis is based on current and projected hydrological data obtained from the a PCR-GLOBWB Global Hydrological Model and five Global Climate Models (GCMs) selected from CMIP5 (Climate Model Intercomparison Project, phase 5). In this research an analysis of the design flood for a sample of about 1400 dams across the world under current, historical and future scenarios of climate change is made, and compared to the original design flood, by building a synthetic spillway design (using re-analysis data from CRU TS 3.2 and ERA-Interim datasets). Results from this study show that changes can be expected for the spillway discharge capacity. A consistent trend of increasing difference of the spillway capacity between the RCP4.5 and RCP8.5 scenarios and the baseline runs shows that there is a direct impact of climate change on the increase of dam failures rates due to overtopping. East Asia, South Asia, Central North America and Western North America are the regions facing the biggest rise in spillway discharge.

Acknowledgements

I would like to first express my sincere gratitude to my supervisor Dr Micha Werner for his continues support and interest in every aspect of this research and for allowing me working and learning from him. I would like to thank my mentor, Dr Daniel Valero for his guidance, motivation, patient and support at every stage of this process. Special thanks to Dr Edwin H. Sutanudjaja from the Department of Physical Geography of Utrecht University for his cooperation in accessing to the PCR-GLOBWB model.

Finally, I would like to thank my family and friends for the support and love you have given me during this year and a half that I have been in The Netherlands.

Table of Contents

List of Figures

List of Tables

Abbreviations

AOGCM	ATMOSPHERE-OCEAN GENERAL CIRCULATION MODEL
CMIP	COUPLED MODEL INTERCONPARISON PROJECT
GCM	GLOBAL CLIMATE MODEL
GHM	GLOBAL HYDROLOGICAL MODEL
GRanD	GLOBAL RESERVOIR AND DAM DATABASE
ICOLD	INTERNATIONAL COMISSION ON LARGE DAMS
IPPC	INTERNATIONAL PLAN PROTECTION CONVENTION
PCR-GLOBWB	PCRASTER GLOBAL WATER BALANCE MODEL
PMF	PROBABLE MAXIMUM FLOOD
PMP	PROBABLE MAXIMUM PRECIPITATION

Chapter 1 Introduction

This chapter briefly describes the actual knowledge about expected changes in the weather over the world due to climate change and its consequences, as the increase of large floods events occurrence. Also, it is mentioned how dam safety may be affected due to the change in the hydrological response of the catchments under climate change scenarios. Hence, it is presented a number of objectives and research questions that motivated the developing of this research to assess the present and future change of risk of dam failure due to overtopping.

1.1 Background information

According to the Fifth Assessment Report of the Intergovernmental Panel on Climate Change IPCC (2014a), climate warning is a reality; the atmosphere and oceans have warmed, the cryosphere has decreased and sea level has risen. These changes in the natural features of the Earth have brought about different consequences to the hydrology cycle, one of them being the alteration of the amount of precipitation.

In many areas of the world in the 21st century, both in the high latitudes and in tropical regions and in winter in the northern mid-latitudes, the frequency of heavy precipitation is likely to rise (IPPC, 2012). The IPCC reports that there is medium confidence that heavy rainfall will increase irrespective of if the total precipitation is projected to decrease (IPCC, 2014b). Consequently it may be expected that the frequency of occurrence of large flood events will be higher in future decades.

Taking climate variability into account and the projected rise of the magnitude of future floods to which the river basins will be exposed under climate change, hydraulic structures may be at an increased risk of failure due to the expected change in the hydrological response. These structures include large dams of which several tens of thousands have been built across the world. According to ICOLD large dams are defined as: “A dam with a height of 15 meters or greater from lowest foundation to the crest, or a dam between 5 meters and 15 meters impounding more than 3 million cubic meters” (ICOLD, 2011). The design of these dams requires the estimation of design floods, based on available hydrological data, such that the safety of the dam and population at downstream is guaranteed.

The accidental failure of a dam leads to the sudden release of significant amounts of water (i.e., dam break flow), with significant impacts on populations and property downstream. The potential inundation area and assets that can be affected due to a dam failure are directly relating to the characteristics of the dam and the flow discharge from the structure during different hydrological scenarios (FEMA, 2012a). Hence, the change of the probability of dam failure over the years leads to a changing risk of level of damage and loss life in the downstream area.

The causes of failure of a dam can be due to different mechanisms; overtopping, piping discharge and foundation problems. According to Bulletin 99 of ICOLD (ICOLD, 1995), for earth and rockfill dams, overtopping is the most frequent source of failure, with 31% of dam failures reporting overtopping as primary cause and 18% as secondary cause; followed by piping in the body the dam (15% as main cause and 13% as secondary cause) and problems in the foundation as the last major cause (12% as primary cause and 5% as secondary cause).

In order to avoid overtopping, it is necessary to establish a design peak discharge of a specific flood event, with the aim to design a spillway that is able to safely pass flood discharge, in particular the design flood, downstream when the reservoir is overflowing (Novak et al., 2007).

The methods to define the design flood event have changed over the last decades and may vary between countries. According to (ICOLD, 2003) there have been three generations of guidelines for selecting design floods: The first generation was based on empirical formulas and safety factors given for the engineer's judgment and applicable to any dam in any situation. The second generation took into account the classification of dams according to the likely consequences that a failure presents and the concept of Probable Maximum Flood (PMF) was introduced, which was calculated using deterministic criteria. This was implemented in the 1980's by the US Army Corps of Engineers. Lastly, in the third generation the selection of the design flood is based on risk and needs risk analysis for assessing the benefits of mitigating the hazards.

It must be noted that most countries have their own guidelines and criteria to select the design flood to ensure dam safety. Nonetheless, design floods are commonly floods with annual exceedance probabilities rarer than 1 in 100 and up to the PMF (ICOLD, 2016), which commonly is represented as twice the value of a return period of 1:10000 (Zhou et al., 2008).

However, there are large dams that were built in the 1930s, 1940s and 1950s, before the implementation of mathematical approaches to solve hydrological problems and when the available hydrological data were limited. These structures were designed during the first generation of design guidelines, and it is likely that the estimation of the design flood is not adequate given the current knowledge of the hydrology of upstream basins, or with the upcoming uncertainties of climate change. This may mean that the risk of failure is higher than would currently be considered acceptable. Dams that were designed and built using the second and third generation of guidelines could present similar problems.

Nowadays, climate models have been built and improved to represent the biogeochemical cycles, important to climate change. These models are among the primary instruments available to investigate the response of the climate system to different forcings (Flato et al., 2013).

As a result of the changing climate several studies have been developed based on climate models, forced with different patterns which represent the alternative futures. These studies have confirmed the increase of the floods in the 21st century at a global scale in different parts of the globe (Arnell & Gosling, 2014; Hirabayashi et al., 2008; Hirabayashi et al., 2013; Milly et al., 2002). Also, other several studies have assessed the likely consequences and changes in different sectors under the prediction of climate change, as the change in hydropower production and the impacts in dam failure and the vulnerability to climate change of selected dams (Chernet et al., 2014; Fluixá-Sanmartín et al., 2018; Fluixá-Sanmartín et al., 2019; Mallakpour et al., 2018; Turner et al., 2017). However, there is no previous work which assesses the changing of risk of dam failure due to climate changing at a global scale.

This research focuses on the study of the impact of the global climate change on the dam failure due to overtopping, determining the drivers that may increase the risk of failure through the analysis of different hydrological scenarios to estimate flood design and re-analysis of the discharge capacity of the dam spillway. This study aims to determine if the estimation of design flood and expected changes in precipitation and discharge in river due to climate change is relevant to increase the risk of failure of dams due to overtopping.

1.2 Problem statement

There are 57,985 Dams registered by the International Commission On Large Dams (ICOLD, 2019). These are spread around the world, and when built their safety was estimated based on different approaches. All methods that have been implemented over the years: statistical, hydro-meteorological and risk-enhanced approaches, hold uncertainty due to their uncertain inputs as the limited length of available hydrological data (Baecher, 2004; Sordo et al., 2014).

Additionally, the influence on the hydraulic safety due to the changing climate and consequent changes in hydrological conditions has not been addressed yet on a global scale. It is of utmost importance to assess the vulnerability of failure due to overtopping (most common failure mode) and estimate if the risk of dam failure (probability of occurrence of the design flood) of each structure has changed, in order to analyse a likely changing risk of damage of assets and loss life base on an increase on the risk of dam failure. This change of risk must take into account both currently available hydrological observations, as well as the influence of climate change on hydrology.

1.3 Objectives and research questions

Different studies have assessed the alterations on the hydrology cycle (precipitation, temperature, evapotranspiration, etc.) due to climate change, showing the potential climate patterns that the world may be face. These changes may have an effect on the development of several sectors around the world such as dam safety. The following objectives and research questions are proposed in order to evaluate the impact of climate change on dam failure due to overtopping.

1.3.1 General objective

Analyse the present and future global risk of dam failure due to overtopping.

1.3.2 Specific objectives

1. Assess the level of safety against overtopping of the dams based on current hydrological data and different design floods.
2. Determine the influence of global climate change on the probability of failure of dams due to overtopping.

1.3.3 Research questions

What is the impact of climate change on the global risk of dam failure due to overtopping?

- What would the flood design of the dams be using the then-available data and used methods?
- What is the level of safety of the dams using the currently available hydrological data?
- How would climate change scenarios influence the risk of failure in the dams?

1.4 Relevance of the research

This study will present an overview of the changing safety level of dams around the world, taking into consideration the available hydrological data and climate change. It will analyse the trends of the changes of dams at risk of overtopping and provide a framework to understand the relationship between climate change consequences and increase of dam failure risk. It also aims to consider aware the impacts of climate change on dams that can lead to failure, thereby impacting people's safety and the economic sectors that relies on them.

The results will provide an estimation of the percentage of change of the spillway design for the period 2015-2050, based on the different climate regions, in order to provide a tool for potential research for individual dams around the world. This research may motivate to take concrete actions against climate change in order to mitigate the potential social and economic impacts of dam failure.

Chapter 2 Literature review

This chapter discusses the models that have been developed the last years with the aim to assess the climatology and hydrological changes around the world due to climate change, through the implementation of global climate models and global hydrological models, and presents the probable changes in precipitation in the future based on different researches. The chapter also presents the theory about the flood design used in the dam design and how is linked to the hydrological conditions.

2.1 Overview of climate change impacts on dam safety

Over the last years, different researches have presented the expected changes on climate change and its impacts in precipitation and runoff that leads to face more floods and droughts events in many areas over the world. Specifically, the increase of precipitation and runoff influence the statistical properties of the discharge that enters to the hydraulic structures, as the probability of occurrence of a specific event that might affect the risk of failure. However, global climate change impacts on risk of dam failure are separately investigated.

For example, Mallakpour et al. (2018) found that in most dams in California the risk of hydrological failure is expected to increase by 2100 due to the change of the flow regime and rise in the probability of occurrence for extreme flood under a warming scenario. Fluixá-Sanmartín et al. (2018) provide a tool to assess the vulnerability of dams taking into account the risk imposed by climate change. Fluixá-Sanmartín et al. (2019) assess the effects of climate change of Santa Teresa dam in Spain under hydrological scenarios, where the main load the dam is exposed to is the floods.

In order to investigate the effects of climate change on dam failure, it is necessary to implement results from other investigations, as the historical and projected time series from Global Climate Models (GHMs) and Global Hydrological Models (GHMs).

2.2 Design flood methods for dam design

As dams retain large volumes of water, the failure of them naturally lead to a potential risk of loss of life, economic damage, and social and environmental impacts downstream. Over the years, different methods to estimate the design flood have been developed with the aim to ensure dam safety. The design flood is an essential quantity that is used to determine the discharge capacity of the spillway, as the spillway should be sufficient to pass the design flood without compromising the safety of the dam.

The oldest method for estimating design floods uses the analysis of recorded extreme flood events that have occurred in the location. This method, however, presents some limitations. For example, data on extreme floods are not enough for all catchment sizes, the peak flow for extreme events may be of poor quality as they are usually estimated from readings of maximum water levels extrapolated from stage-discharge curves and the resulting value from the extrapolation cannot be the optimal frequency of occurrence for estimate floods (Cluckie & Pessoa, 1990).

Another approach for the estimation of the design flood uses the probability of exceedance in any given year of precipitation events based on the construction of Intensity-Duration-Frequency curves (IDF) developed over the basin upstream of the dam. With the estimation of the precipitation corresponding to the design probability of exceedance, a rainfall-model is made which turns precipitation into runoff using a set equations and parameters that describes the catchment (Sitterson et al., 2017). However, the selection of the statistical method can influence the design and represents a source of uncertainty. On the other hand, it is necessary to have a long historical record of discharge to allow the estimation of the parameters of the statistical function with low uncertainty bounds.

Lastly, an economic approach has been introduced, which is based on flood peak probabilities and damages and varies the capacity of the spillway until the total annual cost is minimal (Cluckie & Pessoa, 1990). The Dam Hazard Classification System is based on the potential consequences of a dam failure, the methods of classification are divided into two main approaches: dam classification based on the characteristics of the system (dam height and type, reservoir volume, etc.) and dam classification based on the consequences of dam failure and the evaluation (quantitative or qualitative) of different types of impacts (ICOLD, 2016).

As the selection of the frequency of the design flood is subjective, in the 1980's the terms of Probable Maximum Precipitation (PMP) and Probable Maximum Flood (PMF) were adopted. The PMF is defined as "the flood that may be expected from the most severe combination of critical meteorological and hydrologic condition that are reasonably possible in the drainage basin under study" (FEMA, 2012b). The motivation of this approach is that every physical process has a natural limit with an upper limit equal to the amount of precipitation that may occur over a given region over a specified period (Cluckie & Pessoa, 1990).

Most countries have defined criteria and methods to select the design flood to determine the flood event that should safely be passed, depending also on the physical characteristics of the structure. Table 2.2-1 presents the methods that selected countries have chosen to estimate design flood.

Table 2.2-1 Flood estimation guideline per country (ICOLD, 2016)

Country	Embankment dam	Concrete dam	Height 8m	Height 50 m	Volume 0.5 hm3	Volume 1010 hm3
Australia	10 000-yr	10 000-yr	10 000-yr	10 000-yr	10 000-yr	10 000-yr
Austria	5 000-yr	5 000-yr	5 000-yr	5 000-yr	5 000-yr	5 000-yr
Brazil	PMF	PMF	PMF	PMF	PMF	PMF
Bulgaria	1 000-yr	1 000-yr	1 000-yr	1 000-yr	1 000-yr	1 000-yr
Canada – CDA	1/3 between 1 000-yr and PMF	1/3 between 1 000-yr and PMF	1/3 between 1 000-yr and PMF	1/3 between 1 000-yr and PMF	1/3 between 1 000-yr and PMF	1/3 between 1 000-yr and PMF
Canada – Quebec	1 000-yr	1 000-yr	1 000-yr	1 000-yr	1 000-yr	1 000-yr
China	2 000-yr	2 000-yr	2 000-yr	2 000-yr	200-yr	PMF
Czech	1 000-yr	1 000-yr	1 000-yr	1 000-yr	1 000-yr	1 000-yr
Finland	10 000-yr	10 000-yr	10 000-yr	10 000-yr	10 000-yr	10 000-yr
France	10 000-yr	1 000-yr	1 000-yr	10 000-yr	10 000-yr	10 000-yr
Germany	10 000-yr	10 000-yr	10 000-yr	10 000-yr	5 000-yr	10 000-yr
India	PMF	PMF	PMF	PMF	1 000-yr	PMF
Ireland	10 000-yr	10 000-yr	10 000-yr	10 000-yr	10 000-yr	10 000-yr
Italy	3 000-yr	1 000-yr	3 000-yr	3 000-yr	3 000-yr	3 000-yr
Japan	200*1.2-yr	200-yr	Not specified	200*1.2-yr	200*1.2-yr	200*1.2-yr
New Zealand	10 000-yr	10 000-yr	10 000-yr	10 000-yr	10 000-yr	10 000-yr
Norway	1 000-yr	1 000-yr	1 000-yr	1 000-yr	1 000-yr	1 000-yr
Panama	5 000-yr	5 000-yr	5 000-yr	5 000-yr	5 000-yr	5 000-yr
Poland	1 000-yr	200-yr	1 000-yr	1 000-yr	500-yr	1 000-yr
Portugal	5 000-yr	1 000-yr	1 000-yr	10 000-yr	5 000-yr	5 000-yr
Romania	1 000-yr	1 000-yr	1 000-yr	1 000-yr	1 000-yr	1 000-yr
Russia	100-yr	100-yr	100-yr	100-yr	200-yr	1 000-yr
South Africa	100-yr	100-yr	100-yr	200-yr	100-yr	100-yr
Spain	1 000-yr	1 000-yr	1 000-yr	1 000-yr	1 000-yr	1 000-yr
Sweden	SDF	SDF	SDF	SDF	SDF	SDF
Switzerland	1 000-yr	1 000-yr	1 000-yr	1 000-yr	1 000-yr	1 000-yr
Turkey	1 000-yr	500-yr	1 000-yr	PMF	1 000-yr	1 000-yr
UK	PMF	PMF	PMF	PMF	PMF	PMF
USA	PMF	PMF	PMF	PMF	PMF	PMF

2.2.1 Other design parameters for dams

Although the selection of the peak design flood is the main challenge to guarantee dam safety and to design the hydraulic works of dams (such as the spillway), it is important to take into account other design parameters. According to ICOLD, these parameters are (ICOLD, 2016):

- **Safety check flood:** The spillway capacity design can be more restrictive than the peak flood design. The dam must be able to pass safely the flood, accepting some damages without causing dam failure.
- **Gate availability and reliability:** Problems and lack of maintenance of the gates can have an impact on the spillway capacity during major flood events.
- **Initial conditions for flood routing:** In practice, it is considered the reservoir at its full supply level (FSL) before the arrival of the flood, but if the flood is mainly caused by snowmelt, the reservoir is usually not at the FSL and "conservative" assumptions must be implemented to estimate the initial level of the reservoir.
- **Freeboard:** To reduce the risk of failure due to overtopping the freeboard is taken into account as a safety factor against the uncertainty related to the flood. Normally, for embankment dams, the freeboard is higher than for concrete dams.

2.3 Global climate models

Atmosphere-Ocean General Circulation Models (AOGCMs) reflect physical processes in the atmosphere, sea, cryosphere and land surface. There is considerable confidence that AOGCMs can produce reliable estimations of future climate change at global scale, as they have been able to reproduce observed data of current and past climate changes (Randall et al., 2007).

2.3.1 Climate Model Intercomparison Project (CMIP)

The Climate Model Intercomparison Project has worked since 1995 under the sponsorship of the Working Group on Coupled Modelling (WGCM) with the aim to achieve a better understanding of past, present and future climate, and changes arising from natural and unforced variability (WCRP, 2019). CMIP has coordinated model experiments in collaboration with modelling teams around the world. The project has been developed through different phases, which have improved the quality of the output experiments and the possibility to obtain and share the data. It is noteworthy that the outputs from CMIP have become a central element of international evaluation of climate change; for example, the IPCC supports its reports on these model results (Flato et al., 2013).

The CMIP studies climate simulations based on the model output of different AOGCMs, the first two main phases of the project (CMIP1 and CMIP2) were based on, respectively: the ability of models to simulate current climate and simulation of climate change due to a forced change (1% per year CO2 increase) (Meehl et al., 2000). The fifth and most complete phase of the project is CMIP5, which includes two types of climate change modelling experiments: long-term (century time scale) integrations and near-term integration (10-30 years), the resolution of the coupled models varies for the atmosphere component from 0.5° to 4° and for the ocean from 0.2° to 2°. In total, 35 experiments were made and were key elements for the development of the Fifth Assessment Report (AR5) of the IPPC (Taylor et al., 2012).

The most recent phase of the project is CMIP6, which began in 2013 and an overview of its new organization was launched in 2016. CMIP6 is based on three major elements: first, a group of common experiments called DECK (Diagnostic, Evaluation and Characterization of Klima) and CMIP historical simulations since 1850. Second, this phase includes documentation and common standards to facilitate the distribution of the outputs from the model and third, an ensemble of CMIP-Endorsed Model Intercomparison Projects (MIPs) (Eyring et al., 2016). However, only 31 of 49 CMIP6 models have been presented until now and there is not likely that all the results will be done for the IPPC's Sixth Assessment Report (AR6) in 2021 (Carbon Brief, 2019).

2.3.2 Global Hydrological models (GHMs)

Global Hydrological models (GHMs) are models that describe the hydrological cycle at a global scale and are used to assess the effects of global change on water resources (van Beek & Bierkens, 2008b). These models are close to several stand-alone hydrological models and hydrological components of the GCMs. However, the detail of the processes, spatial and time resolution, and parameter estimation approaches is different (Sood & Smakhtin, 2015).

Currently, at least 12 GHM have been developed since 1989, with each of these models offering different characteristics to estimate the parameters and to calculate the hydrological cycle and energy balance. For instance: methods to estimate potential evapotranspiration (PET), runoff scheme, reservoir storage, vegetation estimation, and soil layers (Sood & Smakhtin, 2015). Due to these differences, uncertainty in the GHMs have to be analysed, the most common process to assess the uncertainty of a hydrological model is by comparing the results with the outputs of other models.

GHMs are useful in research that focuses on assessing the impacts of climate change on hydrology. They can be forced with the climate results provided from the GCMs (e.g. CMIP). Table 2.3-1 presents the available models together with their inception year and main objective.

Table 2.3-1 Existing Global Hydrological Models (Sood & Smakhtin, 2015)

Model	Year	Developed/Maintained by	Objective
HDTM	1989	University of New Hampshire, USA	To study biogeochemical cycles worldwide, linked to Terrestrial Ecosystem Model and Trace Gas Model.
MPI-HM	1998	Institute for Meteorology, Germany	Defining lateral water flow from continents to oceans and connecting with a GCM (ECHAM)
GWAVA	1999	Centre for Ecology & Hydrology, UK	To research global water shortage development due to population growth and climate change.
VIC	2001	University of Washington, Seattle, USA	To develop the previous model VIC by adding two layers of soil and implementing heterogeneity of the sub grid for vegetation storage capacity for soil moisture and precipitation.
LanD	2002	Geophysical Fluid Dynamics Laboratory, Princeton, New Jersey, USA National Oceanic and Atmospheric Administration (NOAA)	Enhance the energy and water balance of the older model.

WaterGAP	2003	University of Kassel; University of Frankfurt, Germany	Combining water supply and water use on t he basis of global economic and technological changes.
PCR-GLOBWB	2004	Utrecht University, The Netherlands	Introduced grid heterogeneity routine for surface runoff, inter-flow and groundwater heat transportation.
LPJmL	2007	Potsdam Institute for Climate Impact Research (PIK), Germany	To simulate the global vegetation's spatial and time dynamics and analyse its impact on global hydrological and carbon cycles.
WASSMOD-M	2007	Department of Earth Sciences, Air, Water and Landscape Sciences, Uppsala University, Sweden	To complement established global models and to create with a set of minimum parameters for measured and ungauged river basins.
H08 (H07)	2008	National Institute of Environmental Studies, University of Tokyo, Japan	To determine the supply of global water on a sub-annual basis.
ISBA-TRIP	2010	Centre National de Recherchés Météorologiques, France	To measure and use GRACE data to verify terrestrial water storage at continental level.

The different GHMs have been used in several researches, being a useful tool to project and assess water variability. The performance of the GHMs have been tested by different researches as in the EartH2Observe project, which made an ensemble of 10 GHMs (Schellekens et al., 2017). The project found that for most of the hydrological variables (i.e. runoff and evaporation) the GHMs present and agreement in their results for large parts over the world, while there are less agreement in snow-dominated zones, tropical rainforests and monsoon regions.

Also, the ability of the GHMs to predict floods has been evaluated ((Gründemann et al., 2018), (Towner et al., 2019)), finding the most influential criteria that affect the performance of the models, as the selection of precipitation datasets and modelling of reservoir operation and water use. In conclusion, GHMs provide good results as long as it is guaranteed resolution, forcing and model parametrization needed.

2.3.3 Representative Concentration Pathways (RCPs)

Based on the principal forcing parameters of climate change, the time series of potential greenhouse gases and air contaminants concentrations and emissions and land-use change, different possible development routes have been developed called Representative Concentration Pathways (RCPs), these are used to perform new climate model experiments and develop new climate scenarios (van Vuuren et al., 2011). These RCPs describe different future scenarios considering the amount of greenhouse gases are emitted.

Currently, four RCPs have been defined, which include one mitigation scenario with a very low level of forcing emission (RCP 2.6), two average stabilization scenarios (RCP4.5 and RCP6) and an extra high emission scenario (RCP8.5) (van Vuuren et al., 2011):

- RCP8.5 represents a rising radiative forcing pathway until 8.5 W/m^2 by 2100

- RCP6 represents stabilization without exceeding 6 W/m^2 after 2100
- RCP4.5 represents stabilization without exceeding 4.5 W/m^2 after 2100
- RCP2.6 presents a peak in radiative forcing at 3 W/m^2 after the first half of the 21^{st} century and then decline to 2.6 W/m^2.

The RCPs are named according to their target level of radiative forcing for 2100, the radiative forcing represents the change in the energy balance of the Earth system, the difference between earth-absorbed insolation and space-radiated heat (Myhre et al., 2013). A higher radiative forcing leads to a warming system.

2.4 Climate change impacts on precipitation

In the last decades, impacts on natural and human process have been observed due to climate change all over the world. Since 1950, there has been a downward trend in cold temperature extremes, increase in extreme heat and temperature extremes, increase in sea levels and a rise in heavy rainfall events in many parts of the world (IPCC, 2014a). Also, it is expected that global warming will lead to increased evaporation and precipitation resulting as the water cycle is accelerated (Del Genio et al., 1991; Held & Soden, 2000).

In response to these facts, studies have been developed to assess the impacts or changes in global precipitation in the future due to climate change. According to the research Global patterns of change in discharge regimes for 2100 (Sperna Weiland et al., 2012), global discharge increase of more than ten percent based on a multi-model ensemble of 12 GCMs can be expected.

On the other hand, a recent study of Global flood risk under climate change (Hirabayashi et al., 2013) suggests that the frequency of occurrence of a 100-yr return period in the 21^{st} century for discharge corresponding to the 20^{th} century 100-year flood will increase across large areas of South Asia, Southeast Asia, Northeast Eurasia, eastern and low-latitude Africa and South America. Using an ensemble of five GCMs (Wan et al., 2018) showed that the change in precipitation is regionally specific, with increase of more than three degrees in temperature and 0.15 mm/day in precipitation most noticeable in Northern high-latitude regions (above 50N), while precipitation decreases in Southern mid-latitude regions (10S-40S).

Figure 2.4-1 and Figure 2.4-2 show the difference of mean precipitation between two periods of time, 1986-2005 and 2081-2100, using two different RCPs and a subset (pre-industrial control) of CMIP5 (KNMI, 2019).

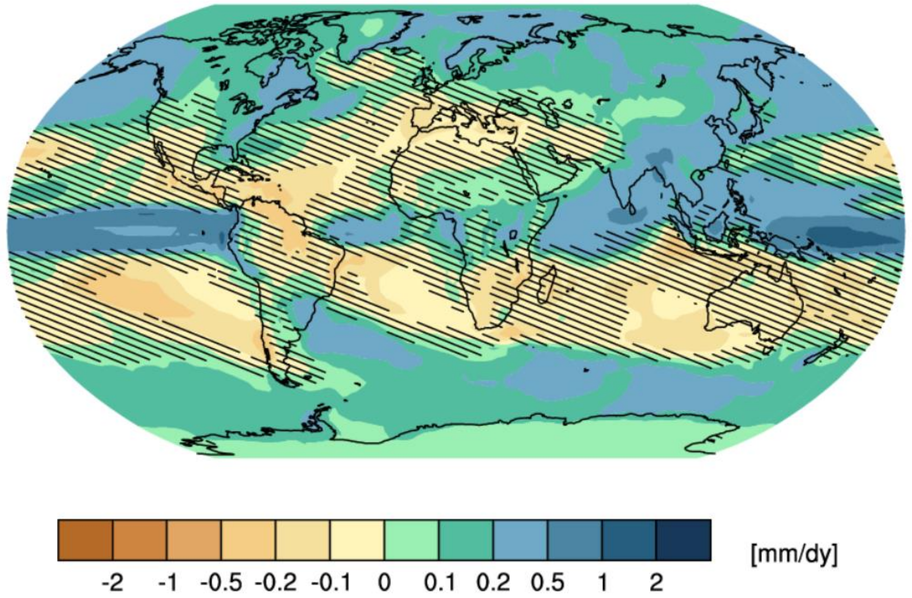

Figure 2.4-1 Difference in mean precipitation between RCP4.5 2081-2100 and 1986-2005 (CMIP5 subset)

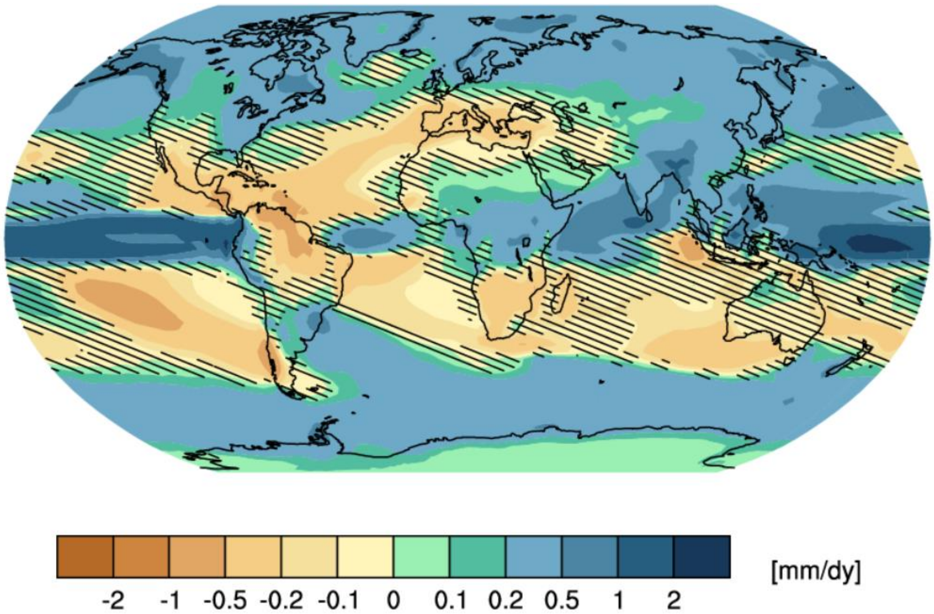

Figure 2.4-2 Difference in mean precipitation between RCP8.5 2081-2100 and 1986-2005 (CMIP5 subset)

Chapter 3 Methodology

This chapter presents the steps developed to achieve the objectives of the research. First, the method used to obtain the hydrological data using a global hydrological model (GHM) and the criteria to select the dams considered is introduced. Subsequently, a detailed explanation of the procedure implemented to estimate the needed parameter, based on available dam databases and discharge data series, to construct a reservoir flood routing scheme that can be implemented to evaluate the risk of overtopping with different data series.

3.1 Overview

As the main objective of the research is to evaluate the change in risk failure for overtopping due to climate change, different scenarios were developed based on the available hydrological data, to compare results and identify this change. Five scenarios were analysed, each with a different period of analysis:

- Re-analysis data (1980-2015)
- Historical climate data (1955-2005)
- Current climate scenario (1980-2015)
- Climate change scenario forced with RCP4.5 and RCP8.5 (2015-2050)

To identify the change to the risk of failure, the design spillway capacity of the dams selected is compared for each of these scenarios. To obtain design capacity, a flood routing scheme was constructed, which allows calculating the spillway capacity and the height over the crest of every dam based on peak floods discharges for different return periods.

The values obtained using the GHM forced using re-analysis data (1980-2015), which is as close to an observed data-set as possible, are referred to as the synthetic design. This is used to find the bias between the real spillway capacities of the dams as defined in the databases and established using observed hydrological data for each dam, and the design discharge that is obtained using the hydrological data from the GHM.

The historical climate data is obtained by forcing the GHM with the climate model outputs run over the historical period (1955-2005). This historical data allows for analysing the estimation of the design discharge for the dam taking into account the year of construction. The change of spillway discharge design is compared to the results from the synthetic design in order to establish the relationship between the results, due to both time series share several years. The same procedure is done with the current climate scenario, though with this the reference values are obtained from the historical scenarios, observing the changes in spillway capacity due to the climate variability between scenarios. Lastly, the results from the climate change scenarios were compared with the historical climate and the current climate scenario, obtaining insight into the change of risk of dam failure due to climate change.

In order to obtain the spillway design discharge for each dam in these scenarios, it was necessary to develop several steps: calculate the design inflow hydrograph, establish the volume-storage relation for each dam to allow routing the hydrograph through the reservoir, and calculating the outflow hydrograph. All data analysis and data processing was made in Python by the implementation of several scripts.

3.2 GHM and time series

3.2.1 PCR-GLOBWB 2: PCRaster Global Water Balance Model

For developing this research, the second version of PCR-GLOBWB global hydrology and water resource model was used to obtain the hydrological data needed. This model is based on a global grid which includes all continents except Greenland and Antarctica. Currently there are two available resolutions of the model (5 and 30 arcmin, equivalent to approximately 8 km and 50km at the equator) and the standard time step implemented for hydrology and water use is one day.

The model is forced based on time series of monthly rainfall, temperature and evaporation from the CRU TS 3.2 data set and with daily values from ERA 40 (1958-1978) and ERA-Interim (1979-2015) which are the data used to obtain the re-analysis scenario. The model offers two versions: the human influence and naturalized version. The first one includes a reservoir operation for more than 6000 human-made reservoirs, takes into account human water consumption (water supply for domestic and industry uses , livestock and irrigation), return flows and includes a land surface module which includes four types of land cover (tall and short natural vegetation, non-paddy irrigated crops and paddy irrigated crops). The naturalized version does not implement reservoir operation or human water use, but it does include the land cover module (Sutanudjaja et al., 2018).

In the two versions of the model, for every cell of the grid at each time step hydrological fluxes and system states are calculated, including soil moisture storage, surface run-off from precipitation and snowmelt, interflow or stormflow, baseflow and riverbed infiltration from and to groundwater. It is possible to simulate flood routing implementing different methods: simple accumulation, simplified dynamic routing or kinematic wave routing (Sutanudjaja et al., 2018).

Sutanudjaja et al., (2018) evaluate the accuracy of discharge results from the model by comparing the simulated results with the observed values from the Global Runoff Data Center (GRDC). This comparison was carried out through the estimation of three parameters: the correlation coefficient (measure of correct timing of high and low discharge), Kling-Gupta efficiency coefficient (KGE) (measure of the bias and difference in timing and amplitude) and anomaly correlation (correlation among monthly time series after the seasonal signal is removed), each of this parameters presented a better performance for the 5 arcmin resolution than the 30 arcmin.

For the 5 arcmin model, 63% of the catchments present a KGE greater than 0, 40% greater than 0.3 and 12% greater than 0.6, where the perfect fit is equal to 1. Due to this research is on a global scale it is not necessary to obtain a complete accuracy of the details provided for the model and most of the catchments on the model presented good quality, then, the model’s results are suitable to achieve the objectives.

For this research, the naturalized version with a resolution of 5 arcmin was selected and the routing was made with the kinematic wave formulation to ensure a good propagation of flood waves. Five GCMs based on the results from CMIP5 and developed by different institutes over the world were taking into account to extract the data (see Table 3.2-1). The data from the GCMs were bias-corrected to the CRU TS 3.2 data by the PCR-GLOBWB.

Table 3.2-1 Selected GCMs

Name Model	Institute	Country	Reference
MIROC-ESM	Center of Climate System Research	Japan	(Watanabe et al., 2011)
IPSL-CM5A	Institute Pierre Simon Laplace	France	(Dufresne et al., 2012)
HadGEM2	Met Office's Hadley Centre for Climate Prediction	United Kingdom	(Jones et al., 2011)
GFDL-ESM2M	Geophysical Fluid Dynamics Centre	USA	(Dunne et al., 2012)
NorESM1-M	University Corporation for Atmospheric Research	Norway	(Bentsen et al., 2013)

The confidence of the selected GCMs was evaluated in the Fifth Assessment Report of the IPPC, showing a very high confidence that models are capable of reproducing the general hydrological components (i.e. surface temperature and precipitation) at global scale (Flato et al., 2013).

Eleven daily time series were extracted: one time series from 1980 to 2015 based on reanalysis of data which is the values resulting from the merge of the CRU TS 3.2 and ERA-Interim, five historical runs from 1955 to 2005 and five climate model from 2006 to 2052. The forcing selected for the climate runs were RCP4.5 and RCP8.5, due to the first one representing a stabilization of the radiative forcing after 2100 and the second embodying the largest raising in the radiative forcing for the next years, which means an extreme variability in future conditions due to higher greenhouse gasses concentration levels. In this way medium and extreme future conditions are represented.

As the extracted time series have different lengths, it was decided to consider a fixed length equal to 36 years for every scenario. Using the same length for all the hydrological data, it is possible to compare the changes on risk of dam failure due to overtopping for a fixed period of time in different scenarios (historical, current and futures). On the other hand, it is also possible to assess the change of risk of dam failure taking into account the full length of the time series (1955-2052), however this research does not develop this approach.

3.2.2 Scenarios and synthetic design

In order to analyse the change of risk of dam failure over the years, four scenarios were developed: Historical, Current, Future RCP4.5 and Future RCP8.5. For every scenario, five time series are available corresponding to the five selected GCMs.

- Historical scenario: The time series corresponding to the historical scenario contains data from 1955 to 2005 and is developed using the GHM forced by each of the five GCM's. In order to extract the needed sample, the year of construction of the dam is taken into account. If the dam was constructed before 1991, the data series begins in 1955 until 1991, if the year of construction is after 1991 but before 2005, the time series begins 36 years before of the year of construction. Finally, if the dam was built after 2005, the data is taken from 1969 to 2005.

- Current climate scenario: This scenario is used to analyse how the risk of failure has changed in the current climate when compared to with the climate when the dam was built. Data was extracted for the time series from 1980 to 2015. This time series is based on a combination between the data from the historical data (which ends in 2005) and results from the climate runs forced with RCP4.5.
- Future RCP4.5 and Future RCP8.5: For the analysis of the change of risk of dam failure under climate change, the time series for RCP4.5 and RCP8.5 begin in 2015 until 2050.

With the results from the re-analysis run (1980-2015) a synthetic design was estimated which is the reference for the results for the historical scenario. The synthetic design was developed to find the bias between the time series from the model and the real data as obtained from the dam databases.

3.3 Selection of large dams

In order to estimate the change of risk of failure due to overtopping at the global scale it is necessary to select a sample of large dams which represents the conditions of these structures over the world. Several criteria were, however, needed to allow for the estimation of the spillway capacity of the dams with different hydrologies. The main criteria needed, besides of the basic characteristics (Name of the dam, Country, Continent and Year of construction to identify each structure) were; River where it is located, Actual spillway capacity (m^3/s), Dam Type, Height (m), Reservoir capacity (m3), Length of the crest (m), Longitude and Latitude, Area of the reservoir and Catchment Area.

To choose the dams that were taken into account to analysis under this research, three (global) databases of dams were used: The Global Reservoir and Dam (GRanD) database (Beames et al., 2019), The World Register of Dams (WRD) (ICOLD, 2018) and the US Dam Inventory (US Army Corps of Engineers, 2018), every database contains one or more of the needed criteria, for this reason it was necessary to use more than one database.

As the WRD database contains more than 50,000 dams located around the world and it is the only one that offers the spillway capacity value, the process to select the dams started with this database, where were selected the dams which have the spillway capacity known. In this step, 20000 dams were extracted approximately. Then, a cross-match was done with the GranD database, to find the dams in which the spillway capacity is known as well as the location (longitude and latitude). Lastly, the same process had to be done with the US Dam Inventory, as none of the dams from the USA in the WRD database include the spillway capacity.

Where multiple dams are defined for which it is possible to obtain all the criteria, the most upstream structure is selected. In the cases where there were more than one dam in a river, this was made taking into account the elevation above the sea level of the dams (from the GranD database), and choosing the one with the larger elevation. This resulted in some 2000 dams included in this list.

Finally, based on the grid that the model PCR-GLOBWB2 implements, a last filter was done through the verification of the locations of the dams, guaranteeing that the area upstream of the location of the dam in the model grid corresponds with the catchment area given in the database. This was done setting a tolerance threshold between the catchment area in the model and the

catchment area reported in the database. The tolerance for the larger catchment is smaller by percentage than the smaller catchments, this is due to for the smaller catchments the difference between areas grow due to the resolution of the model (between 50-70 km^2 every cell). On the other hand, some dams were left because there are other dams in the same cell.
Figure 3.3-1 shows the relation between the reported area and the model area for catchments with less than 50,000 km^2, where the red lines represent the tolerance threshold, the red points dams which its reported area corresponds to the model area and the blue points the dams that are not taken into account for the final selection.

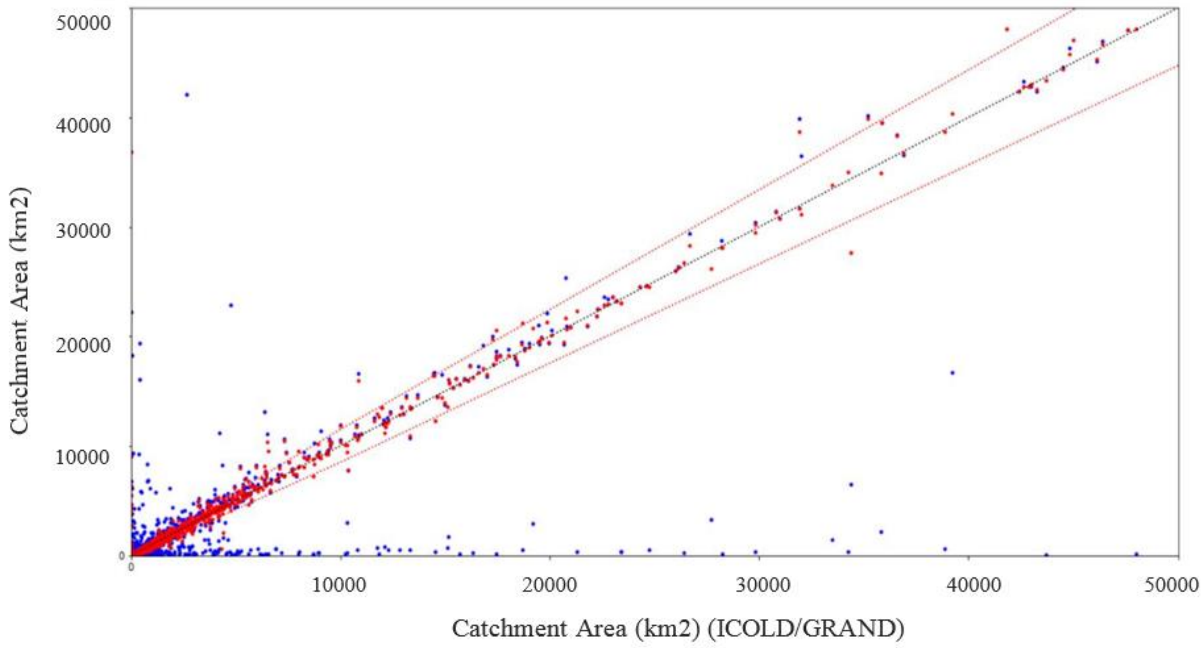

Figure 3.3-1 Relation between the reported area and the model area for catchments less than 50000 km2

At the end, the database for this research has 1447 dams. Figure 3.3-2 presents the global distribution of the selected dams, where every circle represents a dam that is considered. The selected dams are spread over the five continents, although there is a higher concentration in North America and Asia, this was expected due to approximately the 26 % of the dams in the GRanD database belong to USA, the 12% to China and 4% to India (Beames et al., 2019).

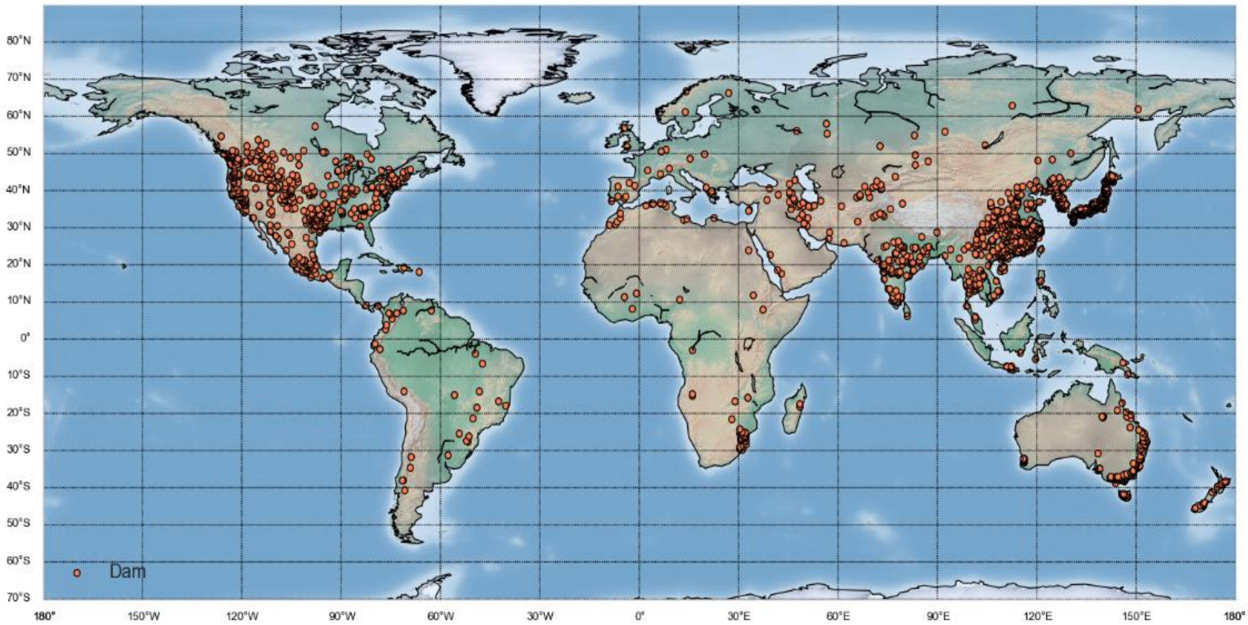

Figure 3.3-2 Global distribution of selected dams

3.4 Deriving the design inflow hydrograph

The inflow hydrograph represents the input of the mass balance that is estimated in the flood routing in order to assess dam safety. An important part in ensuring a safe design of dams is the estimation of flood peaks and the corresponding volumes that belong to the hydrographs. In order to construct the different hydrographs for each dam for different return periods, a method is adopted that is based solely on discharge data series.

The method implemented is explained in the paper *Flood type specific construction of synthetic design hydrographs* (Brunner et al., 2017). This approach develops synthetic design hydrographs (SDHs) by calculating the design value of the maximum flood and volume parameters by fitting probability density function (PDF) to observed flood hydrographs. The method takes into account the dependence between the two design variables; flood peaks and volume, it considers the duration of the event as an independent variable, to restrict the analysis of the data as a bivariate case.

The use of fitting PDF is an advantage in order to obtain a flexible shape for the hydrographs and it is more acceptable than conventional methods for deriving unit hydrographs because of the region under the curve is assumed to be one and may be used as a basis for designing the flood hydrograph. The method combines the use of frequency analysis to calculate the design variables (peak discharges and volumes) making use of the statistical information of the data, and prescribed mathematical functions like to upscaling unit hydrographs (Brunner et al., 2017).

The development of the SDHs is based on the method proposed by (Yue et al., 2002), which employs the PDF of the Beta distribution to represent different shapes of the hydrographs, linking the design variables flood volume (V_T) and duration (D_T) for a determinate return period

(T) and the PDF to obtain the SDH ($Q_T(t)$) (Equation 1). The same principle is used for Brunner et al., (2017) but taking into account different PDFs.

Equation 1

$$Q_T(t) = f(t)\frac{V_T}{D_T}$$

The method can be simplified in six steps that are presented in Figure 3.4-1, which allow to transform a dimensionless shape of the design hydrograph; that it is estimate with a normalization of the events, to a real design flood.

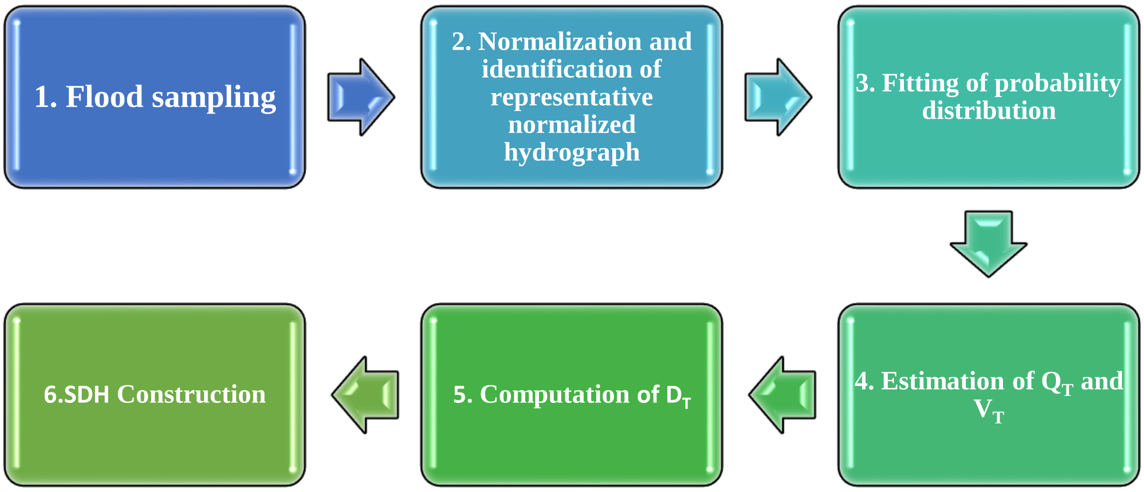

Figure 3.4-1 Method developed to construct SDHs.

3.4.1 Sampling flood events

To sample the events the peak-over-threshold (POT) method was implemented, which extracts all peak discharges that exceed a defined threshold level. This method was chosen as it allows for a bigger sample due to it not being restricted to only one event per year (Lang et al., 1999). To filter the data the *scipy.signal.find_peaks* function available in python was used, which finds all local maxima above a threshold, based on comparing neighbouring values, defining a peak value as a sample with a greater amplitude on two close neighbours (Scipy community, 2019).

The threshold value was calculate based on (Madsen & Rosbjerg, 1993), where it is recommended to use a standard frequency factor (k) and the mean (μ_x) and standard deviation (σ_x) value from the data. The threshold value was calculated with Equation 2.

Equation 2

$$x_0 = \mu_x + k\sigma_x$$

Although, there are several methods to calculate the threshold value based on mathematical and statistical approaches, this method was selected due to allowing to be implemented easily for the amount of data (dam) that this research processed. The k value was chosen in order to extract from two to three events per year (around k=3 to k=5). Figure 3.4-2 shows an example of peak selection for two years of Manapouri Dam, with k equal to 4 extracting the peaks above 1383 m3/s, using the re-analysis data (1979-1981).

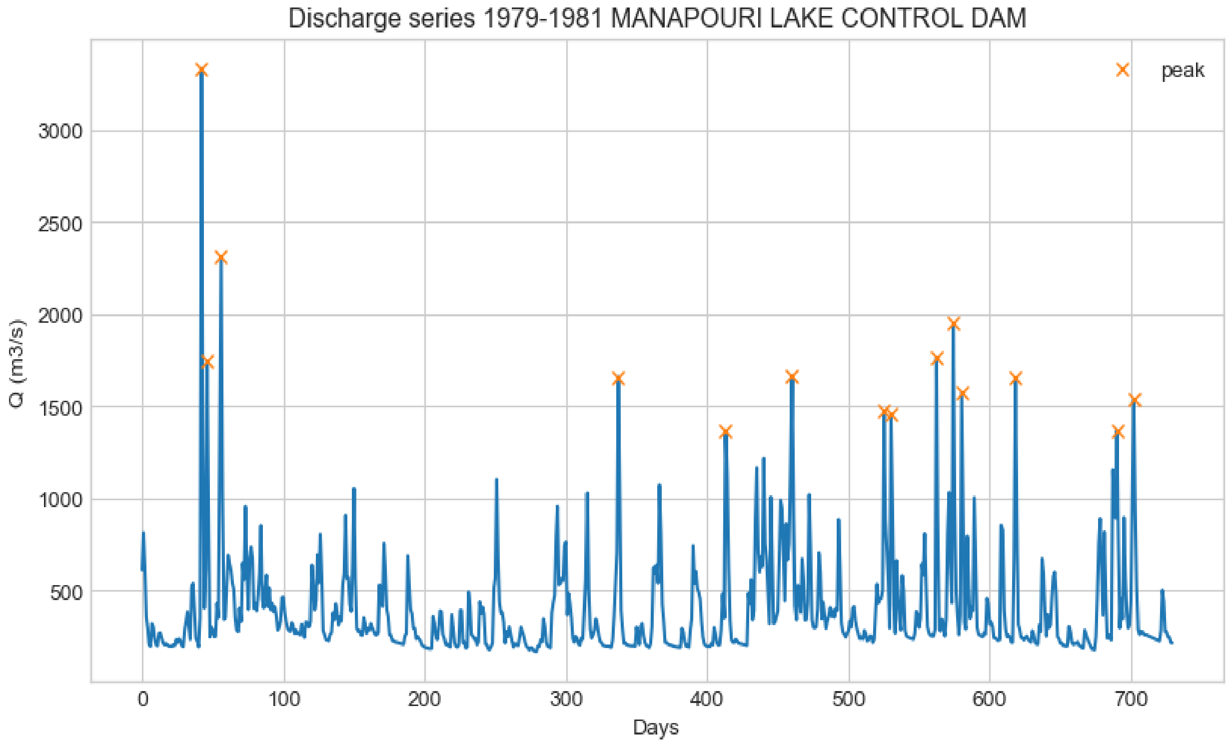

Figure 3.4-2 Manapouri Dam peak selection 1979-1981

The next step after the selection of the peak values is to extract the hydrograph of the flood events from the time series. This is required to establish the distribution of flood event volumes. To achieve this, an initial time to peak (T_p) is assumed that is based on the size catchment, taking into account that the time of concentration of catchments is related directly with the catchment area. Three groups were established in order to give a value for T_p, the selection of the values were based on observations of the time series from the re-analysis data, ensuring that the extracted hydrograph is the best representation of an event that represents the biggest and the quickest flood, which may not be mitigated by the dam and has to be passed over the spillway.

The time of recession (T_r) and time base (T_b) were calculated following the dimensionless unit hydrograph approach, which estimates T_r as 1.67 times T_p (Melching & Marquardt, 1997). However, as the minimum time step available is one day, T_r is taken here as two times T_p., this approximation would overestimate the recession time for larger catchments. Table 3.4-1 presents the T_p, T_r and the total duration T_b according to the catchment area.

Table 3.4-1 Initial hydrograph duration

Area (km^2)	**T_p**	**T_r**	**T_b**
A≤20.000	1	2	3
20.000<A≤500.000	3	6	9
500.000<A≤900.000	6	12	18
A>900.0000	15	30	45

For each of the events that were extracted, the flood volume is calculated by taking into account the fixed duration as defined. The flood volume is then found by calculating the area under the curve of the hydrograph using the trapezium rule as shown in Equation 3.

Equation 3

$$V = \sum_{i=1}^{N-1} (t_{i+1} - t_i) \left(\frac{Q_{i+1} + Q_i}{2}\right)$$

Lastly, probability distributions were fitted to the peaks and volumes obtained. According to extreme value theory, the series obtained with POT follow a generalized Pareto distribution (GPD) (Robson & Reed, 2008). Hence the peak values were fitted to the GPD. As the volumes were not selected with POT and not necessarily represent annual maxima, Brunner et al., 2017 suggests using GEV distribution to fit the flood volumes.

Equation 4 and Equation 5 represent the probability density function of GEV and GPD distribution. Then, the three parameters for each of the distribution were estimated (location μ, scale σ and shape ξ), taking into account the approach that was implemented in the sampling.

Equation 4

$$F_x(x) = 1 - \left(1 + \xi\left(\frac{x-\mu}{\sigma}\right)\right)^{-\frac{1}{\xi}} \quad \xi \neq 0$$

Equation 5

$$F_y(y) = \exp\left(1 + \xi\left(\frac{x-\mu}{\sigma}\right)\right)^{-\frac{1}{\xi}} \quad \xi \neq 0$$

In order to ensure the quality of the results, the fit of the GPD distribution for discharges was evaluated using the Kolmogorov-Smirnov test, which is a useful tool to compare two distributions. The approach consists of assessing if two samples are substantially different, where one of the samples is a known distribution and the null hypothesis states that both samples are from the same identical distribution (Hassani & Silva, 2015). The results of the Kolmogorov test were obtained using the *stats.ks_2samp* python package, which calculate the K-S statistic (absolute maximum distance between the cumulative distribution function) and the p-value (probability to accept or reject the null hypothesis) (Scipy, 2019).

The Kolmogorov test was applied to the results obtained from the re-analysis data, as this data is used to calibrate the results from the model. Dams where a significance (1-(p-value)) higher than 5% was found, were removed from the analysis.

3.4.2 Identification of the representative normalized hydrograph

To allow a probability distribution function to be fitted to the flood hydrograph for the catchment upstream of each dam, a normalized hydrograph representative of that catchment is derived. This representative normalized hydrograph (RNH) is obtained by transforming the base width and volume of the hydrographs so that these are equal to one. This was done by dividing the total duration (t_b) of each flood hydrograph by t_p and t_r, and dividing the ordinates of each hydrograph by the ratio of the flood volume V and duration corresponding to each event (Brunner et al., 2017) . The RNH is then selected from the normalized hydrographs of all events as the median normalized hydrograph. The median is taken as this is not susceptible to the extremes as might be the case if the mean hydrograph were taken

3.4.3 Fitting a probability distribution to the representative normalized hydrograph

To represent the characteristics of flood events, synthetic design hydrographs the SDHs are computed based on peak and volume flood. To define the shape of the design hydrograph probability density function (PDF) was fitted to the RHN. The area below the curve of the hydrograph and PDF is equal to one and the PDF is able to take different shapes (Brunner et al., 2017). There are several available derived expression for the unknown values of the density functions in terms of time to peak (t_p) and the peak discharge (q_p) developed by (Nadarajah, 2007). However, based on Brunner et al., 2017 the lognormal density function is implemented, as they find this provides the best fit to model their RHNs.

Based on the time to peak (t_p) and peak discharge (q_p) obtained from the RHN, Equation 6 and Equation 7 proposed by Nadarah, 2007 were implemented to find the two parameters (location μ and scale σ) for the Lognormal distribution. Through this it was possible to determine the shape of the SDH for the catchments upstream of each of the dams considered in the analysis.

.

Equation 6

$$t_p q_p = \frac{1}{\sqrt{2\pi}\sigma} \exp\left(\frac{-\sigma^2}{2}\right)$$

Equation 7

$$\mu = \sigma^2 + \ln t_p$$

3.4.4 Design of event discharge and volume (Q_T and V_T)

In order to find the pair of discharge and volume with respect to a given return period (Q_T, V_T), a joint cumulative distribution function (F_{xy}) of the two variables (X,Y) is defined, which allows to define the probability $F_{xy}(x,y)$ that both X and Y do not exceed given values x and y (Brunner et al., 2016). As the variables volume and discharge are dependent, it was necessary to model their dependency. This is dependency is modelled using a copula model.

A copula is a bivariate function which defines, regardless of marginal laws involved, the dependency structure between random variables which have a uniform distribution (Salvadori et al., 2007). The copula approach is based on Sklar theorem, which says that the joint cumulative distribution can be written as:

Equation 8

$$F_{XY}(x,y) = C(F_X(x), F_Y(y) = C(u,v)$$

Where $F_X(x)$ denote by u and $F_Y(y)$ denoted by v are the representation of the marginal distributions of X and Y whose dependence is modelled by a copula C (Brunner et al., 2016). For this research, $F_X(x)$ represent the marginal distribution of the flood volume values and $F_Y(y)$, the marginal distribution of the peak discharge values.

There are different copulas families, such as Gaussian, Archimedean and Extreme value. To select the most suitable dependence model between the families the behaviour of different copulas needs to be evaluated, and the results compare using different criteria such as the

Akaike or Bayesian information criterion (Brunner et al., 2016). Also, nonparametric measures of dependence are usually computed as Spearman's rho and Kendall's tau (Genest & Favre, 2007), the last one was implemented in this analysis.

Various research studies have analysed the estimation of the return period of hydrological events with copulas. (Salvadori & De Michele, 2004) showed that the use of copulas can simplify the calculation for bivariate analysis and provides a simple and efficient tool for performing risk analysis. (Favre et al., 2004) concluded that bivariate probabilities obtained from using copulas are more accurate than classical multivariable models and allows the modelling of a broad range of correlations that are observed in hydrology. (Li et al., 2013) compared the results from bivariate designs using copulas with historical floods in the Three Gorges reservoir, and found that results of copulas are more precise than univariate design results.

However, in order to implement the modelling of copulas in python using the *Copulaslib* library was chosen. This only offers three copulas: Clayton, Frank and Gumbel, which are part of the Archimedean family (Tomer, 2011). With the python package it is possible to generate 1000 samples of the joint cumulative distribution based on the variables volume and peak discharge and estimate the dependence parameter of each copula (θ), which is fundamental to estimate the design event.

It is important to highlight, that there are different approaches to define the return period using copulas which are based on developing joint return periods that are called: the joint OR return period and the joint AND return period. The OR return period represents the probability of events where either discharge or food volume exceeds a given threshold, while the AND return period describes when both peak discharge and flood volume exceed the threshold (Brunner et al., 2016). The return period for this research was not calculated using these approaches, as the return periods normally used to design the spillway capacity are already known from the literature (either 1000 years, 10000 years return period and PMF).

On the other hand, the type of joint return period was taken into account to calculate the level curves of the copula, which are isolines that represent pair of values with the same probability of occurrence. For this research, we use the OR return period due to both conditions could lead to dam overtopping. Equation 9 (Salvadori, 2004) provide the level curves of Frank copula for the OR return period; which is one of the available copulas in the python package.

Equation 9

$$v = L_t(u) = \frac{1}{\ln(\theta)} \ln\left(1 + \frac{(\theta - 1)(\theta^t - 1)}{\theta^u - 1}\right), \qquad t \leq u \leq 1$$

Equation 9 depends of θ, which was calculate with the python package and t that represents the different return periods. However, for establishing the design hydrograph it necessary to extract one value from the curve levels. To find this value, a linear regression is proposed between the values of peaks discharges and volumes. The intersection point between the linear regression and the level curves chosen as the event for the respective return period is extracted. The point extracted has two components (u and v), which were inverted into their marginal probability distribution (GPD and GEV), obtaining Q_T and V_T for different return periods.

To estimate the design pair for the PMF, which has no predefined return period we implement the ratio between the PMF and 10000 year flood period as proposed by (Zhou et al., 2008). This ratio is not a constant value, but it depends of the coefficient of variation (Cv) of the series of annual flood maxima. Equation 10 presents the ratio proposed for a 10000 year flood.

Equation 10

$$\frac{Q_{10.000-yr}}{Q_{PMF}} = \frac{1 + 15 * Cv}{1 + 6.731 * Cv}$$

According to this, the PMF to 10000 year flood ratio varies from 1.53 to 2.66, with most common being in the order of 2 (Zhou et al., 2008).

3.4.5 Computation of event duration (D_T)

As the analysis done is bivariate and the dependence between duration, flood volume and peak discharge is not considered, the estimation of the duration of the event (D_T) is calculated based on Q_T and V_T (Brunner et al., 2017). Equation 11 presents how to calculate D_T, where $f(t_p)$ is the value of the Lognormal distribution at the time to peak t_p, which is calculated with the parameters found in the fitting of the SDH (section 3.4.3) and Equation 12 which is the Lognormal density function.

Equation 11

$$D_T = f(t_p)\frac{V_T}{Q_T}$$

Equation 12

$$F(x) = \frac{1}{x\sigma\sqrt{2\pi}}\exp\left(-\frac{(\ln x - \mu)^2}{2\sigma^2}\right)$$

3.4.6 Construction of the design hydrographs

To construct the design hydrographs, the duration (D_T) and the ratio between volume and discharge (V_T/D_T) from the values for 500, 1000 and 10,000 year return period and the PMF (see section 3.4.4.), were used to obtain the final inflow hydrographs, implementing Equation 13 and the values of the ordinates found fusing from the lognormal distribution.

Equation 13

$$Q_T(t) = f(t)\frac{V_T}{D_T}$$

3.5 Elevation and storage relation

The elevation storage curve of a reservoir determines the water volume for any water stage, this curve is an important characteristic of the reservoir that is needed to complete the flood routing from the elevation of the permanent pool to at a slightly higher elevation than the top of the dam (Serrano-Lombillo et al., 2011).

Generally, for each dam it is possible to estimate the relation elevation storage from observed data or from contour maps. However, these data are not included in the global dam databases and as this research works with approximately 1500 dams it was necessary to implement a simpler method to find this relationship.

The same theoretical relationship used in the construction of PCR-GLOBWB2 model is implemented (van Beek & Bierkens, 2008a). The relationship between stage and storage of a reservoir, according to (Liebe et al., 2005) is given by Equation 14:

Equation 14

$$V = \frac{1}{3}Ad$$

Where A is the surface area of the reservoir (m^2), d is the maximum depth of the reservoir (m) and V is the maximum storage (m^3). With this theoretical relationship is possible to find the storage based on a changing surface area and on a changing depth.

The reservoir surface area and maximum depth are available information in the global dam databases, with these data the following steps to calculate the elevation-storage relationship were taken:

1. Estimate ratio between maximum depth and surface area of the reservoir
2. Discretize the area in ten equal intervals
3. Calculate the depth for each discretized area (Area*Ratio)
4. Calculate the volume for each interval using Equation 14.

This provides a table with Area, Depth and Volume information for each dam at different stages. With this a power law is fitted to find the coefficients to build an equation that represents the elevation storage curve of every dam with the form:

Equation 15

$$d = a * V^b$$

Where *a* and *b* are the parameters of the power law and d (m) is the elevation at storage V (m^3)

3.6 Outflow relationship

To determine the outflow over the spillway, it was assumed for simplicity that all dams have an ogee spillway (the most widely used), and unconstrained flow, meaning that it was considered that gated spillways are raised during the design flood. Equation 16 describes the discharge over the weir.

Equation 16

$$Q = \frac{2}{3}C_d b H_t \sqrt{2gH_t}$$

Where Q is the flow rate (m3/s), Cd is the discharge coefficient, b is the spillway width (m), H_t is the upstream energy head (m) in every time step and g is gravity acceleration (m/s^2) (Montes, 1998). To calculate the Cd we implement Equation 17 which was proposed by (Vischer & Hager, 1998) for ogee weirs, where H_d is the design head over the crest (m).

Equation 17

$$Cd = \frac{1}{\sqrt{3}}\left(1 + \frac{4X}{9 + 5X}\right) \ ; X = \frac{Ht}{Hd}$$

It is important to highlight that the ogee crest shape has the capability to change its discharge capacity if the height of the head (H_t) is different to the design head (H_d) , due to the fact that when the head over the crest is larger or smaller than the design head (H_d) this leads to changes in pressure: a wider shape reduces the discharge and a narrow crest shape increase the discharge (US Bureau of Reclamation, 1976). Taking into account this variability in the analysis of the risk of overtopping, allows to ensure that the dams can increase the spill discharge in case that the head over the crest is larger than the design, using the narrow space provided by the freeboard.

To estimate the maximum outflow discharge of the spillway, the physical characteristics of the spillway (spillway width and height over the crest) are needed. Unfortunately these parameters are not available for all dams in the databases. It is important to highlight that the width of the spillway is an independent variable and it is designed based on the designer criteria and economic factors.

However, it was possible to extract the spillway width for around 1000 dams from the US Dam Inventory for which the maximum spillway discharge capacity is known. These data we use to parametrize the hydraulic characteristics of the dams and develop a multivariate regression based on the available physical characteristics. This is then used to estimate the spillway width of all dams in the analysis.

Once the physical characteristics of the dam are calculated, the height of the crest can be found using Equation 18, where Hcrest is the height for full supply of the reservoir, FB is the freeboard, H_{dam} is the coronation height (total height of the dam) and H_d is the maximum head over the weir for the spillway design.

Equation 18

$$H_{crest} = H_{dam} - H_d - FB$$

To define a freeboard value for each dam, the type of dam is taken into account, considering if it is either a concrete dam or an embankment dam. According to (Novak et al., 2007), the freeboard is calculated using the concept of significant wave height (H_s), that is the average height of the third wave height of a train with approximately 14% of waves higher than Hs. It is recommended to use $1.3H_s$ for earth dams and 0.75Hs for concrete dams to estimate the freeboard. H_s is estimated based on the Donelan/JPNSWAP equation (Donelan, 1980):

Equation 19

$$H_s = \frac{UF^{0.5}}{1760}$$

Where U is the velocity of the wind (m/s) and F is the maximum free distance over the reservoir known as fetch. To estimate the fetch of each reservoir it was assumed that the surface area of the reservoir is triangular, then with the length of the dam (B) and the reservoir surface area (A), the fetch was calculated:

Equation 20

$$F = \frac{2 * A}{B}$$

To obtain the wind speed we use the open access Global Wind Atlas database developed by the World Bank and the Technical University of Denmark, which provides a unified and high resolution public domain dataset for wind characteristics over the world (Badger & Ejsing

Jorgensen, 2011). From its website a GIS file was obtained with the average wind speed around the world at 10 m height. Figure 3.6-1 shows the data obtained from the Global Wind Atlas and the location of the dams. With this dataset it was possible to extract the velocity for each dam based on its location.

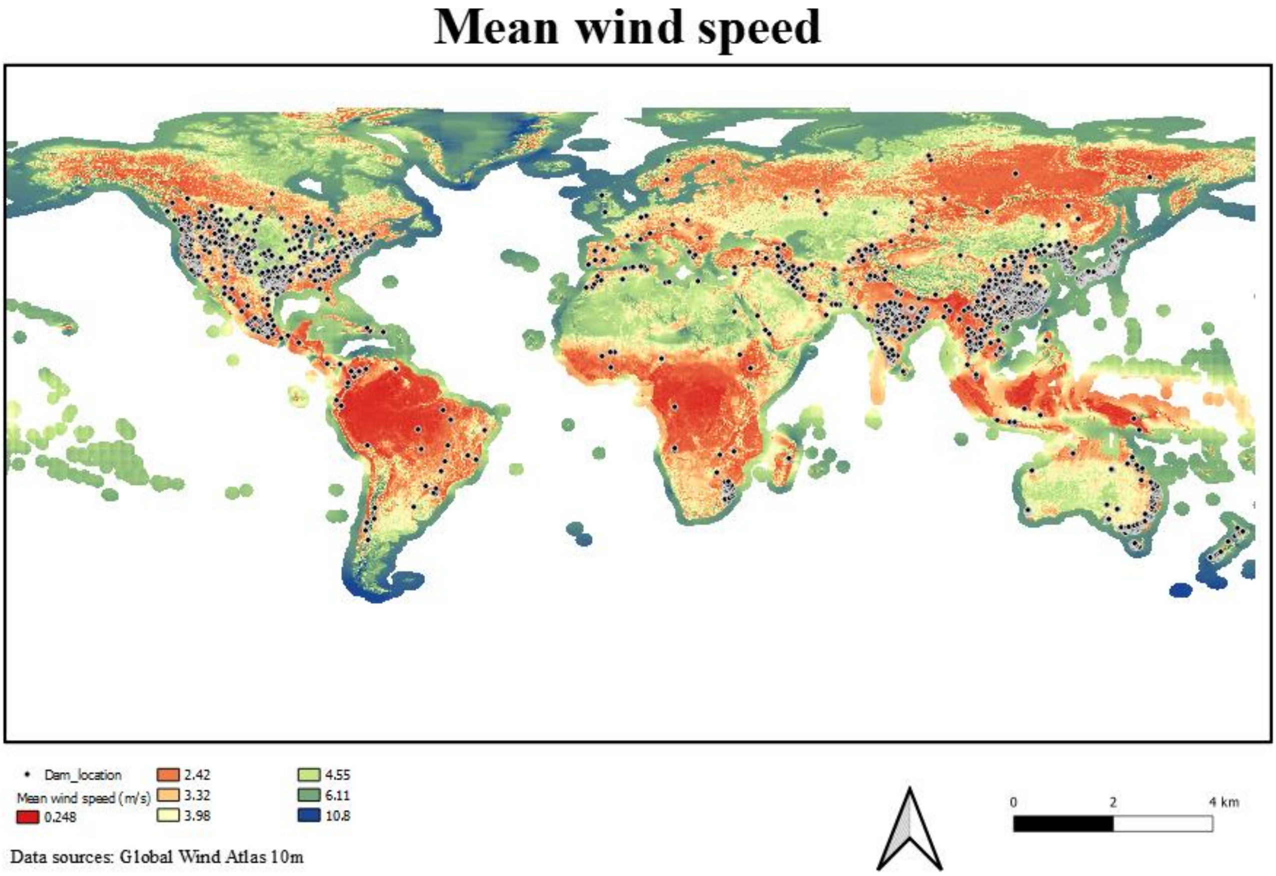

Figure 3.6-1 Mean wind speed global map at 10 m

With the calculated freeboard based on Equation 19, second check was done based on the criteria for minimum freeboard that is used in Switzerland, which gives constants values depending on the type and height of the dam,(ICOLD, 2016). Table 3.6-1 presents the guideline. This was done due to some of the selected dams having been built before 2000, and it is probable that the method proposed by (Novak et al., 2007) was not used.

Table 3.6-1 Minimum Freeboard Switzerland (ICOLD,2016)

Dam height	**H<10 m**	**10m<H<40m**	**H>40m**
Concrete dam	0.5 m	1.0 m	1.0 m
Embankment dam	1.0 m	1.5m-2.0m	2.0m-3.0m

The final value of freeboard was obtained comparing the value obtained from Hs equation and the Swiss guideline, guaranteeing that concrete dams have at least 1 m of freeboard and embankment dams between 10m and 40 m high at least 1.75 m and dams with a dam higher than 40 m having a freeboard of at least 2.5 m.

3.7 Flood routing

To determine if a dam is on risk to fail due to overtopping, a flood routing routine was developed to simulate the attenuation of the inflow hydrograph through the reservoir, based on the hydrological data obtained from the PCR-GLOBWB2 model and the characteristics of the reservoir and spillway described using the approach in the previous sections. Every dam is designed based on a flood peak discharge, to guarantee the safety and minimize damage downstream due to a flood event. The procedure to determine the outflow hydrograph is named flood routing, which from the inflow hydrograph into the reservoir, elevation crest, storage and physical characteristics of the spillway can solve a mass equation assuming outflow discharge and volume storage capacity are directly related (USDA & NRCS, 2014).

Equation 21

$$I - O = \frac{dV}{dt}$$

Equation 22

$$\frac{V_2 - V_1}{\Delta t} = \frac{I_1 + I_2}{2} - \frac{O_1 + O_2}{2}$$

At the start of each event, it is assumed that the reservoir is full until the crest of the spillway, which is the most critical condition. The initial volume is then calculated based on the relation storage-elevation found in section 3.5 and the crest height calculated in section 3.6. The outflow values are calculated with the outflow curve (Equation 16) and the inflow values are from the inflow hydrograph.

To estimate the value for the spillway design, the point where the inflow hydrograph and the outflow hydrograph intersect is chosen. This represents the highest point of the outflow curve and thus the maximum required capacity of the structure. This point represents the maximum discharge and thus also the maximum height that the water may reach over the crest (Ht). The flood routing approach was implemented for the design inflow hydrographs for 500, 1000, 10,000 years return period, as well as for the PMF.

3.7.1 Synthetic design

As it was mentioned before, a synthetic design of the spillway discharge capacity was calculated using the re-analysis data (1979-2015). The aim of this synthetic design capacity is to provide a tool to use as reference to compare the change of risk of dam failure between the scenarios. The synthetic spillway design consist in two parts: estimation of H_{crest} and H_d and calculation of the spillway discharge capacity.

To estimate the initial value for H_d (maximum height over the crest), the value for discharge coefficient (Cd) was chosen equal to 0.7, which represents a medium value for an ogee weir based on Equation 17. With the value of Cd and the equation for the outflow curve (Equation 16), H_d is calculated based on the real spillway discharge capacity for every dam, and H_{crest} is estimated with Equation 18. These results were named H_d* and H_{crest}*.

However, as the calculation of these values are from the real spillway discharge capacity and the hydrological data used in this research are not the same data that was available at the time of the design the dams, it was necessary to correct H_d* and H_{crest}* using the hydrological time series provided by the re-analysis. To make the correction, and find the synthetic value for H_{d_syn} and H_{crest_syn}, a series of iterations with the flood routing scheme were made.

The procedure to make the iteration was:

1. Estimate spillway discharge capacity using H_d* and H_{crest}* and the flood routing scheme, obtaining $H_{d(i)}$ and $H_{crest(i)}$.
2. Calculate spillway discharge with $H_{d(i)}$ and $H_{crest(i)}$, obtaining $H_{d(i+1)}$ and $H_{crest(i+1)}$.
3. Calculate the difference between $H_{crest(i+1)}$ with $H_{crest(i)}$.
4. If the difference is greater than 1% of $H_{crest(i)}$, flood routing is estimated with $H_{d(i+1)}$ and $H_{crest(i+1)}$, and the process repeats from step 2.
5. If the difference is smaller than 1% of $H_{d(i)}$ and $H_{crest(i)}$, H_{d_syn} and H_{crest_syn} are equal to these values.

Finally, the values of H_{d_syn} and H_{crest_syn} were used to calculate the spillway discharge capacity for all scenarios. The spillway discharge capacity and height over the crest for 500, 1000, 10,000 years flood and PMF were computed with H_{d_syn} , H_{crest_syn} and the re-analysis data as well.

Chapter 4 Results

This chapter presents the results from the analysis proposed in Chapter 3. The first part shows the outcomes of the flood routing scheme as inflow hydrograph, relation storage-elevation and outflow curve. Then, it presents the synthetic spillway design which is computed to obtain reference values in order to analyse the changes of spillway discharge for future scenarios (RCP4.5 and RCP8.5), due to there is not a clear relationship between the real values and the results from this research.

Next, an analysis of the relationship between synthetic design and spillway discharge capacity from historical and current scenario provides the tools to understand the bias between the available hydrological data and the run-off time series from the GHM. Finally, the results of the impacts of climate change on the necessary spillway discharge capacity and dam overtopping provide an overview of the trend to increase dam failure in specific parts of the world.

4.1 Deriving the design inflow hydrograph

4.1.1 Identification of the representative normalized hydrograph

Following the process presented in section 0, the representative normalized hydrograph (RNH) was estimated for each of the dams and for each scenario. Figure 4.1-1 shows the results for six selected dams of varying catchment size. The grey lines show the hydrographs of the selected flood events (normalized), while the red line shows the median flood event, which is taken as the representative normalized hydrograph (RNH).

It can be observed that for the larger catchments the shape of the normalized hydrographs is not uniform, while for smaller catchments the events have a similar shape.

This difference is due to the time to peak was fixed for all events base on the catchment area. For larger catchments (area greater than 500.000 km^2), the time of the base was assumed to be 45 days. This allows a large time period in which observe more variation of event is observed. For smaller catchment, this behaviour was not observed because of their time to peak correspond to the minimum time step of the time series (see Table 3.4-1)

However, as the median normalized hydrograph was selected as the representative normalized hydrograph (RNH), the flood events with more variation did not represent a problem

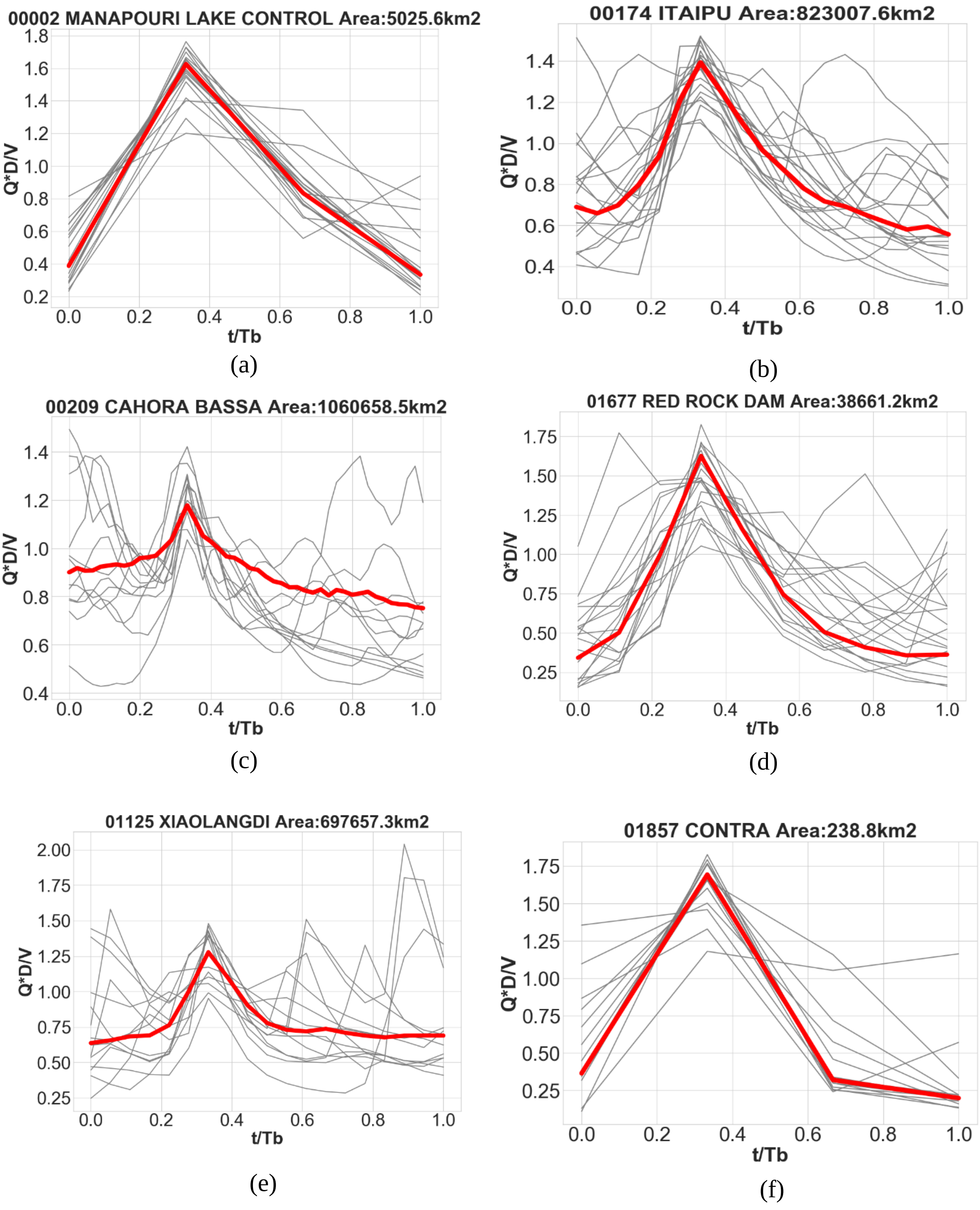

Figure 4.1-1Representative normalized hydrograph. Red line represents the median RHN (a) Manapouri Lake control dam in New Zealand, (b) Itaipu dam in Brazil/Paraguay, (c) Cahora Bassa dam in Mozambique, (d) Red Rock dam in United States (e) Xiaolangdi Dam in China, (f) Contra Dam in Switzerland

4.1.2 Fitting a probability distribution to the representative normalized hydrograph

The flood peak and the time to peak were extracted for each RNH in order to estimate the parameters μ and σ of the lognormal density distribution (Equation 6 and Equation 7). This allows obtaining a SDH with the shape of the lognormal distribution with the RHN's characteristics. Figure 4.1-2 presents the shape of six RNH with the fitting of the lognormal distribution and the RHN. It must be noted that for bigger catchments (e.g., Itaipu and Cahora Bassa dam) the shape of the hydrograph is wider due to the time base and the fit of the lognormal distribution is more accurate for smaller catchments.

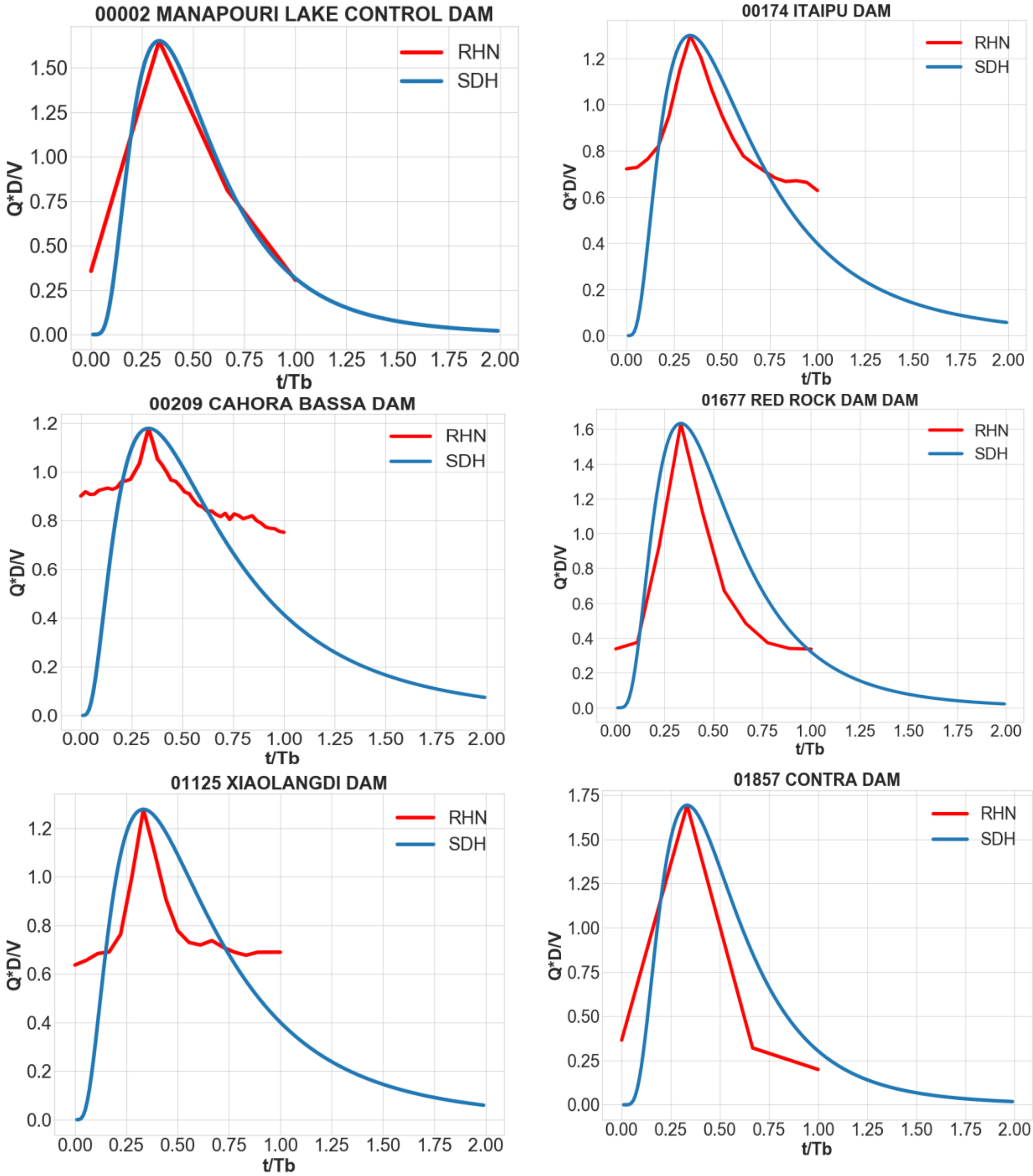

Figure 4.1-2 Fitting Lognormal distribution

4.1.3 Design of flood discharge and volume (Q_T andV_T)

Frank copulas were used to estimate the peak flood discharge and volume (Q_T and V_T, respectively) for a specific return period, as presented in section 3.4.4. For each copula that was fitted, the Kendall's tau coefficient was calculated, which measures the correlation between the two variables and a value equal to 1 means a perfect covariance.

Figure 4.1-3 presents the distribution of the Kendall's tau coefficient estimated with the data from the re-analysis discharges, mean value is 0.75 and most of the values tends to be skewed towards the positive side, which shows a good correlation in the estimated copulas.

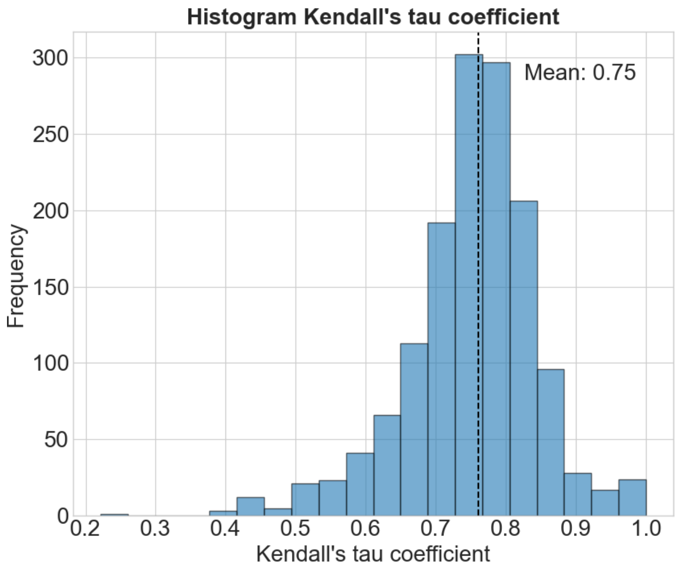

Figure 4.1-3Histogram Kendall's tau coefficient

Figure 4.1-4 shows the joint distribution of discharge and volume variables, green points represent random points generated by Frank copulas function. Additionally, it was observed that the joint distribution between discharge and volume for dams located in smaller catchment have a better correlation than the bigger catchments. A better fit for the larger may well be obtained using other families of copula, though this was not explored here.

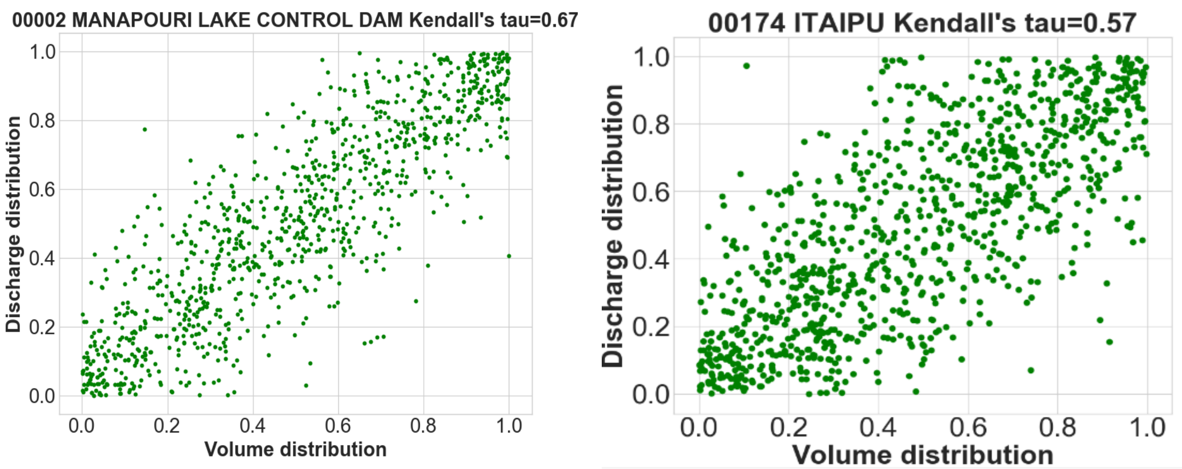

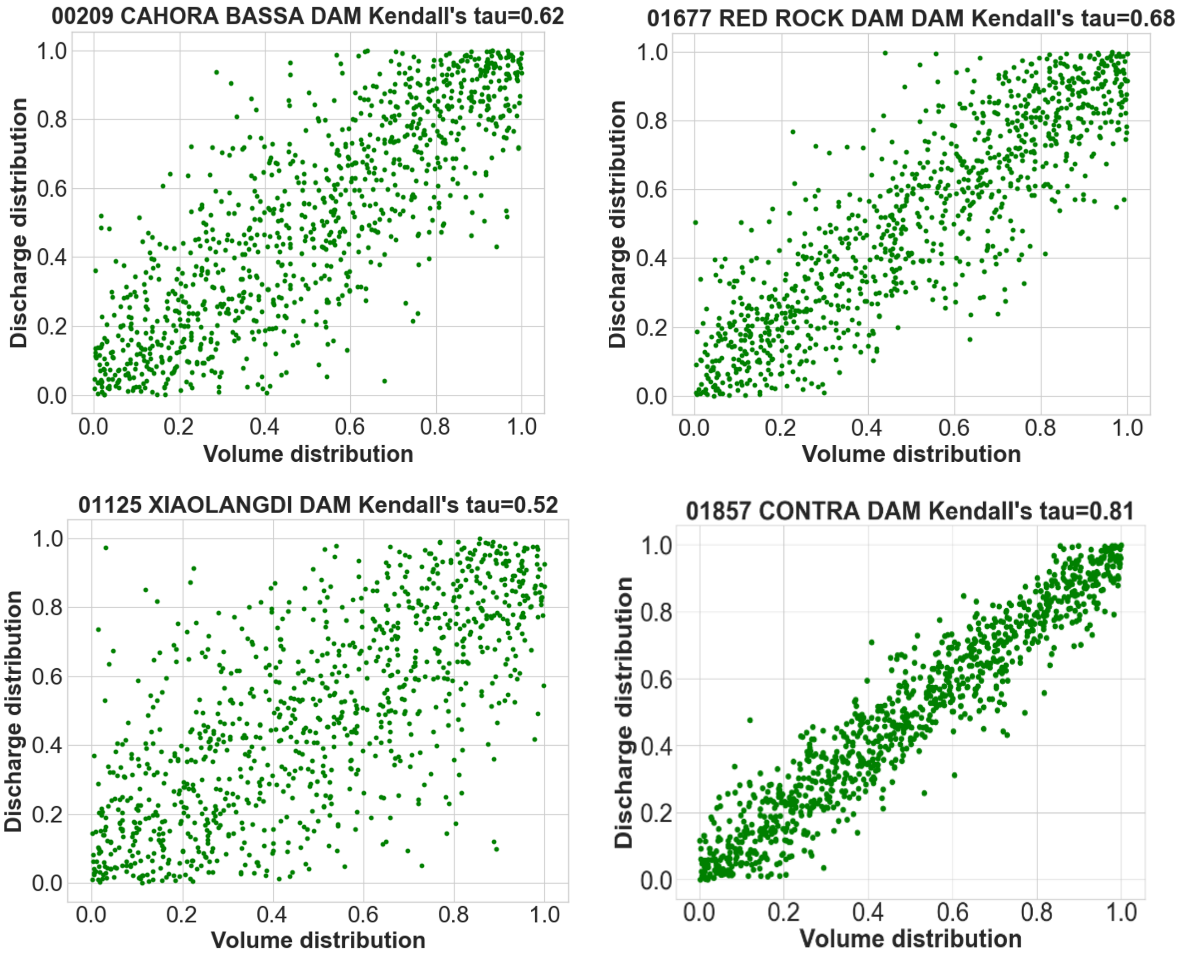

Figure 4.1-4 Frank copulas simulation (Kendall's tau coefficient)

The level curves for Frank copula were calculated for 100, 500, 1000 and 10,000 year return period floods. These isolines represent all the points of the joint distribution which have the same probability of occurrence. All points over this line hold the same probability of occurrence.

The analysis of the level curves for six dams is presented in Figure 4.1-5, where it is possible to see that the level curve corresponding to bigger probability of occurrence have bigger values of the representation of the marginal distributions for volume (u) and discharge (v). The red line shows the linear regression between discharge and volume samples, and the intersection of this line with the level curves was chosen to extract the components u and v to establish the Q_T and V_T for the design hydrograph. The values u and v represent the probability of occurrence of each of the variables in their probability distribution function and applying the inverse of the GPD and GEV distribution the values for Q_T and V_T were calculated.

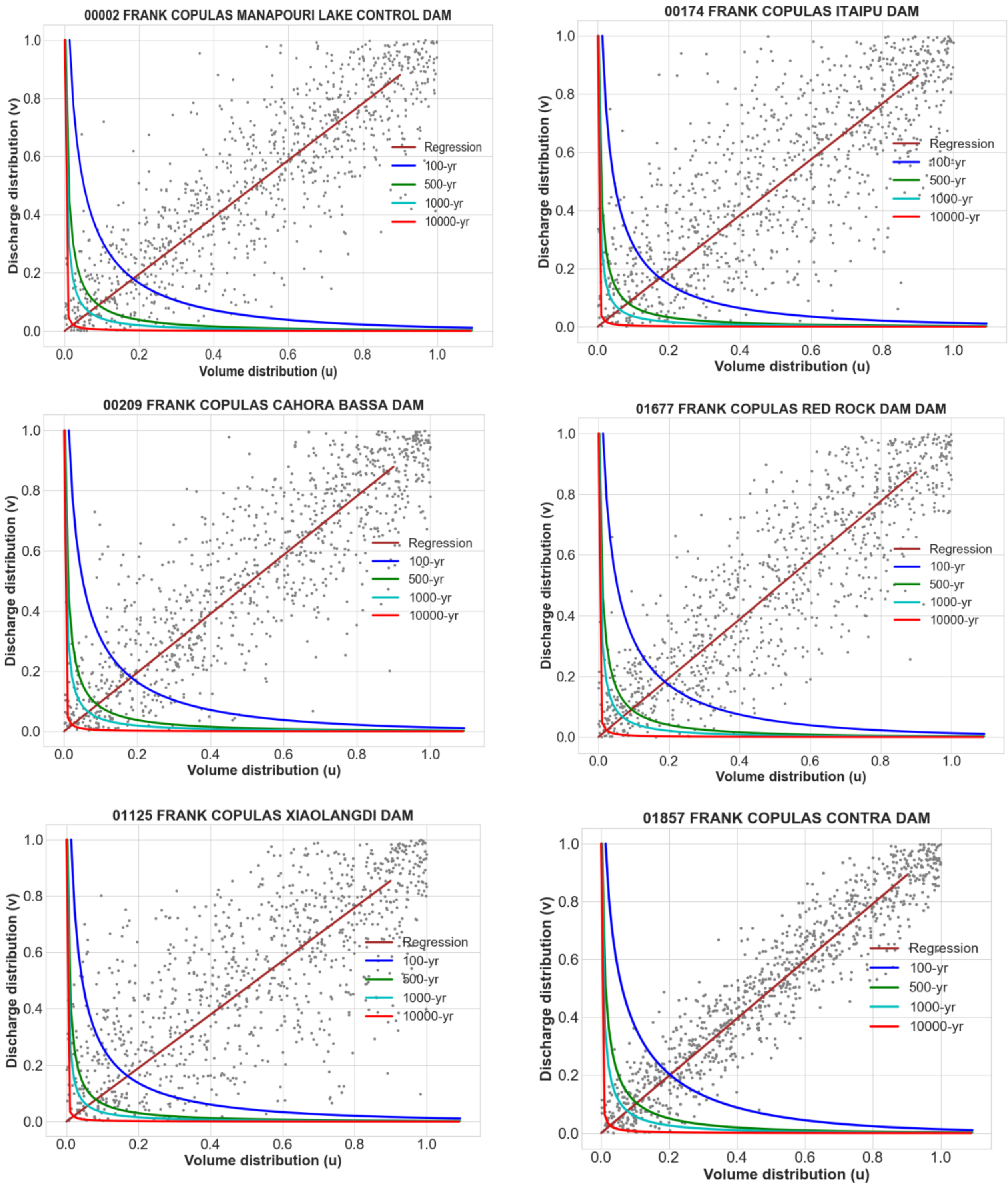

Figure 4.1-5 Level curves Frank copulas

4.1.4 Construction of the design hydrographs

With the definition of Q_T, V_T, D_T (Equation 12) and the shape of the hydrograph, Equation 13 was applied to obtain the values for the final hydrograph. Four hydrographs were developed for each dam: 500, 1000, 10,000 years flood and PMF. The chosen return periods to construct the hydrographs correspond to the most common values which countries use as guidelines for dam design (ICOLD, 2016), in order to obtain spillway discharge capacity values as similar as possible to real values.

Figure 4.1-6 presents the final hydrographs for six dams, it can be observed that the discharges of the PMF hydrograph are approximately double the 10,000-yr return period flood due to the ratio between 10,000-yr flood and PMF was implemented to calculate the PMF and it was expected to be between 1.56 and 2.66 (see section 3.4.4).

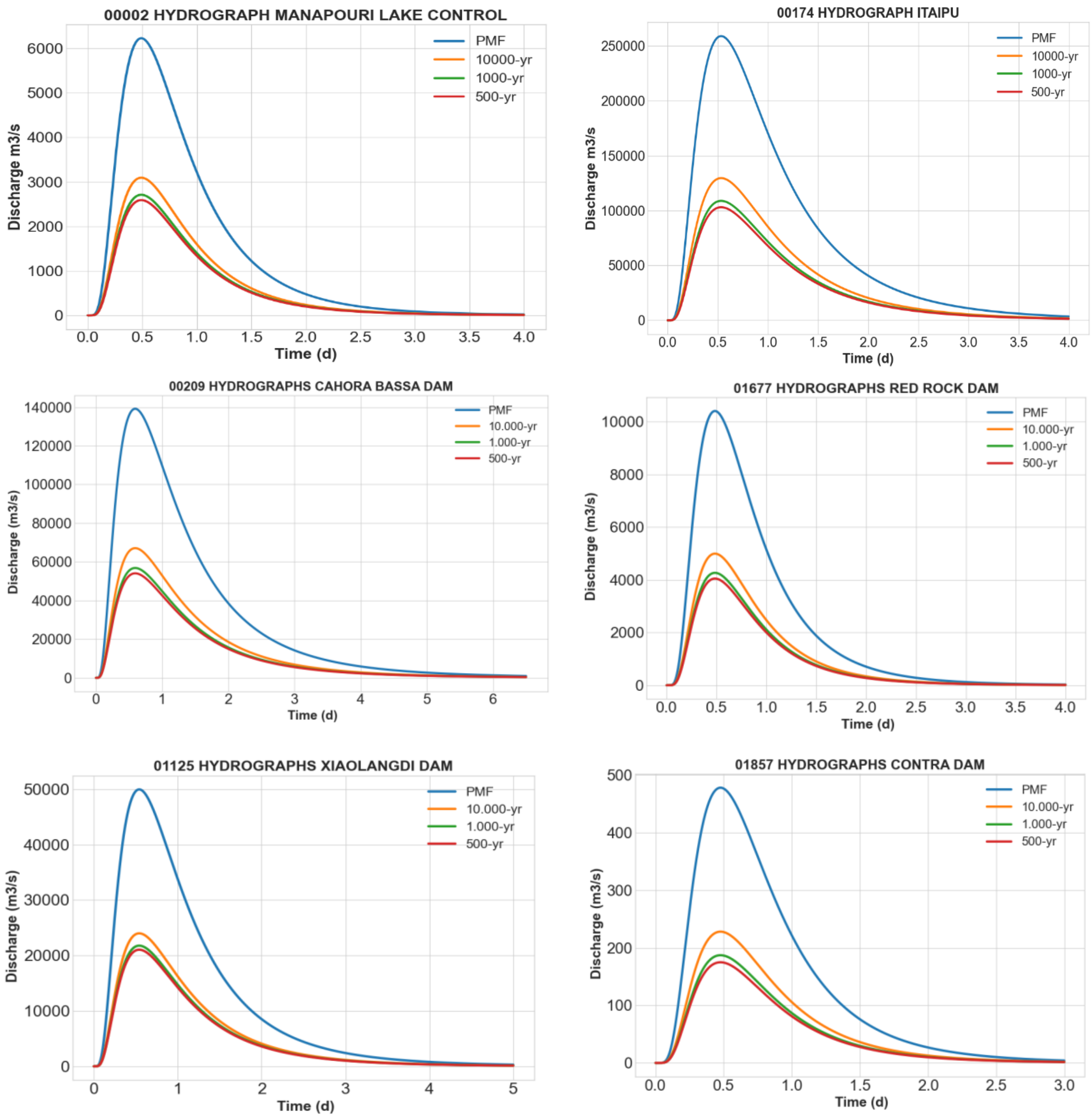

Figure 4.1-6 Design hydrographs for 500,1000,10,000 year return period and PMF floods

4.1.5 Elevation-storage relation

Following the procedure presented in section 3.5, the values for parameter *a* and *b* were estimated for every dam, in order to construct the power function that represents the relation elevation storage. With these values, a table was created for the elevation-storage relationship to be used in the flood routing. Parameter *b* is equal to 0.5 for all dams, due to it was assumed that the geometry of all reservoirs correspond to a pyramid. An example of the values found for the parameters power law is shown in Table 4.1-1

Table 4.1-1 *Power function parameters for the elevation-storage relation.*

ID	Dam name	Country	Total H (m)	Max storage (m3)	Parameter a	Parameter b
00002	MANAPOURI LAKE CONTROL	New Zealand	15	470,000,000	0.000542	0.5
00174	ITAIPU	Brazil	196	5,100,000,000	0.0016	0.5
00209	CAHORA BASSA	Mozambique	171	52,000,000,000	0.00051	0.5
01125	XIAOLANGDI	China	160	12,650,000,000	0.00133	0.5
01677	RED ROCK	USA	34	2,004,367,996	0.00123	0.5
01857	CONTRA	Switzerland	220	105,000,000	0.02967	0.5

4.1.6 Outflow relationship

Taking into account the parameters involved in the calculation of the outflow discharge (To determine the outflow over the spillway, it was assumed for simplicity that all dams have an ogee spillway (the most widely used), and unconstrained flow, meaning that it was considered that gated spillways are raised during the design flood. Equation 16 describes the discharge over the weir.

Equation 16), the first parameter estimated was the spillway width for the synthetic design. Using the available data (spillway discharge capacity, spillway width and dam length) of 1000 dams from the US Dam Inventory (see section 3.6), correlation factors were calculated between the physical characteristics of the dams. Table 4.1-2 presents the results, where Q is the spillway discharge capacity, b is the width of the spillway, H_{dam} is the height of the dam and B is the coronation width of the dam:

Table 4.1-2 Correlation factors

Parameters	Correlation
Q and b	0.63
Q and H_{dam}	0.20
B and b	0.60

Figure 4.1-8 and Figure 4.1-7 present the relation between the parameters which were chosen to make the multivariable regression. It is observed that the relationship between the spillway width, spillway discharge capacity and dam length present a similar behaviour which was expected according to the correlation factors.

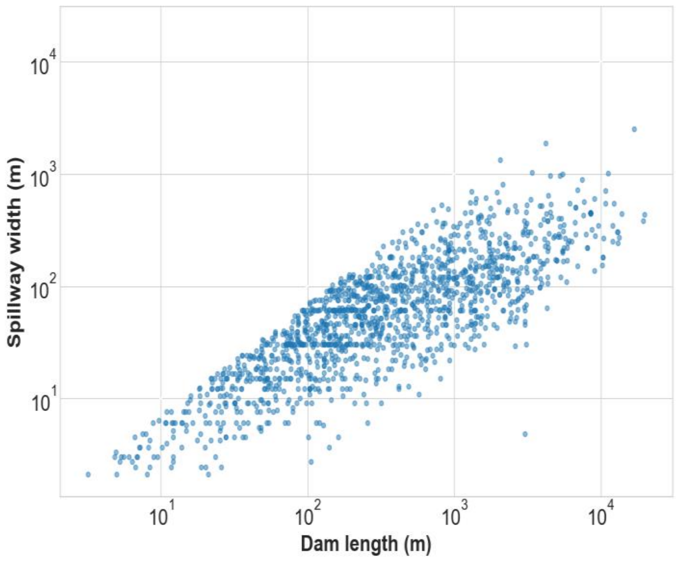

Figure 4.1-8 Dam length and spillway width relationship

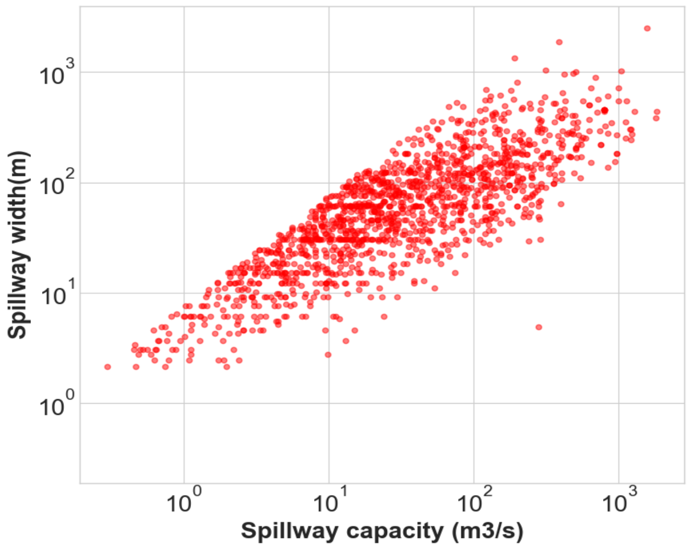

Figure 4.1-7 Spillway capacity and spillway width relationship

The correlation factors allowed to identify how the parameters might determinate the spillway width. As the correlation between Q and b and B and b were the greatest values, a multivariable linear regression was calculated with the flow discharges of the spillway and the length of the dam to calculate the width of the spillway.

Equation 23 is the result from the multivariate linear regression, where B is the length of the dam, Q the spillway discharge capacity and b the width of the spillway. The multivariate regression has a value of 0.33 for R-squared.

Equation 23

$$b = 24.54 - 0.00145B + 0.032188Q$$

$$R^2 = 0.33$$

Figure 4.1-9 shows the results for the spillway width using Equation 23 and the original values of the 1000 dams from US Dam Inventory. The results of the multivariate linear regression presented a trend to overestimate the spillway width compared with the original value. Then, the values of the spillway width used for the synthetic design might be bigger than the real design of the selected dams.

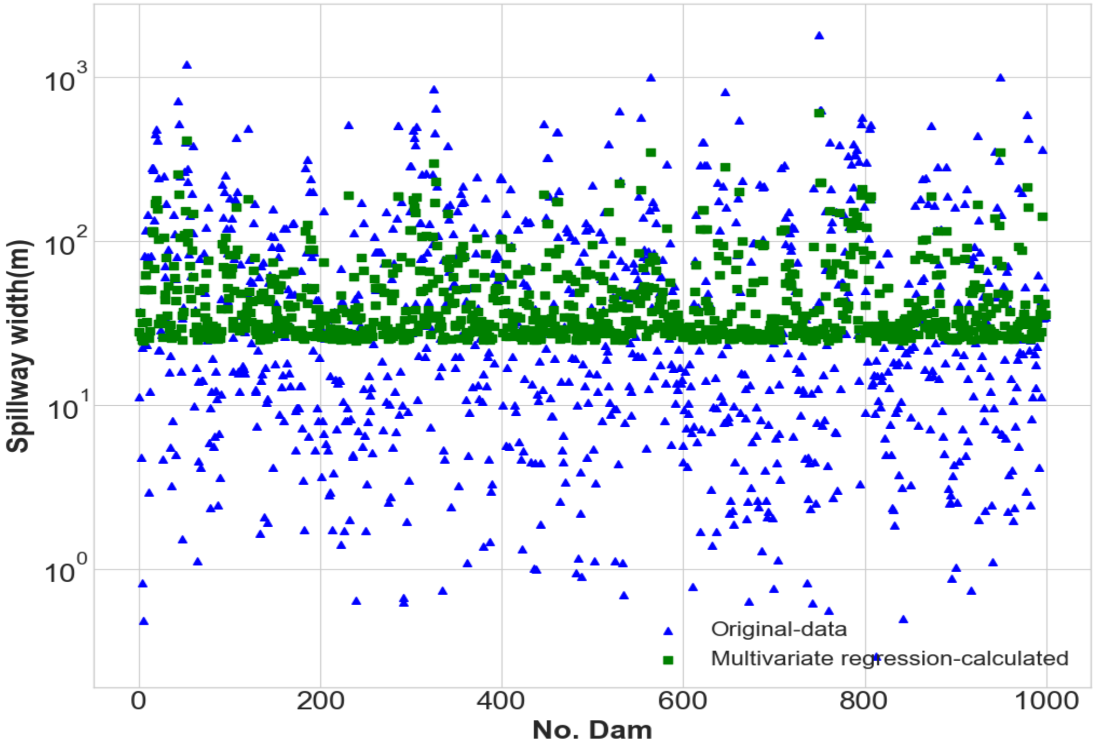

Figure 4.1-9 Estimation spillway width multivariable regression

Obtaining the spillway width for the selected dams, the initial assumption of the height over the crest (H_{d*}) was calculated using the real spillway discharge capacity and To determine the outflow over the spillway, it was assumed for simplicity that all dams have an ogee spillway (the most widely used), and unconstrained flow, meaning that it was considered that gated spillways are raised during the design flood. Equation 16 describes the discharge over the weir.

Equation 16. Besides, the estimation of the crest height of the dams (H_{crest}*) was calculated based on H_d* and the freeboard (see section 3.7.1). An example of the initial assumptions for height over the crest and crest height is presented in Table 4.1-3.

Table 4.1-3 Initial assumptions of height over the crest and crest height

ID	Name	Real Spillway capacity (m3/s)	Height dam (m)	Height over the crest H_{d*} (m)	Crest height H_{crest}*(m)	FB (m)
00002	MANAPOURI LAKE CONTROL	1,500	15	3.8	9.5	1.75
00174	ITAIPU	62,200	196	6.1	187.4	2.5
00209	CAHORA BASSA	13,400	171	7.9	157.6	5.5
01125	XIAOLANGDI	17,000	160	5.9	151.6	2.5
01677	RED ROCK	10,704	34	5.8	26.4	1.75
01857	CONTRA	2,154	220	5.0	214	1.0

4.1.7 Spillway design discharge

With the inflow hydrographs and the physical characteristics of the dam, the flood routing was carried out for different return period flood. Figure 4.1-10 presents the results of the flood routing for six dams for the PMF, similar results were obtained for dams in the analysis. The intersection point between the inflow and outflow represent the spillway design discharge for every analysed dam. Additionally, based on the estimated spillway discharge capacity established with the flood routing approach, height over the crest (H_d) corresponding to the maximum discharge of the outflow curve is extracted.

The design of the spillway discharge was observed to depend on several variables that could influence the response of the dams to a flood event as reservoir capacity and spillway width. Reservoir capacity has a significant impact on attenuation of the peak flood event, it has been observed that larger reservoirs (e.g. Cahora Bassa dam) have a greater capacity to attenuate the flood than smaller reservoir as Contra dam. Spillway width can influence a similar response, larger length of the spillway increases the capacity. Manapouri dam presents a large attenuation of the flood although its reservoir is not large, but the width of the spillway is approximately one third part of the crest length.

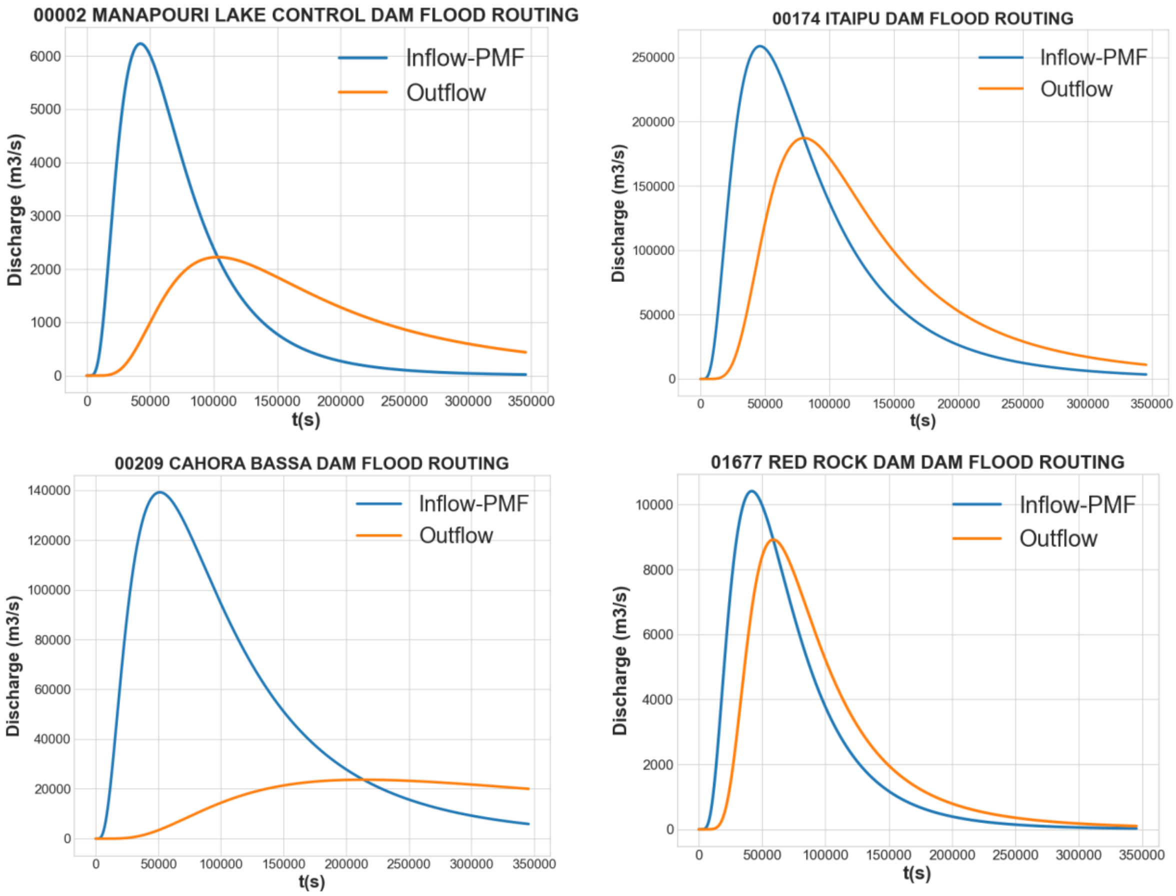

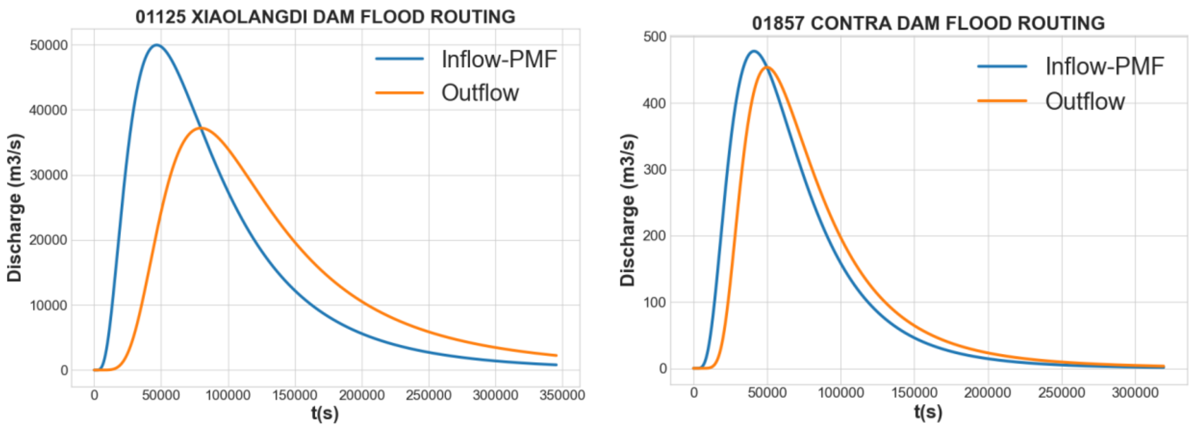

Figure 4.1-10 Flood routing-PMF inflow

4.2 Synthetic spillway design

The first set of hydrological data implemented in this study was the re-analysis data which is available from 1980 to 2015. The spillway discharges calculated with these data were compared with the real discharge capacity that is reported in the dam databases (ICOLD, US inventory of dams).

The synthetic spillway design consists in two parts: estimation of H_{crest} and H_d and calculation of the spillway discharge capacity. In order to compute the values for the synthetic design, approximately four flood routing iterations were made for each dam to determinate the values for H_{crest} and H_d, as to ensure that the values satisfied the given criteria (see section 3.7.1).

As the return period used to design the dams is not known, the synthetic design computed the spillway discharge capacity and height over the crest for 500, 1000, 10,000 year return period flood and PMF for all dams. The height of the crest and the head over the weir which are estimated by the synthetic design (H_{crest_syn}, H_{d_syn}), are the values taken into account for estimating the flood routing in each scenario. Table 4.2-1 illustrate a glimpse into the synthetic design results.

Table 4.2-1 Synthetic design results

ID	**Dam Name**	**H_{crest_syn} (m)**	**Qd 500**	**Hd 500**	**Qd 1,000**	**Hd 1,000**	**Qd 10,000**	**Hd 10,000**	**Qd PMF**	**Hd PMF**
00002	MANAPOURI LAKE CONTROL	12.2	85.0	0.96	90.9	0.97	110.5	0.99	298.8	1.07
00174	ITAIPU	192.3	19,080	1.10	20,568	1,15	26,075	1.20	65,285	1.30
00209	CAHORA BASSA	164.3	4,639	1.0	4,993	1.06	6,366	1.10	18,018	1.16
01125	XIAOLANGDI	156.3	8,219	1.10	8,588	1.10	9,727	1.12	24,332	1,17
01677	RED ROCK	31.1	1,050	1.1	1,106	1.10	1,283	1.10	3,234	1.16
01857	CONTRA	218.0	174.5	0.8	186.8	0.9	227.74	0.92	477.8	1.0

Figure 4.2-1 shows the comparison between synthetic design and real spillway discharge capacity for 10,000 year return period flood and the PMF (the two most common approaches

to establish the design flood). The grey line represents the perfect proportionality between the two variables. The synthetic designs and the real spillway discharge capacity do not present a clear relationship. This may be due to the fact that the hydrological data used to calculate the synthetic design do not correspond to the available data used when the dams were constructed. Additionally, the final decision on the design discharge of the spillway can be subject to other unknown factors

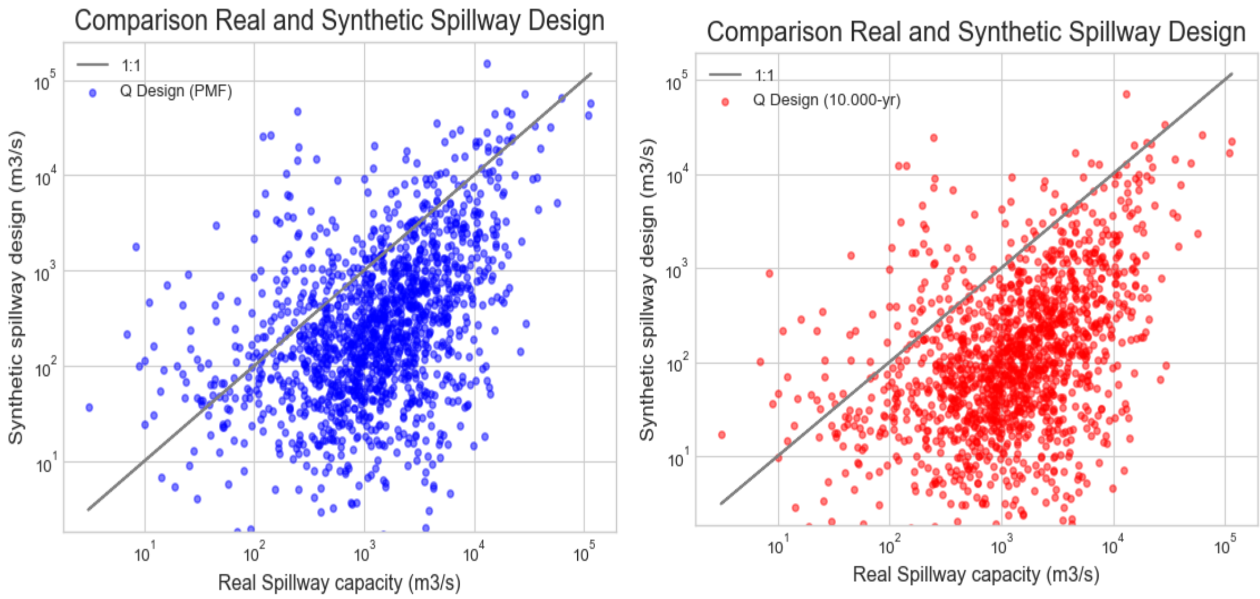

Figure 4.2-1 Comparison between real spillway capacity and synthetic design for PMF and 10.000-yr flood

The results show that the real spillway discharge capacity values is commonly larger than the synthetic design in both cases, the percentage of dams with a smaller synthetic design than the real one (below the grey line) is approximately 80% and 90% (for the PMF and 1:10,000 year return period flood respectively).

Although the data from the re-analysis calculations has the same period of record as the current scenario, the spillway discharge design between the synthetic design and the design for the current scenario presented differences in the five climate models. This can be seen in Figure 4.2-2. The differences in the results are a consequence of the performance of the GHM, due to the data from the re-analysis is based on observed precipitation and temperature data and the data for the current scenario is result of the historical and climate runs of the GHM.

In addition, it has been observed that the results of the five models show a similar trend in relation to the synthetic spillway design. This shows that the results of the five models are consistent and that the five model are suitable for further analysis in the next chapters.

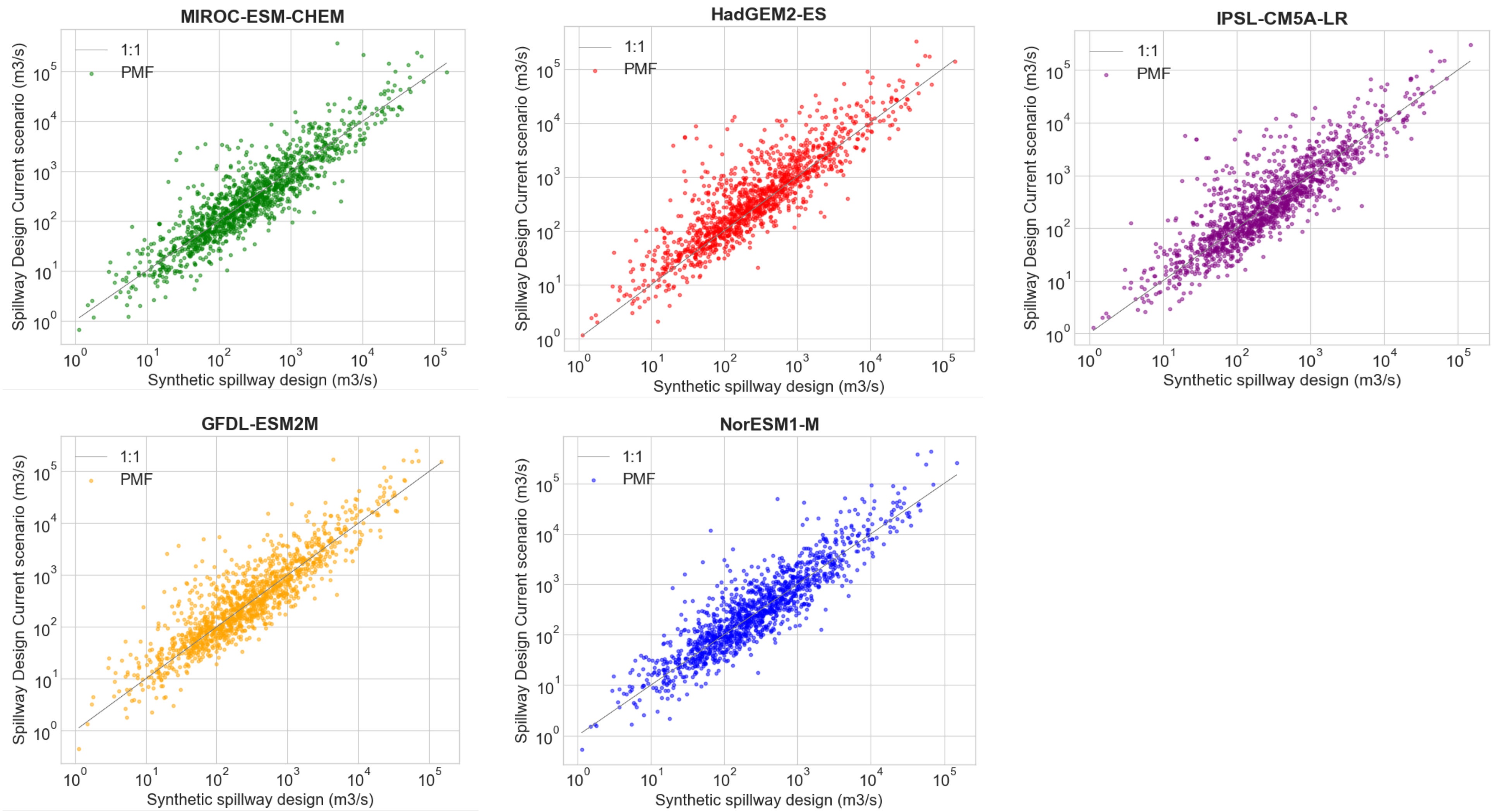

Figure 4.2-2 Comparison synthetic spillway design and spillway design in current scenario

4.3 Influence of climate change on the spillway discharge capacity

As explained four scenarios were developed to establish the spillway design discharge: Historical, Current, RCP4.5 and RCP8.5. Spillway discharge design and height over the crest were computed in every scenario with different hydrological time series that represent past, present and future conditions.

The aim of the computation of these values in every scenario is to give the tools to analyse how the spillway discharge capacity changes under different hydrological conditions. The changes in spillway discharge design are compared between scenarios (e.g. current vs RCP4.5 and current vs RCP8.5). These variations represent the likelihood of an increase in the failure of dam due to climate change. For example, if a dam presents a higher design discharge in the RCP4.5 scenario than in current scenario, this leads to analyse a likely dam overtopping for the mid-century.

On the other hand, the height over the crest from each scenario was compared with the value of the synthetic design due to the values that are compared are based on the physical characteristics of the dam (H_{crest} and FB). These physical values were calculated from the synthetic design (see section 4.2).

4.3.1 Change between historical and current scenario

Given that the time series used for the historical scenario are from 1955 to 2005 and the data for the current scenario is from 1980 to 2015, there is a significant overlap in the time series. It can be expected that the design spillway discharge capacity for both cases is similar.

Figure 4.3-1 and Figure 4.3-2 present the comparison between the results for the historical and current spillway design for two climate models, for a 500-years flood and PMF. For the five climate models, it is observed that the values show a linear relationship. However, some values presented an increase or decrease of more than 50% of the spillway discharge design found in the current scenario. These variations can be explained due to the short period of record (36 years) from which flood peaks are sampled. This may mean selected flood events may be present in the years that only belong to the current or to the historical time series, thus influencing the extrapolation of the data to estimate the flood peak and thus impacting the estimation of $Q_{d.}$

Additionally, the spillway discharges for 500-years flood show a better linear relationship than the results for PMF, this is due to the extrapolation that is made to calculate the peak discharge. The extrapolation for 500-year flood is less uncertain than for 10,000-year flood. This uncertainty is linking with the short period of record, as well.

.

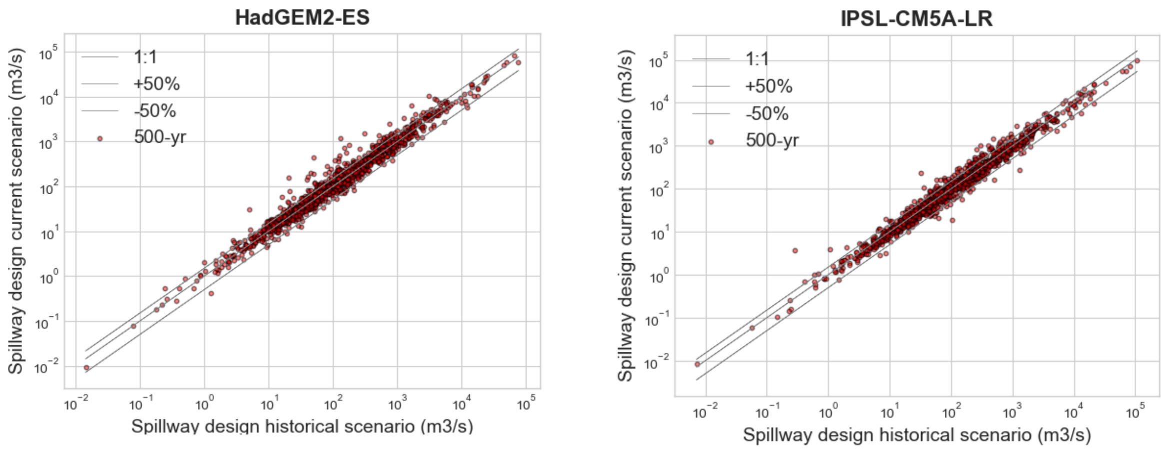

Figure 4.3-1 Comparison historical and current scenario (500-yr flood)

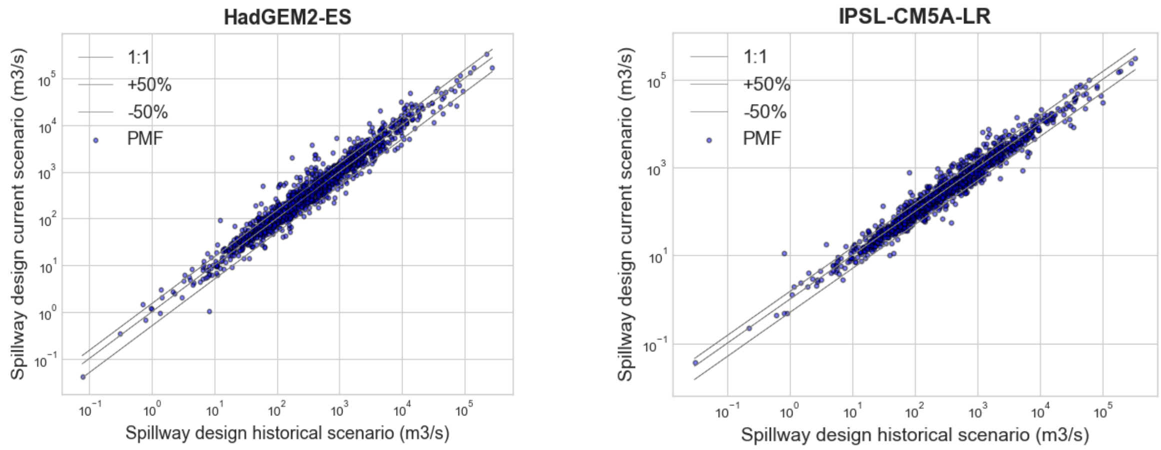

Figure 4.3-2 Comparison historical and current scenario (PMF)

.

Figure 4.3-3 presents the difference in spillway discharge between the historical and current scenarios, where red dots represent increase and blue dots show decrease of spillway discharge. Most of the dams present a decrease or no change in spillway discharge, especially dams in Australia, India and Central North America. However, dams that show an increase in the spillway dicharge may be at risk of failure due to the changes of hydrological condition in the last years (1980-2015).

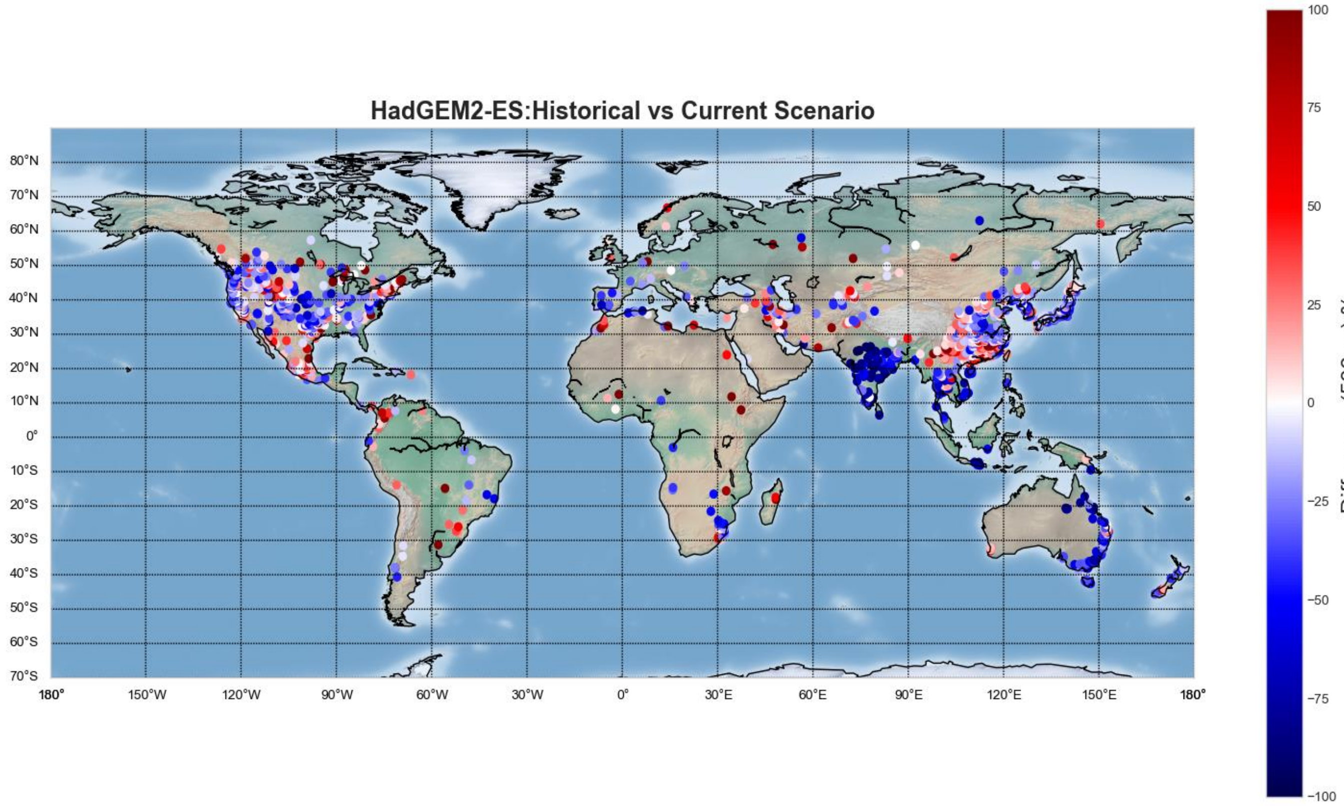

Figure 4.3-3 Difference Qd between historical and current scenario (500-yr)

4.3.2 Changes between current and RCP4.5 and RCP8.5 scenario

Following the same procedure, the spillway discharge design was estimated with the flood routing scheme and the time series from the climate runs forced with RCP4.5 and RCP8.5 (2015-2050). The difference between the discharge design for the current scenario and the discharge design for the future climate runs, due to the projected influence of climate change on the variability in the upcoming years.

Figure 4.3-4 presents the distribution and median value of the difference in spillway discharge capacity (percentage) between the current scenario and RCP4.5 and RCP8.5 for the five models, comparing the designs for a flood of 500-yr. The differences between the current and RCP4.5 scenario show a similar distribution in the five models, GFDL-ESM2M model has the highest median value, while NorESM1-M model have a median value below zero. This means, that GFDL-ESM2M model is the scenario where there are more dams which have increased of spillway discharge.

On the other hand, the results of the five models follow the same trend, higher median values for the comparison between current and RCP8.5 than for comparison between current and RCP4.5, and in general the differences are also higher. The differences between current and RCP8.5 scenario show that the projected hydrological conditions for this future scenario would have a greater impact on the spillway discharge design.

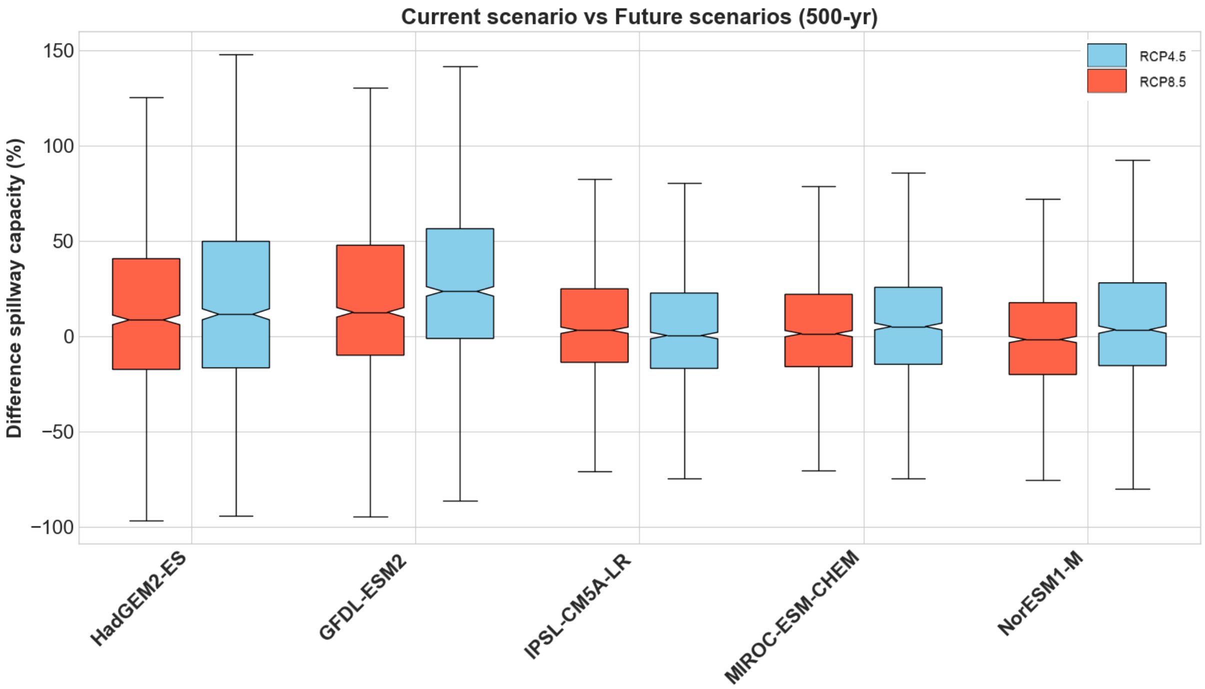

Figure 4.3-4 Difference current scenario vs RCP4.5 and RCP8.5

4.3.3 Geographical analysis of changes between current and RCP4.5 and RCP8.5 scenario

A geographical analysis was made of the results from these scenarios, Figure 4.3-5 and Figure 4.3-6 show the global representation of the change in the design capacity of the spillway between the current scenario and the climate run forced with RCP4.5 and RCP8.5 for the HadGEM2-ES model. These two maps present the trends where the necessary spillway discharge design will increase, decrease or continue equal for the period 2015-2050.

The results are to some extent consistent with the results presented in different research about expected floods in the next century as the research presented by Sperna et al., (2012), which was developed using the same GHM was used in this research. This study shows that some regions are expected to become wetter for the period 2080-2100: such as East and Southeast Asia, Northern Europe, Western Africa, Eastern North America and Northwester South America.

Although, the dams which present a higher increase of the spillway discharge design are located in the zones where it is expected to be wetter in the next years under climate change effects, the dams located in Southern Africa and South Asia (zones expected to be drier) also show an increase of the computed spillway discharge capacity. This would be due the uncertainty of the outputs of the GCMs implemented.

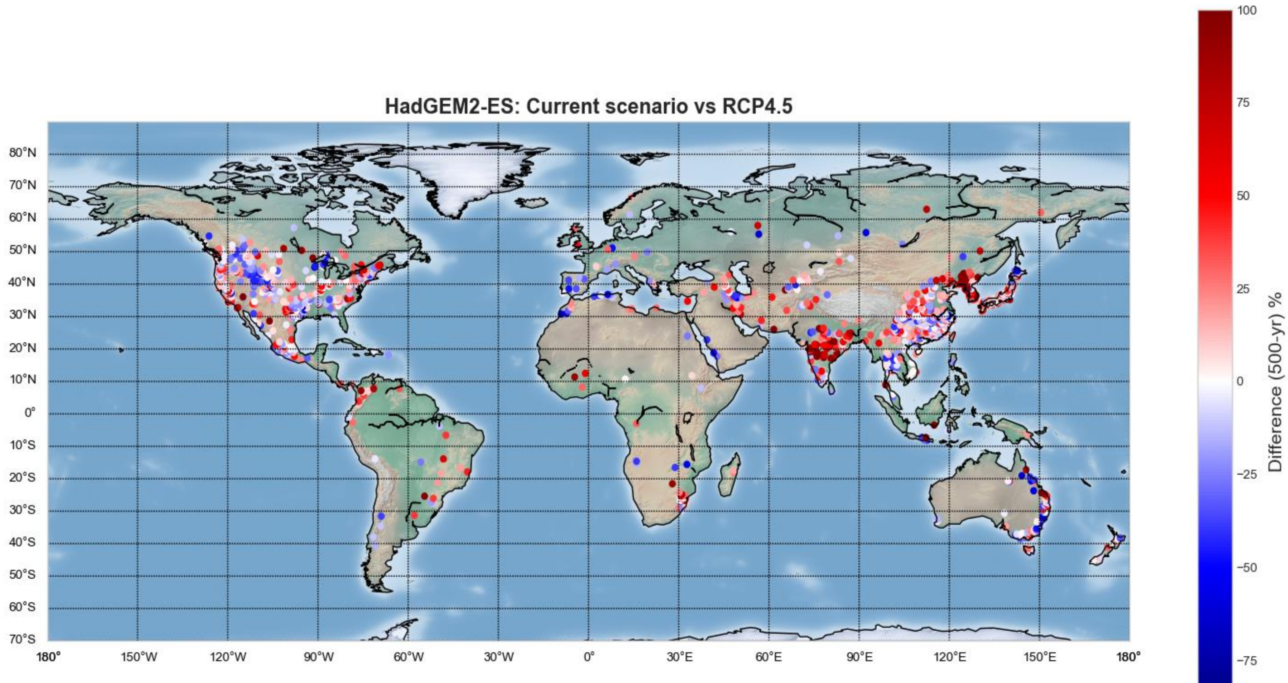

Figure 4.3-5 HadGEM2-ES: Difference Qd between current scenario and RCP4.5 (500-yr)

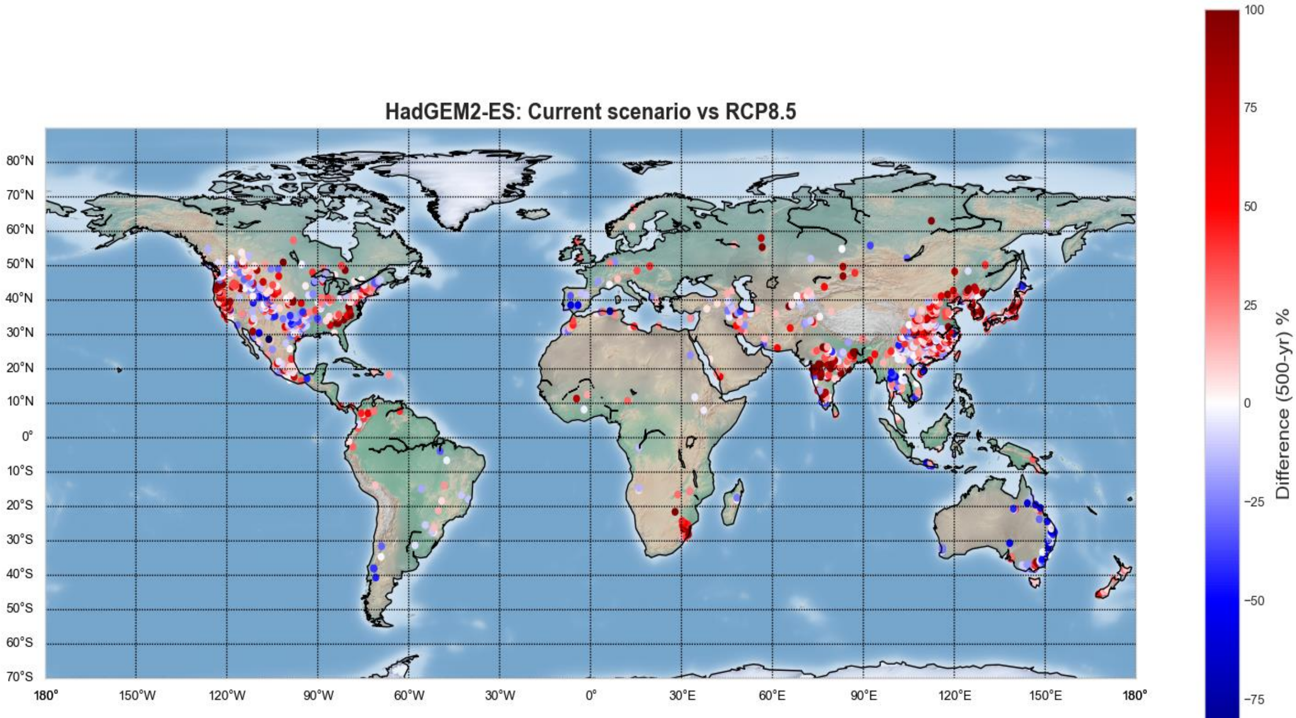

Figure 4.3-6 HadGEM2-ES: Difference Qd between current scenario and RCP8.5 (500-yr)

To understand the effects of climate in the variation of the necessary spillway discharge capacity to face the effects of climate change, it was divided the location of the dams using the global climate regions proposed by (Giorgi & Francisco, 2000). Table 4.3-1 shows the names and acronyms of the global climate regions used. Figure 4.3-7 shows the climate region of each dam used in this study and the number of dams belonging to each region.

Table 4.3-1 Global climate regions (Giorgi & Francisco, 2000)

Name	Acronym	Latitude	Longitude	No. Dams
Australia	AUS	45–11◦ S	110–180◦ E	103
Amazon Basin	AMZ	20◦ S–12◦ N	82–34◦ W	20
Southern South America	SSA	56–20◦ S	76–40◦ W	11
Central America	CAM	10–30◦ N	116–83◦ W	43
Western North America	WNA	30–60◦ N	130–103◦ W	184
Central North America	CAN	30–50◦ N	103–85◦ W	101
Eastern North America	ENA	25–50◦ N	85–60◦ W	66
Mediterranean Basin	MED	30–48◦ N	10◦ W–40◦ E	32
North Europe	NEU	48–75◦ N	10◦ W–40◦ E	8
Western Africa	WAF	12◦ S–18◦ N	20◦ W–22◦ E	5
East Africa	EAF	12◦ S–18◦ N	22–52◦ E	4
Southern Africa	SAF	35–12◦ S	10◦ W–52◦ E	29
Southeast Asia	SEA	11◦ S–20◦ N	95–155◦ E	52
Est Asia	EAS	20–50◦ N	100–145◦ E	488
South Asia	SAS	5–30◦ N	65–100◦ E	97
Central Asia	CAS	30–50◦ N	40–75◦ E	42
Tibet	TIB	30–50◦ N	75–100◦ E	6
North Asia	NAS	50–70◦ N	40–180◦ E	10

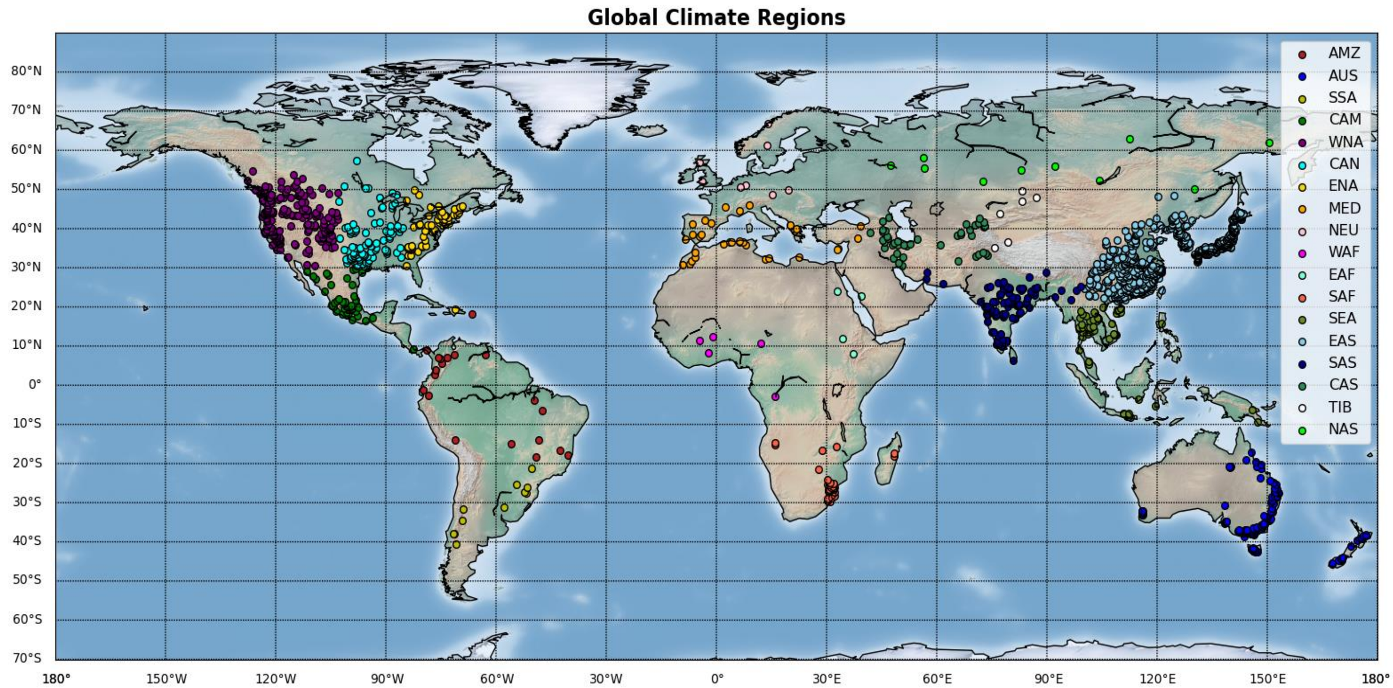

Figure 4.3-7 Global climate regions-Dam location. (See Table 4.3-1 for regions notation).

Figure 4.3-8 shows the histograms of the difference of spillway discharge capacity between current scenario; and RCP4.5 and RCP8.5 divided in climate regions. As there are several climate regions where there are only few dams selected in this research, the results were grouped in nine regions as it is shown in the legend of the histograms.

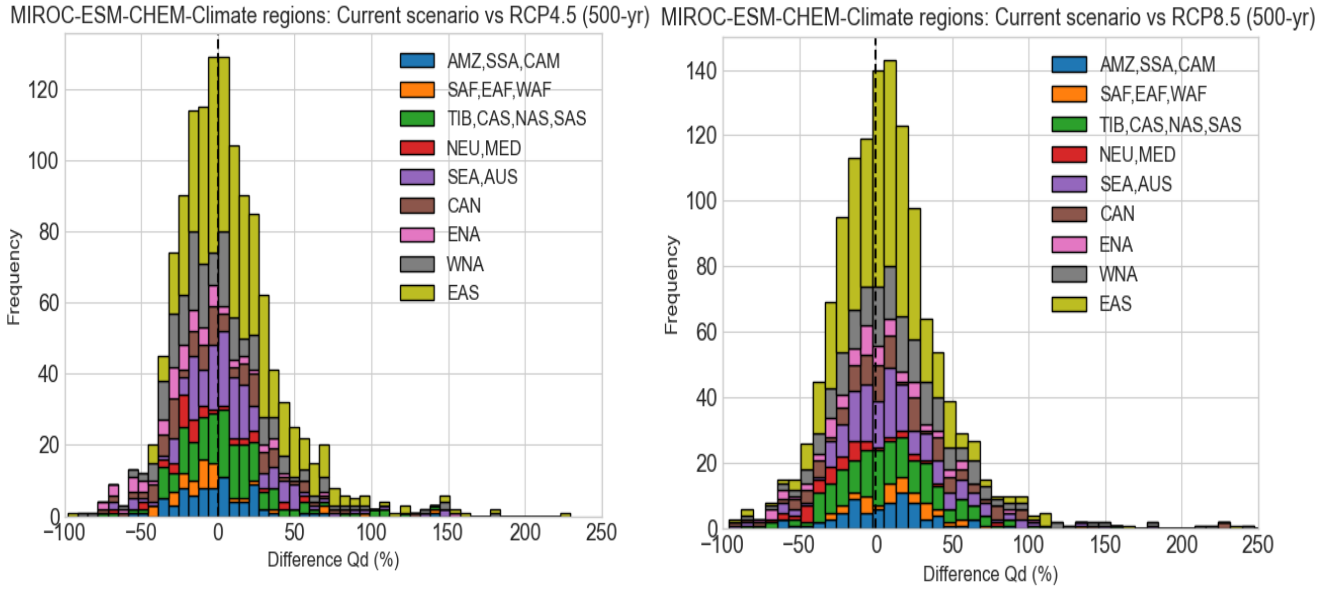

Figure 4.3-8 Histograms difference Qd between current, RCP4.5and RCP8.5 scenario (See Table 4.3-1 for regions notation)

The histograms show how the dams in every climate region tend to lean to a negative or positive change in the spillway design discharge, this change is directly associated with the expected change in climate. Because of this, the hydrograph that represents the changes for the RCP8.5 scenario tends to be skewed towards the positive side, due to most of the selected dams are located in the zones where are expected to be wetter (EAS and ENA).

To give a better understanding of the behaviour of the change of the necessary spillway discharge capacity, Figure 4.3-9 shows box-whiskers plots of the difference between current and RCP4.5 and RCP8.5 scenario for MIROC-ESM-CHEM model, where it is possible to observe the distribution of the values per every climate region.

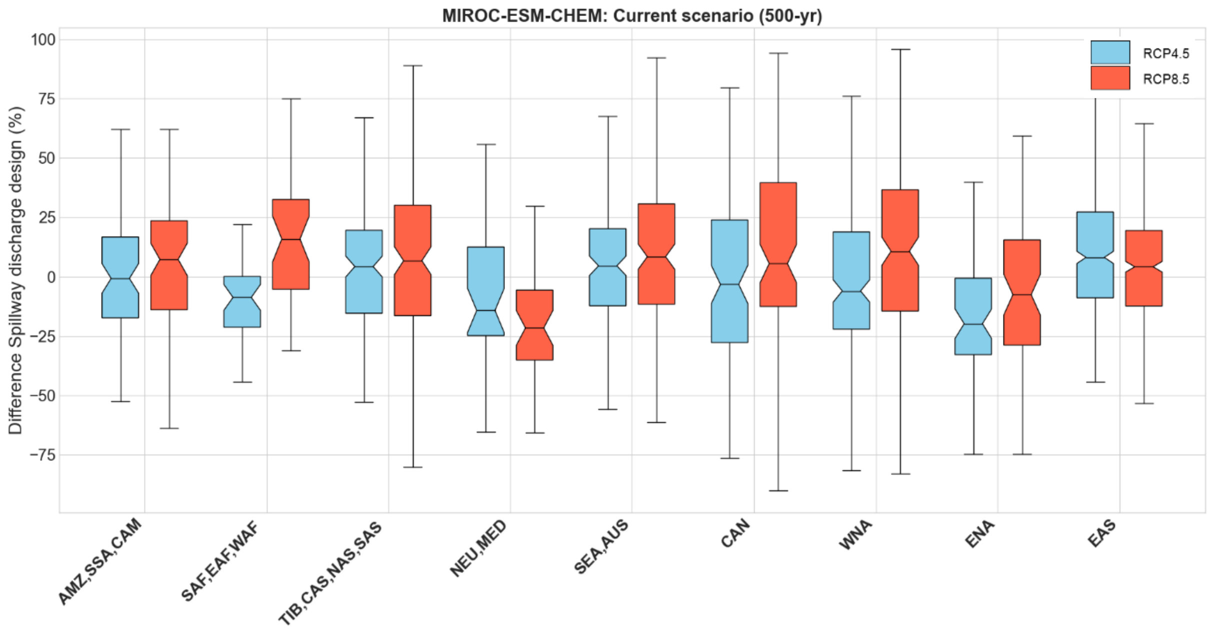

Figure 4.3-9 Distribution difference spillway discharge design by climate regions between current and RCP4.5 and RCP8.5 scenario (MIROC-ESM-CHEM model-500-yr)

The results show that EAS, SEA-AUS and TIB-CAS-NAS-SAS regions tend to be skewed towards the positive values for the RCP4.5 runs, as their median values are greater than zero and 25% of their values present a difference greater than 20%. On the other hand, the dams located in Africa (SAF, EAF, and WAF) and ENA regions tend to be skewed towards the negative values. For approximately 75% of the dams the difference of spillway discharge capacity is smaller than zero. The CAN, WNA and AMZ-SSA-CAM regions have a uniform distribution where approximately 50% of the values are greater than zero and 50% smaller than zero.

For the RCP8.5 scenario, it was found that NEU-MED and ENA are the regions that present reduction in the spillway design discharge (median value smaller than zero), 50% of the dams in the NRE-MED regions present a reduction between the 10% and 25%. On the other hand, the other seven regions present an increase in necessary spillway discharge capacity. As the RCP8.5 scenario represents the expected climate under extreme high emissions, the increase in the spillway discharge is greater than the estimated in the RCP4.5 scenario. Appendix A presents the box-whiskers plots for the other four models, where it is observed the consistency of the GCMs.

Table 4.3-2 contains the ranges of changes between current scenario and RCP4.5 and RCP8.5 for the interquartile range (IQR) (range between the 25% and 75% of data) of the sample according by climate region and model. A median range was estimated for the difference for RCP4.5 and RCP8.5 scenario.

The ranges are consistent for the five models, where the upper boundary of the range tends to increase for RCP8.5, while the lower boundary is roughly the same value for RCP4.5 and RCP8.5 for all climate regions where is expected to be wetter.

Table 4.3-2 Range of difference of spillway discharge design (%) for IQR

	IPSL-CM5A-LR		MIROC-ESM-CHEM		HadGEM2-ES		GFDL-ESM2M		NorESM1-M		Median Range	
Climate Region	**RCP4.5**	**RCP8.5**	**RCP4.5**	**RCP8.5**	**RCP4.5**	**RCP8.5**	**RCP4.5**	**RCP8.5**	**RCP4.5**	**RCP8.5**	**RCP4.5**	**RCP8.5**
AMZ-SSA-CAM	(-31%, 16%)	(-32%, 11%)	(-17%, 17%)	(-14%, 24%)	(-12%, 26%)	(-11%, 20%)	(-22%, 26%)	(-13%, 35%)	(-32%, 19%)	(-29%, 19%)	**(-22%, 19%)**	**(-14%, 20%)**
SAF-EAF-WAF	(1%, 27%)	(-12%, 26%)	(-21%, 1%)	(-5%, 32%)	(-11%, 31%)	(-2%, 78%)	(13%, 149%)	(12, 138%)	(-22%, 1%)	(-1%, 39%)	**(-11%, 27%)**	**(-2%, 39%)**
TIB-CAS-NAS-SAS	(-22%, 35%)	(-16%, 27%)	(-15%, 20%)	(-16%, 30%)	(-2%, 60%)	(-6%, 59%)	(-10%, 50%)	(22%, 136%)	(-20%, 25%)	(-13%, 5%)	**(-15%, 35%)**	**(-13%, 30%)**
NEU-MED	(-27%, 9%)	(-24%, 16)	(-25%, 12%)	(-35%, 6%)	(-32%, 18%)	(-20%, 25%)	(-24%, 14%)	(-25%, 9%)	(-23%, 2%)	(-15%, 32%)	**(-25%, 12%)**	**(-24%, 9%)**
SEA-AUS	(-4%, 45)	(-19%, 23%)	(-12%, 20%)	(-12%, 31%)	(-21%, 16%)	(-31%, 13%)	(-27%, 17%)	(-23%, 30%)	(-14%, 24%)	(-15%, 32%)	**(-14%, 20%)**	**(-19%, 30%)**
CAN	(-10%, 36%)	(-1%, 44%)	(-28%, 24%)	(-12%, 40%)	(-14%, 24%)	(-18%, 24%)	(-12%, 22%)	(-6%, 41%)	(-18%, 14%)	(-26%, 4%)	**(-14%, 24%)**	**(-12%, 40%)**
ENA	(-12%, 39%)	(-5%, 26%)	(-33%, 1%)	(-29%, 15%)	(-8%, 30%)	(-6%, 46%)	(-22%, 18%)	(-6%, 41%)	(-7%, 27%)	(-3%, 56%)	**(-12%, 27%)**	**(-6%, 41%)**
WNA	(-19%, 19%)	(-27%, 8%)	(-22%, 19%)	(-14%, 37%)	(-20%, 18%)	(-11%-42%)	(-9%, 57%)	(-4%, 49%)	(-28%, 10%)	(-11%, 31%)	**(-20%, 19%)**	**(-11%, 37%)**
EAS	(-10%, 18%)	(-19%, 19%)	(-9%, 28%)	(-12%, 19%)	(-7%, -30%)	(0%, 42%)	(1%, 61%)	(10%, 55%)	(-15%, 17%)	(-13%, 25%)	**(-9%, 28%)**	**(-12%, 25%)**

4.4 Dam overtopping

Given the synthetic design as reference, an assessment can be made of the risk of dam failure due to overtopping. This is achieved, by comparing the height over the crest (H_d) resulting from the design discharge for every scenario with the values of H_{d_syn} and freeboard from the synthetic design. A dam is considered to fail due to overtopping when the maximum level in the reservoir is larger than H_d plus freeboard.

As the spillway discharge design was estimated for 500, 1000, 10,000 years flood and PMF in all scenarios, it was evaluated whether a dam designed with a specific return period will be safe for the same return period under the future hydrological conditions. Then, the synthetic design for each return period was compared with the same designs in current, RCP4.5 and RCP8.5 scenario.

Table 4.4-1 presents the number of dams that presented overtopping for current, RCP4.5 and RCP8.5 scenario compared with the synthetic design. Figure 4.4-1 show how the percentage of dams failing changes for both future scenarios for climate models. The RCP8.5 scenario clearly shows a higher number of dams failing for all five models. This was expected due to this scenario presented the highest differences of spillway discharge capacity as well (see section 4.3.2).

On the other hand, the current scenario presents a median value of 3.8% of dams failing in case of a PMF event happens now. Since the time series used for estimating the spillway design for current scenario and synthetic design share the same recorded years, these results may be due to the bias between the time series from the model and time series from the re-analysis.

Table 4.4-1 Number of dams failing due to overtopping

Model	**Current**				**RCP4.5**				**RCP8.5**			
	500-yr	**1000-yr**	**1.000-yr**	**PMF**	**500-yr**	**1000-yr**	**10000-yr**	**PMF**	**500-yr**	**1000-yr**	**10000-yr**	**PMF**
NorESM1-M	7	9	16	50	7	10	12	43	6	9	13	45
IPSL-CM5A-LR	12	14	23	63	12	15	23	67	9	10	17	57
GFDL-ESM2M	6	7	14	46	9	10	16	55	11	13	18	66
HadGEM2-ES	15	15	23	75	20	21	30	83	18	21	34	88
MIROC-ESM-CHEM	4	5	8	38	2	2	10	37	2	2	4	41
Median Value	**7**	**9**	**16**	**50**	**9**	**10**	**16**	**55**	**9**	**10**	**17**	**57**
Percentage (%)	**0.5**	**0.7**	**1.2**	**3.8**	**0.7**	**0.8**	**1.2**	**4.2**	**0.7**	**0.8**	**1.3**	**4.6**

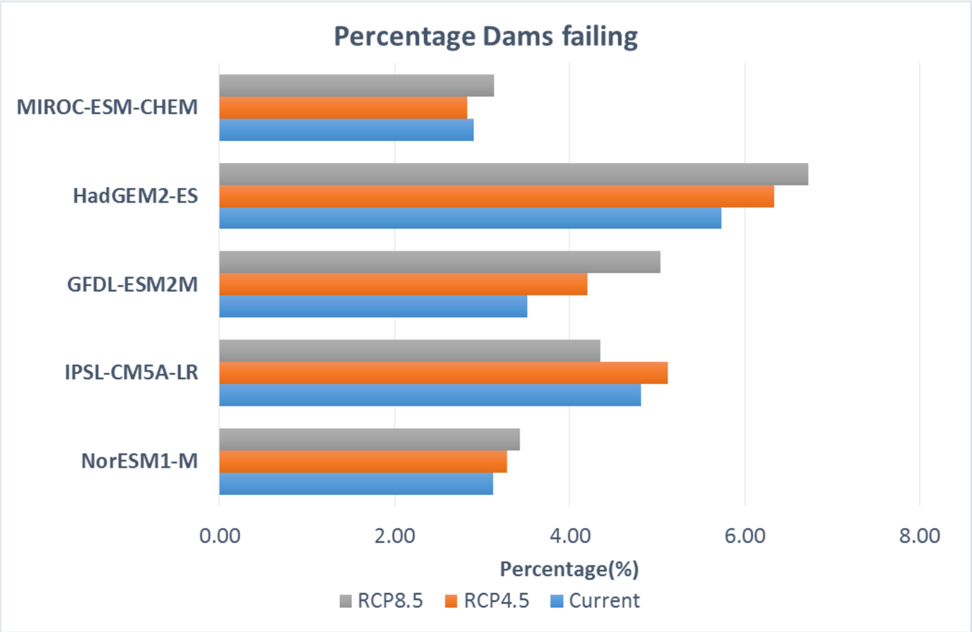

Figure 4.4-1 Percentage dams failing per model (PMF)

Additionally, the results show an increase in the percentage of dams failing due to the effects of climate change. The results suggest that 4.5% of the selected dams would fail due to overtopping in case of the PMF occurs.

Figure 4.4-3and Figure 4.4-2 show the location of the dams failing due to overtopping with the PMF event for the RCP4.5 and RCP8.5 scenario, the red dots represent the dams that fail due to overtopping while the blue dots show the dams that can safely pass the PMF. The zones with a higher concentration of failing dams correspond to the zones with a higher difference of spillway discharge design (EAS, SAS and CNA). However, it is important to highlight that it is in these zones that are the majority of dams used in this research are located.

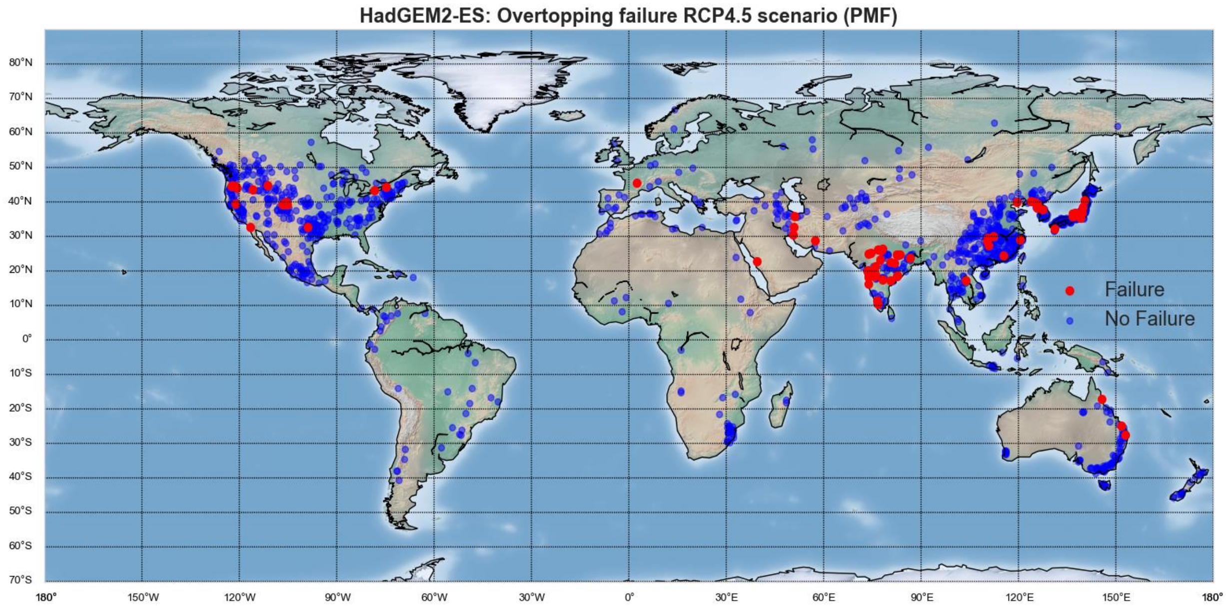

Figure 4.4-3 Dams failing due to overtopping RCP4.5 scenario

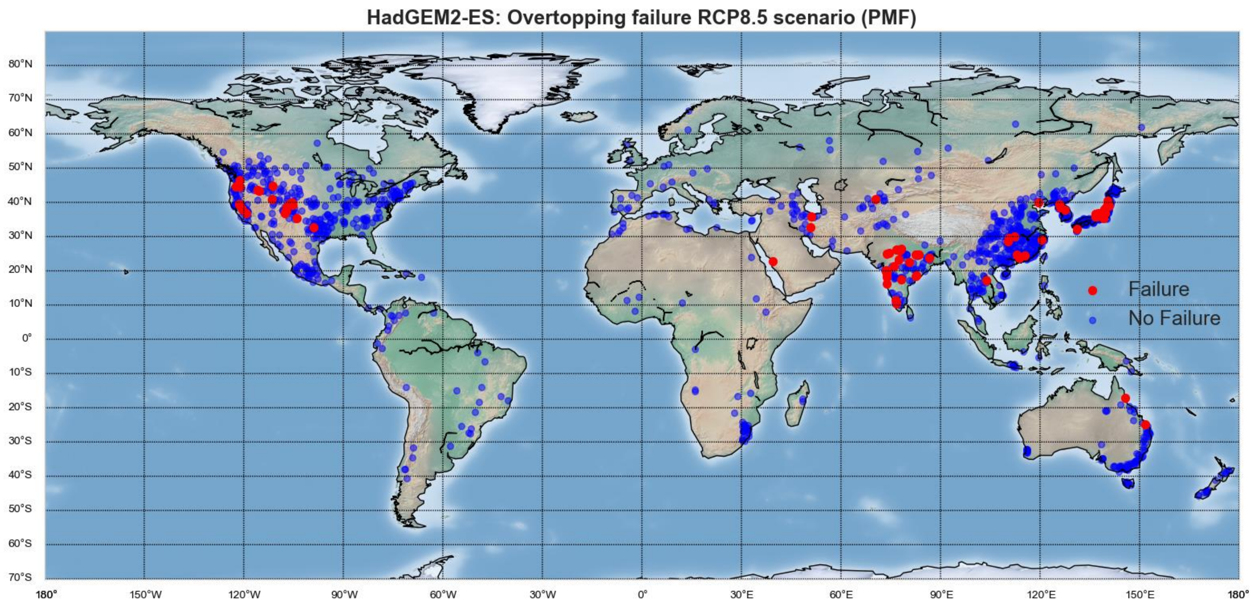

Figure 4.4-2 Dams failing due to overtopping RCP8.5 scenario

To understand the criteria that affects dam overtopping in addition to the climate change, it was analysed the type of dam. For this research, the dams were classified into two groups: concrete dam and embankment dam. For the selected dams 30% are concrete dams and 70% are embankment dams. Figure 4.4-4 shows the type of each dam used in this study, where red dots are embankments dams and yellow dots, concrete dams.

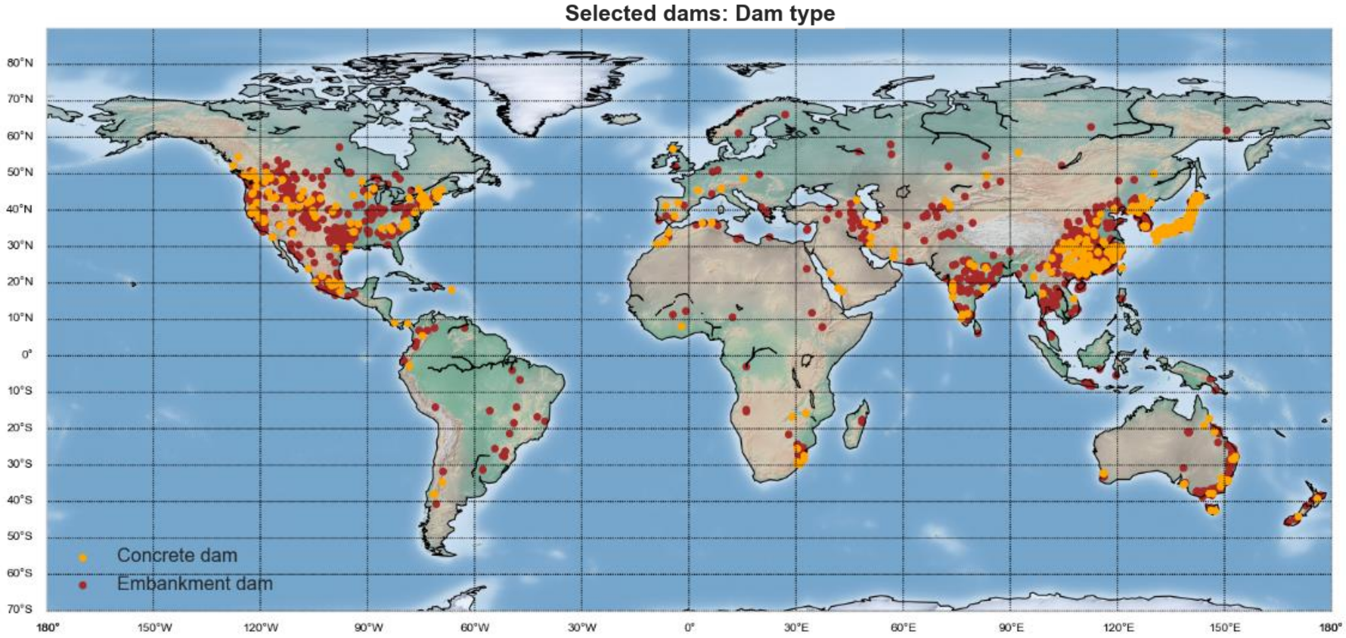

Figure 4.4-4 Dam type classification

Figure 4.4-5 shows the percentage of concrete and embankment dams that fail in comparison with the total number of dams of each type. The most of the dams that fail are concrete dams for both scenarios (RCP4.5 and RCP8.5).The reason why concrete dams have a higher risk to present overtopping than embankment dams is the reduced freeboard. Usually, the freeboard is smaller in concrete dams than in embankment dams, this is because embankment dams are constructed with erodible material and need more protection than concrete.

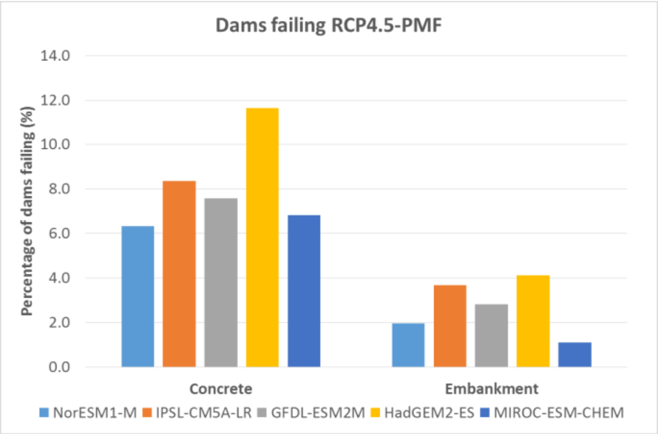

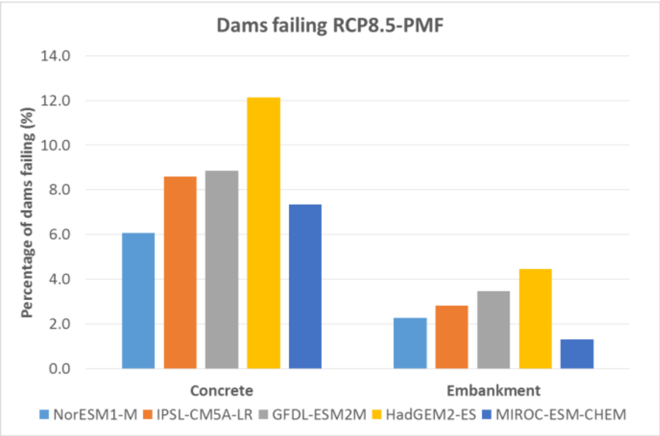

Figure 4.4-5Type of dams failing

Chapter 5 Discussion

Although several studies have been tackled climate change and its impacts on different economic and social sectors, scarce research is available about consequences of climate change on dam safety. This research has faced this problem by analysing how the necessary spillway discharge capacity can change as a result of climate change on a global scale and whether such change could cause dam overtopping. Based on five GCMs and a re-analysis data set, four scenarios were computed analysing roughly 1300 dams around the world. The first part of the study was focused on constructing a flood routing scheme suitable for all dams to estimate the spillway discharge design. The second part was focused on the analysis and comparison of the different results from every scenario. Table 4.4-2 presents some upstanding findings from the comparison of the results between scenarios.

Table 4.4-2 Results comparison between scenarios

Reference scenario	Spillway discharge capacity	Comments
Real spillway discharge capacity	Synthetic design (1980-2015)	Real spillway discharge capacity values are commonly larger than the synthetic design in both cases. There is not a clear relationship, then the synthetic design was chosen as reference.
Synthetic design (1980-2015)	Current climate scenario (1980-2015)	The differences in the results are a consequence of the performance of the GHM due to the fact that both time series share the same period of record.
Historical scenario (1955-2005)	Current climate scenario (1980-2015)	The values show a linear relationship, as there is significant overlap in the time series. Observed differences may be due to selected flood events present in the years that only belong to the current or to the historical time series.
Current climate scenario (1980-2015)	Future RCP4.5 (2015-2050)	Differences are due to the projected influence of climate change. The major increase of the necessary spillway discharge design is observed for RCP8.5.
	Future RCP8.5 (2015-2050)	

5.1 Design flood of the dams using the then-available data

The estimation of the spillway design based on the then-available hydrological data was done in the historical scenario, which takes a period of 36 years before the year of construction of the dam, a historical spillway design was estimated. Taking into account that results for the synthetic design compare with the current scenario presented a similar performance, it is possible to deduce that the historical scenario do not have a relationship with the real data.

It is important to notice the limitations of this research and how may affect the results of the spillway design. The bias of the model and time step (one day) of the hydrological series could affect the selection of floods events and thus the spillway design estimation. For smaller catchments, the time step could produce a large deviation. Also, the time recession time for larger catchment may have been overestimated, and the shape of the hydrograph may be affected. Then in reality flood peaks may be higher

The unknown physical characteristics of the dams, including the spillway width and the relation elevation-storage had to be parametrized. Essentially, the values of these parameters were calculated based on simplified hypotheses and may not be similar to the real values. However, it was possible to find the trends of the changes of spillway design between the results from the scenarios. For the estimation of the peak flood, the discharge data was extrapolated up to 10,000-year flood. Therefore, the short period of record may affect the estimation of the design flood.

Also, estimation of spillway capacity depends on a variety of factors related to physical characteristics, design approaches and available hydrological data. The parametrization of these criteria for the selected dams does not allow to find a relationship between the results from the research with the real data.

However, the mentioned limitations were not a restriction in this study due to the results were compared between scenarios and not with the real data, so there was not propagation of uncertainty.

5.2 Level of safety of the dams using the currently available hydrological data

The comparison between the spillway design of the historical and current scenario, showed that most of the dams have a decrease or not change in the spillway discharge due to climate variability. However, the results of the analysis of dams at risk of overtopping for current climate scenario showed that 3.8% of the selected dams would not survive design conditions.

It is important to highlight that dam overtopping comparison is made in relation to the synthetic design, while the variation of spillway design is done between scenarios. Differences between the synthetic (reference) and current scenario can lead to an increase the number of dams that are at risk of failure.

5.3 Influence climate change on the risk of failure

Climate change has a significant influence on the risk of failure, it was found that under climate change conditions (RCP4.5 and RCP8.5 scenario) several areas over the world present an increase in the spillway discharge design, which are related with the expected raising of precipitation and discharge and the increase of probability of occurrence of flood events (Hirabayashi et al., 2013; Sperna Weiland et al., 2012).

Consistency of climate models was a significant factor in the analysis of these results, although some of the climate models showed lower or higher ranges of variation in the necessary spillway discharge capacity for the future scenario, in general the five models presented the same trend (increase or decrease) for dams in the same region. The results of the GCMs is consistent with the evaluation carried out by Flato et al, 2013, which showed that the signal of the models follow the same trend in relation with the median CMIP5 error.

The areas with the largest increase in spillway discharge capacity due to climate change were East Asia, South Asia, Central North America and Western North America and, in some scenarios, Western South America. It is important to take into account this changes, as there is a high concentration of dams in these areas and their safety might be threatened under current available climate predictions. Although the necessary spillway discharge capacity tends to increase, for both future scenarios that does not directly lead to the failure of the dams, because the freeboard allows discharging over design conditions.

It was possible estimated how much the necessary spillway discharge capacity might increase depending on the climate region where the dam is located. The ranges of change in spillway discharge capacity were estimated in order to measure the possible interventions required by the dams to mitigate climate change impacts.

How climate change impact on the failure of dams was also analysed estimating the percentage of dams that will be prone to overtopping under possible future conditions. This evaluation was carried out base on the comparison of the height over the crest produced by the necessary spillway discharge capacity in RCP4.5 and RCP8.5 scenario, assisted by synthetic dam design which allows overcoming lack of data on each dam. Although, the synthetic design could not be linked with the real spillway discharge capacity, it was a tool to use as a reference in order to observe the changes over periods of time.

The trend of the percentage of dams at risk of overtopping in the future scenarios showed a consistent growth. Therefore, climate change has a major effect on dam safety. The results showed that the percentage of dams failing for RCP4.5 was 4.2% and for RCP8.5 was 4.6% in relation with the total of the selected dams.

5.4 Implications to society

Despite the necessary hypotheses embraced in this research, results provided an overview of the probable future situation that dam stakeholders will face. This work highlights the need to develop better adaptation and mitigation strategies on a global scale to counter the projected increase on dam overtopping risk. In addition, the results may encourage to develop more detail researches of dam safety for individual dams as such Mallakpour et al., 2018 and Fluixá-Sanmartín et al., 2019 presented for dams in California and Spain.

Chapter 6 Conclusion and recommendations

6.1 Conclusion

In this study the impact of climate change on risk of dam failure due to overtopping on a global scale is analysed. Changes in spillway capacity under various climate and hydrological scenarios were used as an approach to assess these impacts. During the development of this research, several observations were made regarding the process to estimate spillway discharge design and assess risk of dam overtopping:

- This study is based on five GCMs and re-analysis data from the merged CRU TS 3.2 and ERA-Interim datasets. The results of the GCMs show a consistent trend is found in the different sections of this study, including the difference in the spillway capacity and percentage of dams failing due to overtopping. These trends are consistent with the evaluation of climate models carried out by Flato et al., 2013. Then, there is confidence in the results of this research.
- Reservoir capacity plays a major role on the capacity of a dam to safely pass a flood event, dams with larger reservoirs showed a higher attenuation of the peak flood than dams with medium and smaller reservoirs.
- Increase of the required spillway capacity for future scenarios (RCP4.5 and RCP8.5) is clearest in specific climate regions such as East Asia, South Asia, Central North America and Western North America. This is consist with the results of the researches which projected increase of run-off for 2100 in the these areas (Hirabayashi et al., 2013; Sperna Weiland et al., 2012), though the larger sample of dams in these regions may introduce a bias.
- The need for an increased design capacity of the spillway due to the projected change in hydrological conditions will not directly lead to an unacceptable risk of dams overtopping as the available freeboard in most dams the allows more water to be discharged than the original design. As the freeboard is typically smaller for concrete dams than for earth-fill dams, most of the dams that have an increased risk of failure due to overtopping are concrete dams. However, despite larger freeboard provided by earth-fill dams meaning the risk of failure may not be unacceptably high, the results do show that the safety factor provided by the freeboard is reduced.
- The percentage of dams at risk of overtopping shows a consistent trend to grow in future scenarios. The percentage of dams failing due to overtopping is higher in RCP8.5 scenario than RCP4.5 scenario, suggesting that significant extreme changes in climate are contributing to a higher risk of dam overtopping. The locations of dams that show an increased risk of failing due to overtopping are consistent with the regions which show larger differences in spillway design.

6.2 Recommendations

6.2.1 Scientific recommendations

Certain improvements can be suggested for future research:

- Review available methods to extract flood events from discharge time series in order to have more accurate time of recession, thereby enhancing the estimation of volume and design peak.
- Make an in-depth analysis of different probability distributions to define the shape of design hydrographs, especially for larger catchments.
- Assess the impacts of climate change for current hydrological scenario by implementing an alternative approach where the period of record of the time series is from the year of construction of the dam until 2015.
- Extend the analysis to include climate projections to extend the analysis to 2100.

6.2.2 Societal recommendation

The consistent trend of increasing spillway capacity required to assure the safety of overtopping in dams for future climate scenarios leads calls for more in-depth analysis for individual dams to be developed, in particular dams located in regions that are also projected to become wetter due to climate change and show higher increase of the spillway capacity (East Asia, South Asia, Central North America and Western North America).

References

Arnell, N. W., & Gosling, S. N. (2014). The impacts of climate change on river flood risk at the global scale. *Climatic change, 134*, 387-401. doi:10.1007/s10584-014-1084-5

Badger, J., & Ejsing Jorgensen, H. (2011). A high resolution global wind atlas-improving estimation of world wind resources. *Energy Systems and Technologies for the coming Century*, 215-225, Roskilde: Danmarks Tekniske Universitet, Risø Nationallaboratoriet for Bæredygtig Energi. Denmark. Forskningscenter Risoe. Risoe-R, No. 1776(EN)

Baecher, G. B. (2004). Uncertainty in dam safety risk analysis. *Georisk: Assessment and Management of Rrisk for engineered Systems and Geohazards, 10,* 1-17. doi:10.1080/17499518.2015.1102293

Beames, P., Lehner, B., & Anand, M. (2019). Global Reservoir and Dam (GRanD) Database. *Technical Documentation, Version 1.3*. Retrieved from Global Dam Watch website: http://globaldamwatch.org/data/#core_global

Bentsen, M., Bethke, I., Debernard, J. B., Iversen, T., Kirkevåg, A., Seland, Ø., . . . Kristjánsson, J. E. (2013). The Norwegian Earth System Model, NorESM1-M – Part 1: Description and basic evaluation of the physical climate. *Geosci. Model Dev, 6,* 687-720. doi:10.5194/gmd-6-687-2013

Brunner, M. I., Seibert, J., & Favre, A. C. (2016). Bivariate return periods and their importance for flood peak and volume estimation. *WIRES water, 3*, 819-833. doi:10.1002/wat2.1173

Brunner, M. I., Viviroli, D., Sikorska, A. E., Vannier, O., Favre, A. C., & Seibert, J. (2017). Flood type specific construction of synthetic design hydrographs. *Water resources research, 53*, 1390-1406. doi:10.1002/2016WR019535

Carbon Brief. (2019). CMIP6: the next generation of climate models explained (Hausfather, Z.) Retrieved from website: https://www.carbonbrief.org/cmip6-the-next-generation-of-climate-models-explained.

Chernet, H. H., Alfredsen, K., & Midttomme, G. H. (2014). Safety of Hydropower Dams in a Changing Climate. *Journal of Hydrologic Engineering,, 19(3)*, 569-582. doi:10.1061/(ASCE)HE.1943-5584.0000836

Cluckie, I. D., & Pessoa, M. L. (1990). Dam safety: an evaluation of some procedures for design flood estimation. *Hydrological Sciences Journal, 35*, 547-569. doi:10.1080/02626669009492458

Del Genio, A. D., Lacis, A. A., & Ruedy, R. A. (1991). Simulations of the effect of a warmer climate on atmospheric humidity. *Nature, 351*, 382-385. doi:10.1038/351382a0

Donelan, M. A., Canada Centre for Inland Waters & National Water Research Institute (1980). Similarity Theory Applied to the Forecasting of Wave Heights, Periods, and Directions. *National Water Research Institute*, 47-61.

Dufresne, J.-L., Foujols, M.-A., Denvil, S., Caubel, A., Marti, O., Aumont, O., . . . Vuichard, N. (2012). Climate change projections using the IPSL-CM5 Earth System Model: from CMIP3 to CMIP5. *Clim. Dynam*. doi:10.1007/s00382-012-1636-1

Dunne, J. P., John, J., Adcroft, A., Griffies, S., Hallberg, R. W., Shevliakova, E., . . . Zade, N. (2012). GFDL's ESM2 Global Coupled Climate–Carbon Earth System Models. Part I: Physical Formulation and Baseline Simulation Characteristics. *Journal of climate, 25*, 6646-6665. doi:10.1175/JCLI-D-11-00560.1

Eyring, V., Bony, S., Meehl, G. A., Senior, C., Stevens, B., Stouffer, R. J., & Taylor, K. E. (2016). Overview of the Coupled Model Intercomparison Projects Phase 6 (CMIP6) experimental design and organization. *Geoscientific Model Development, 9*, 1937-1958.doi: 10.5194/gmd-9-1937-2016

Favre, A. C., El Adlouni, S., Perreault, L., & Thiémonge, N. (2004). Multivariate hydrological frequency analysis using copulas. *Water resources research, 40*. doi:10.1029/2003WR002456

FEMA. (2012a). *Assesing the consequences of dam failure: A How-to guide.* Retrieved from Federal Emergency Management Agency website: https://damsafety.org/sites/default/files/files/FEMA%20TM%20AssessingtheConsequencesofDamFailure%20March2012.pdf.

FEMA. (2012b). *Summary of existing guidelines for hydrologic safety of dams. Chapter 3: Evolution of design flood selection for spillways.* Retrieved from Federal Emergency Management Agency website:https://www.fema.gov/media-library-data/20130726-1849-25045-1538/01_hydrosafetydam_intro.pdf.

Flato, G., Marotzke, J., Abiodun, B., Braconnot, P., Chou, S. C., Collins, W., . . . Rummukainen, M. (2013). *Evaluation of Climate Models. In: Climate Change 2013: The Physical Science Basis. Contribution of Working Group I to the Fifth Assessment Report of the Intergovernmental Panel on Climate Change [Stocker, T.F., D. Qin, G.-K. Plattner, M. Tignor, S.K. Allen, J. Boschung, A. Nauels, Y. Xia, V. Bex and P.M. Midgley (eds.)]*. Cambridge, United Kingdom and New York, NY, USA. Retrieved from website: https://www.ipcc.ch/report/ar5/wg1/

Fluixá-Sanmartín, J., Altarejos-García, L., Morales-Torres, A., & Escuder-Bueno, I. (2018). Review article: Cimate change impacts on dam safety. *Natural Hazards and Earth System Sciences, 18*, 2471-2488. doi:10.5194/nhess-18-2471-2018

Fluixá-Sanmartín, J., Morales-Torres, A., Escuder-Bueno, I., & Paredes-Arquiola, J. (2019). Quantification of climate change impact on dam failure risk under hydrological scenarios: a case study from a Spanish dam. *Natural Hazards and Earth System Sciences*. doi:10.5194/hness-2019-141

Genest, C., & Favre, A. C. (2007). Everything You Always Wanted to Know about Copula modeling but Were Afraid to Ask. *J. Hydrology. Eng.*, *12*, 347-368. doi:10.1061/(ASCE)1084-0699-2007

Giorgi, F., & Francisco, R. (2000). Uncertainties in regional climate change prediction: a regional analysis of ensemble simulations with the HADCM2 coupled AOGCM. *Clim. Dynam, 16*, 169-182. doi:10.1007/p100013733

Gründemann, G. J., Werner, M., & Veldkamp, T. I. E. (2018). The potential of global reanalysis datasets in identifying flood events in Southern Africa. *Hydrol. Earth Syst. Sci., 22*, 4667-4683. doi:10.5194/hess-22-4667-2018

Hassani, H., & Silva, E. S. (2015). A Kolmorogov-Smirnov based test for comparing the predictive accuracy of two sets of forecasts. *Econometrics, 3*, 590-609. doi:10.3390/econometrics3030590

Held, I. M., & Soden, B. J. (2000). Water vapor feedback and global warming. *Annu. Rev. Energy Environment, 25*, 441-475. doi:10.1146/annurev.energy.25.1.441

Hirabayashi, Y., Kanae, S., Emori, S., Oki, T., & M., K. (2008). Global projections of changing risks of flood and droughts in a changing climate. *Hysrology Science Journal, 53*, 754-772. doi: 10.1623/hysj.53.4.754

Hirabayashi, Y., Roobavannan, M., Sujan, K., Lisako, K., Dai, Y., Satoshi, W., . . . Shinjiro, K. (2013). Global flood risk under climate change. *Nature climate change, 3*. doi:10.1038/nclimate1911

ICOLD. (1995). *Dam failures statistical analysis. Bulletin 99.* Retrieved from International Commission on Large Dams website:https://www.icold-cigb.org/GB/publications/bulletins.asp

ICOLD. (2003). *Dams and floods, guidelines and case histories. Bulletin 125.*, Paris. Retrieved from International Commission on Large Dams website:https://www.icold-cigb.org/GB/publications/bulletins.asp

ICOLD. (2011). *Constitution Statuts*. Retrieved from International Commission on Large Dams website:https://www.icoldcigb.org/userfiles/CIGB/INSTITUTIONAL_FILES/Constitution2011.pdf

ICOLD. (2016). *Flood evaluation and dam safety*. Retrieved from International Commission on Large Dams website:https://www.icold-cigb.org/GB/publications/bulletins.asp

ICOLD. (2018). *The World Register of Dams. Starting guide.* Retrieved from International Commission on Large Dams website:https://www.icold-cigb.org/GB/world_register/database_presentation.asp

ICOLD. (2019, September 2019). General syntesis. Retrieved from International Commission on Large Dams website: https://www.icold-cigb.org/GB/world_register/general_synthesis.asp

IPCC. (2014a). *Climate Change 2014: Synthesis Report. Contribution of Working Groups I, II and III to the Fifth Assessment Report of the Intergovernmental Panel on Climate Change [Core Writing Team, R.K. Pachauri and L.A. Meyer (eds.)]*. Retrieved from website: https://www.ipcc.ch/site/assets/uploads/2018/05/SYR_AR5_FINAL_full_wcover.pdf

IPCC. (2014b). Summary for policymakers. In: Climate Change 2014: Impacts, Adaptation, and Vulnerability. Part A: Global and Sectoral Aspects. Contribution of Working Group II to the Fifth Assessment Report of the Intergovernmental Panel on Climate Change [Field, C.B., V.R. Barros, D.J. Dokken, K.J. Mach, M.D. Mastrandrea, T.E. Bilir, M. Chatterjee, K.L. Ebi, Y.O. Estrada, R.C. Genova, B. Girma, E.S. Kissel, A.N. Levy, S. MacCracken, P.R. Mastrandrea, and L.L.White (eds.)]. Retrieved from website: https://www.ipcc.ch/site/assets/uploads/2018/03/ar5_wgII_spm_en-1.pdf

IPPC. (2012). *Managing the Risks of Extreme Events and Disasters to Advance Climate Change Adaptation. A Special Report of Working Groups I and II of the Intergovernmental Panel on Climate Change [Field, C.B., V. Barros, T.F. Stocker, D. Qin, D.J. Dokken, K.L. Ebi, M.D. Mastrandrea, K.J. Mach, G.-K. Plattner, S.K. Allen, M. Tignor, and P.M. Midgley (eds.)]*. Retrieved from Cambridge, UK, and New York, NY, USA. Retrieved from website: https://www.ipcc.ch/site/assets/uploads/2018/03/SREX_Full_Report-1.pdf

Jones, C. D., Hughes, J. K., Bellouin, N., Hardiman, S. C., Jones, G. S., Knight, J., . . . Zerroukat, M. (2011). The HadGEM2-ES implementation of CMIP5 centennial simulations. *Geosci. Model Dev, 4*, 543-570. doi:10.5194/gmd-4-543-2011

KNMI. (2019). KNMI Climate change atlas.Retrieved from KNMI Climate explorer: https://climexp.knmi.nl/plot_atlas_form.py

Lang, M., Ouarda, T., & Bobée, B. (1999). Towards operational guidelines for over-threshold modeling. *Journal of Hydrology, 225*, 103-117. doi:10.1016/S0022-1694(99)00167-5

Li, T., Guo, S., Chen, L., & Guo, J. (2013). Bivariate Flood Frequency Analysis with Historical Information Based on Copula. *Journal of Hydrologic Engineering, 18*, 1018-1030. doi: 10.1061/(ASCE)HE.1943-5584.0000684

Liebe, J., van de Giesen, N., & Andreini, M. (2005). Estimation of small reservoir storage capacities in a semi-arid environment. A case study in the Upper East Region of Ghana. *Physics and Chemistry of the Earth, 30*, 448-454. doi:10.1016/j.pce.2005.06.011

Madsen, H., & Rosbjerg, D. (1993). Application of the Partial Duration Series Approach in the Analysis of Extreme Rainfalls. In Z. W. Kundzewicz, D. Rosbjerg, S. P. Simonovic, & K. Takuchi (Eds.), Proceedings of the Yokohama Symposium: Extreme Hydrological Events: Precipitation, Floods and Droughts (Vol. IAHS Publication No. 213, pp. 257-266). Great Britain: IAHS Press.

Mallakpour, I., AghaKouchak, A., & Sadegh, M. (2018). Climate-Induced changes in the risk of hydrological failure of major dams in California. *Geophysical Research Letters, 46*, 213-2139. doi:10.1029/2018GL081888

Meehl, G. A., Boer, G. J., Covey, C., Latif, M., & Stouffer, J. (2000). The Coupled Model Intercomparison Project (CMIP). *Bulletin of the American Meteorological Society*. doi: 10.1175/1520-0477(2000)081<0313:TCMIPC>2.3.CO:2.

Melching, C. S., & Marquardt, J. S. (1997). *Equations for Estimating Synthetic Unit-Hydrograph Parameter Values for Small Watersheds in Lake County, Illinois*. Retrieved from United States Geological Survey (USGS) website: https://pubs.usgs.gov/of/1996/0474/report.pdf.

Milly, P., Wetherald, R., Dunne, K., & Delworth, T. (2002). Increasing risk of great floods in a changing climate. *Nature climate change, 415*, 514-517. doi: 10.1038/415514a.

Montes, S. (1998). Hydraulics of Open Channel Flow. ASCE Press.

Myhre, G., Shindell, D., Bréon, F.-M., Collins, W., Fuglestvedt, J., Huang, J., . . . Zhang, H. (2013). *Anthropogenic and Natural Radiative Forcing. In: Climate Change 2013: The Physical Science Basis. Contribution of Working Group I to the Fifth Assessment Report of the Intergovernmental Panel on Climate Change [Stocker, T.F., D. Qin, G.-K. Plattner, M. Tignor, S.K. Allen, J. Boschung, A. Nauels, Y. Xia, V. Bex and P.M. Midgley (eds.)]*. Retrieved from website: https://www.ipcc.ch/site/assets/uploads/2018/02/WG1AR5_Chapter08_FINAL.pdf

Nadarajah, S. (2007). Probability models for unit hydrograph derivation. *J. Hydrology, 344*, 185-189. doi:10.1016/j.jhydrol.2007.07.004

Novak, P., Moffat, A. I. B., Nalluri, C., & Narayanan, R. (2007). *Hydraulic Structures*. Abingdon, Oxon: E & FN SPON.

Randall, D. A., Wood, R. A., Bony, S., Colman, R., Fichefet, T., Fyfe, J., . . . Taylor, K. E. (2007). *Cilmate Models and Their Evaluation. In: Climate Change 2007: The Physical Science Basis. Contribution of Working Group I to the Fourth Assessment Report of the Intergovernmental Panel on Climate Change [Solomon, S., D. Qin, M. Manning, Z. Chen, M. Marquis, K.B. Averyt, M.Tignor and H.L. Miller (eds.)]*. Cambridge, United Kingdom and New York, NY, USA. Retrieved from website: https://www.ipcc.ch/site/assets/uploads/2018/02/WG1AR5_Chapter09_FINAL.pdf

Robson, A., & Reed, D. (2008). Statistical procedures for Flood Frequency Estimation: Volume 3 of the Flood Estimation Handbook. *Wallingford: Centre for Ecology & Hydrology, 338*.

Salvadori, G. (2004). Bivariate return periods via 2-Copulas. *Statistical Methodology, 1*, 129-144. doi:10.1016/j.stamet.2004.07.002

Salvadori, G., & De Michele, C. (2004). Frequency analysis via copulas: Theoretical aspects and applications to hydrological events. *Water resources research, 40*, W12511. doi:10.1029/2004WR003133

Salvadori, G., De Michele, C., Kottegoda, N., & Rosso, R. (2007). Extremes in Nature. An approach using Copulas. (Vol. 56). Springer.

Schellekens, J., Dutra, E., Martínez-de la Torre, A., Balsamo, G., van Dijk, A., Sperna Weiland, F., . . . Weedom, G. (2017). A global water resources ensemble of hydrological models: the eartH2Observe Tier-1 dataset. *Earth Syst. Sci, 9*, 389-413. doi:10.5194/essd-9-389-2017

Scipy community. (2019). scipy.stats.ks_2samp. Retrieved from Scipy.org website: https://docs.scipy.org/doc/scipy-0.14.0/reference/generated/scipy.stats.ks_2samp.html

Scipy community. (2019). *Scipy reference guide. Release 1.4.1*. Retrieved from Scipy.org website: https://docs.scipy.org/doc/scipy/scipy-ref-1.4.1.pdf

Serrano-Lombillo, A., Fluixá-Sanmartín, J., & Espert-Canet, V. J. (2011). Risk Analysis, Dam Safety and Critical Infrastructure Managemento: Flood routing studies in risk analysis. Taylor & Francis Group. Valencia, Spain.

Sitterson, J., Knightes, C., Parmar, R., Wolfe, K., Muche, M., & Avant, B. (2017). *An overview of rainfall-runoff model types. U.S. Environmental Protection Agency, Washington, DC, EPA/600/R-17/482*.

Sood, A., & Smakhtin, V. (2015). Global hydrological models: a review. *Hydrological Sciences Journal, 60:4*, 549-565. doi:10.1080/02626667.2014.950580

Sordo, A., Bianucci, P., Garrote, L., & Granados, A. (2014). How Safe is Hydrologic Infrastructure Design? Analysis of Factors Affecting Extreme Flood Estimation. *Journal of Hydrologic Engineering*., *19*(12). doi:10.1061/(ASCE)HE.1943-5584.0000981

Sperna Weiland, F. C., van Beek, L. P. H., Kwadjik, J. C. J., & Bierkens, M. F. P. (2012). Global patterns of change in discharge regimes for 2100. *Hydrol. Earth Syst. Sci., 16*, 1047-1062. doi:10.5194/hess-16-1047-2012

Sutanudjaja, E., H., van Beek, R., Wanders, N., Wada, Y., Bosmans, J. H. C., Drost, N., . . . Bierkens, M. F. P. (2018). PCR-GLOBWB 2: a 5 arcmin global hydrological and water resources model. *Geoscientific Model Development, 11*, 2429-2453. doi:10.5194/gmd-11-2429-2018

Taylor, K. E., Stouffer, R. J., & Meehl, G. A. (2012). An overview of CMIP5 and the experiment design. *American Meteorological Society*.,*1,485-498*. doi:10.5194/gmd-9-1937-2016

Tomer, S. K. (2011). Copulalib 1.1.0. Retrieved from Python package website: https://pypi.org/project/copulalib/

Towner, J., Cloke, H. L., Zsoter, E., Zachary, F., Hoch, J. M., Bazo, J., . . . Stephens, E. M. (2019). Assessing the performance of global hydrological models for capturing peak river flows in the Amazon basin. *Hydrol. Earth Syst. Sci., 23*, 3057-3080. doi:10.5194/hess-23-3057-2019

Turner, S. W. D., Hejazi, M., Kim, S. H., cLARKE, l., & Edmons, J. (2017). Climate impacts on hydropower and consequences for global electricity supply investment needs,. *Energy*, *141*, 2081-2090.

US Army Corps of Engineers. (2018). National Inventory of Dams. Retrieved from National Inventory of Dams website: https://catalog.data.gov/dataset/national-inventory-of-dams.

US Bureau of Reclamation. (1976) Design of gravity dams. Retrieved from Bureau of Reclamation website: https://usbr.gov/tsc/techreferences/mands/mands-pdfs/GravityDams.pdf.

USDA, & NRCS. (2014). *Part 630 Hydrology National Engineering Handbook. Chapter 17: Flood routing*. Retrieved from Natural Resources Conservation Service website: https://www.nrcs.usda.gov/wps/portal/nrcs/detailfull/national/water/?cid=stelprdb1043063

van Beek, L. P. H., & Bierkens, M. F. P. (2008a). *The Global Hydrological Model PCR-GLOBWB: Conceptualization, Parameterization and Verification, Report Department of Physical Geography Utrecht University, Utrecht, The Netherlands*. Retrieved from http://vanbeek.geo.uu.nl/suppinfo/vanbeekbierkens2009.pdf

van Beek, L. P. H., & Bierkens, M. F. P. (2008b). *The Global Hydrological Model PCR-GLOBWB: Conceptualization, Parameterization and Verification, Report Department of Physical Geography, Utrecht University, Utrecht, The Netherlands*. Retrieved from http://vanbeek.geo.uu.nl/suppinfo/vanbeekbierkens2009.pdf.

van Vuuren, D. P., Edmons, J., Kainuma, M., Riahi, K., Thomson, A., Hibbard, K., . . . Rose, S. K. (2011). The representative concentration pathways: an overview. *Climate change, 109,* 5-31. doi:10.1007/s10584-011-0148-z

Vischer, & Hager. (1998). Dam hydraulics. Wiley series on Water Resources Engineering.

Wan, W., Zhao, J., Li, H. Y., Mishra, A., Hejazi, M., Lu, H., . . . Wang, H. (2018). A holistic view of water management impacts on future droughts: A global multimodel analysis. *Journal of Geophysical Research: Atmosphere, 123*, 5947-5972. doi:10.1029/2017JD027825

Watanabe, S., Hajima, T., Sudo, K., Nagashima, T., Takemura, T., Okajima, H., . . . Kawamiya, M. (2011). MIROC-ESM 2010: model description and basic results of CMIP5-20c3m experiments. *Geosci. Model Dev, 4*, 845-872. doi:10.5194/gmd-4-845-2011

WCRP. (2019). WCRP Coupled Model Intercomparison Project (CMIP). Retrieved from World Climate Research Programme website: https://www.wcrp-climate.org/wgcm-cmip

Yue, S., Ouarda, T., Bobée, B., Legendre, P., & Bruneau, P. (2002). Approach for describing statistical properties of flood hydrograph. *J. Hydrology Eng., 7(2)*, 147-153. doi:10.1061/(ASCE)1084-0699(2002)7:2(147)

Zhou, R. D., Donnelly, C. P., & Judge, D. (2008). *On the relationship between the 10000 year flood and probable maximum flood*. Paper presented at the HydroVision 2008. doi: 10.13140/2.1.3015.8406

Appendices

Appendix A. - Difference spillway design between current and future scenarios

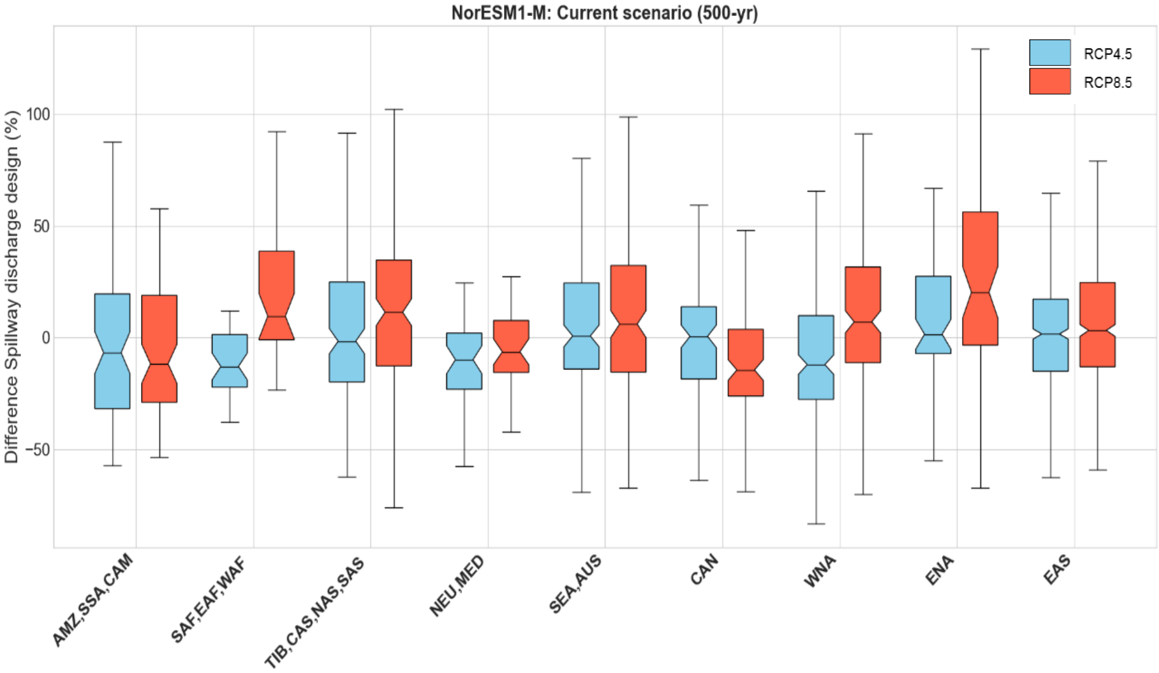

Figure 6.2-1 Distribution difference spillway discharge design by climate regions between current and RCP4.5 and RCP8.5 scenario (NorESM1-M model-500-yr)

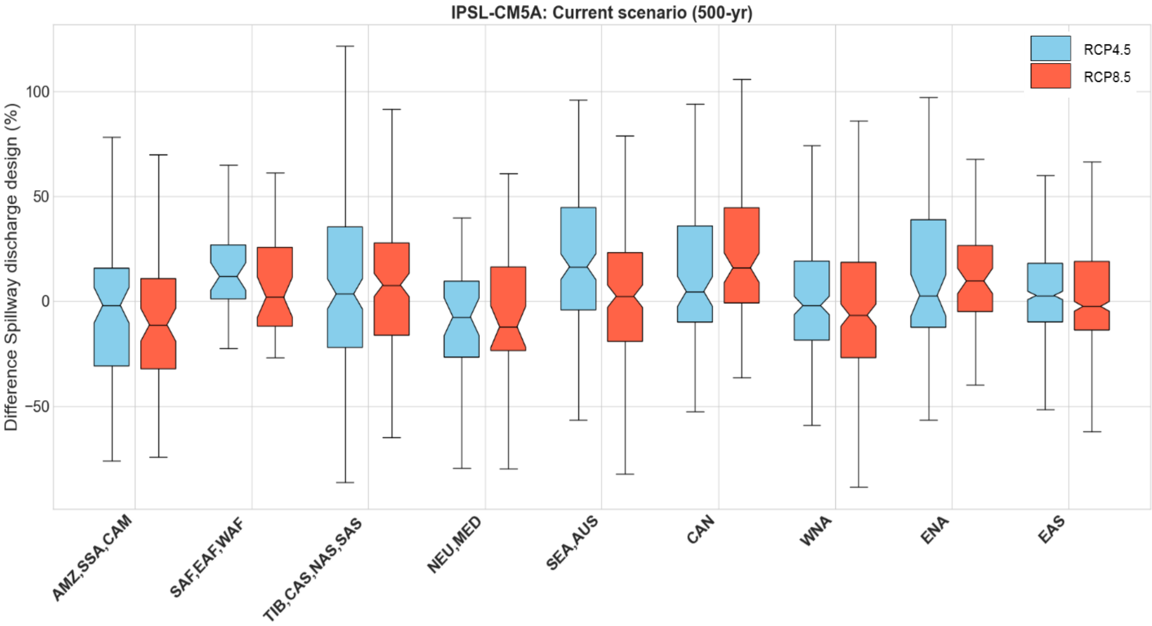

Figure 6.2-2Distribution difference spillway discharge design by climate regions between current and RCP4.5 and RCP8.5 scenario (IPSL-CM5A model-500-yr)

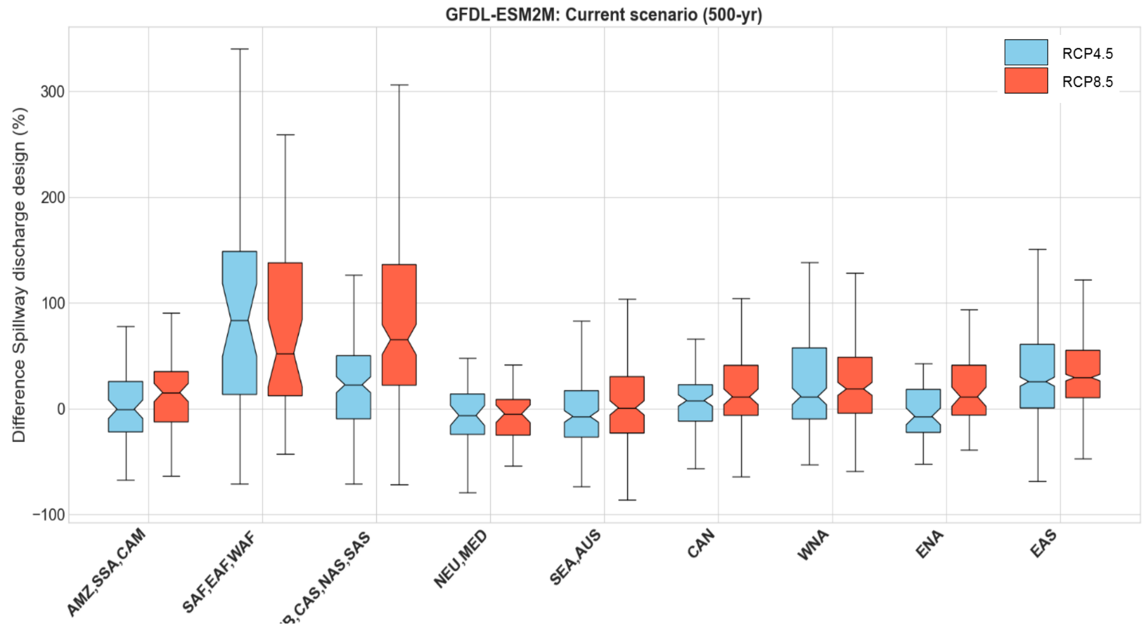

Figure 6.2-3 Distribution difference spillway discharge design by climate regions between current and RCP4.5 and RCP8.5 scenario (GFDL-ESM2M model-500-yr)

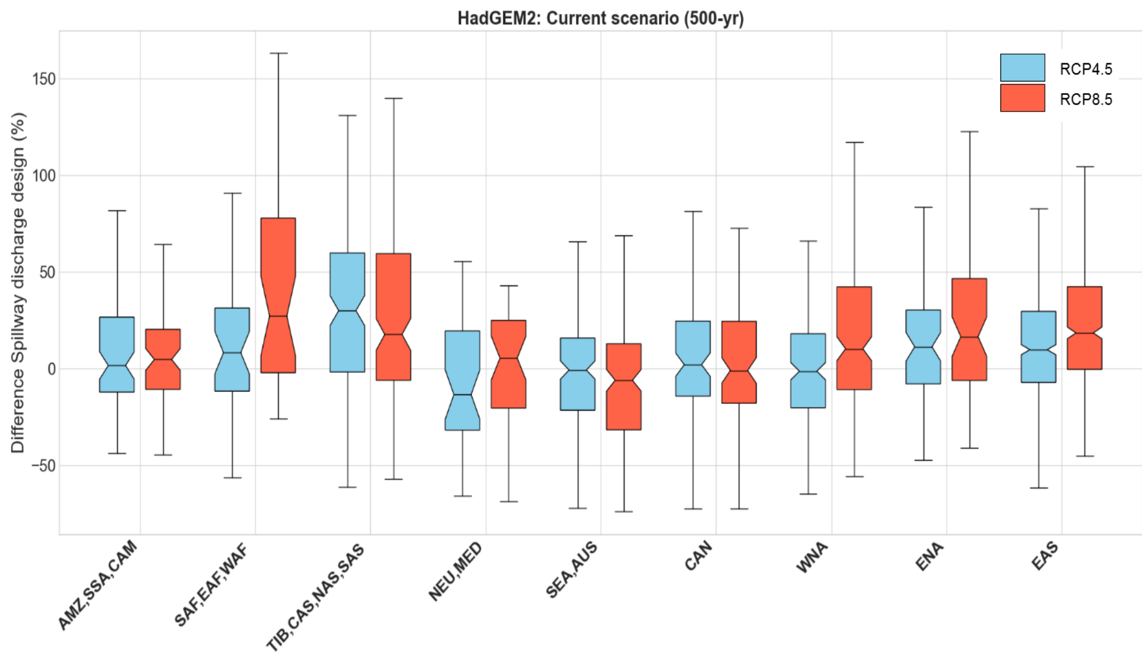

Figure 6.2-4 Distribution difference spillway discharge design by climate regions between current and RCP4.5 and RCP8.5 scenario (HadGEM2 model-500-yr)

Appendix B. - Research Ethics Declaration Form

Research Ethics Committee
IHE Delft Institute for
Water Education
E ResearchEthicsCommitee@un-ihe.org

Date: 2020-03-16
To: Nathalia Silva Cancino
MSc Programme: WSE- HERBD
Approval Number: IHE-RECO 2020 -072

Subject: Exemption for further ethical review

Dear Nathalia Silva Cancino,

Based on your application for Ethical Approval, your proposal Analysis of the impact of climate change on the global risk of dam failure due to overtopping has been exempted from further revision by the Research Ethics Committee (RECO), IHE Delft. You need to notify the RECO of any modifications to your research protocol.

Please keep this letter for your records and include a copy in the final version of MSc. Thesis.

On behalf of the Research Ethics Committee, I wish you success in the completion of your research.

Yours sincerely,

Angeles Mendoza
Acting Ethics Coordinator

Copy to: Academic VP.
Copy to: Reviewer

Part 1

1.1 General Information

Date:	November 11th 2019		
Researcher	Nathalia Silva Cancino		
Student number	1045587	E-mail	nsi002@un-ihe.org
Department or MSc. Programme	Water science and engineering.		
Mentor	Daniel Valero	E-mail	d.valero@un-ihe.org
Supervisor	Micha Werner	E-mail	m.werner@un-ihe.org
Country where research will take place	The Netherlands		
Project or funding source			
Title of Research proposal	Analysis of the impact of climate change on the global risk of dam failure due to overtopping.		
Summary	This study aims is to analyse the impacts of climate change on the failure of dams due to overtopping in a global scale. The last report of the Intergovernmental Panel on Climate Change (IPPC) presented medium confidence to expect heavy rainfall will increase regardless of the total precipitation is projected to decrease. Besides, other studies have assessed the projected precipitation and have agreed with the IPPC assessment. These changes in climate present a concern about the risk of failure on the large dams, due to most of these structures were built at the end of the 20th century with different methods and limited hydrological data, facing uncertainty in the design capacity of the spillways. The analysis will be based on current and projected hydrological data obtained and the outputs from a Global Hydrological Model and a Global Climate Model where it will be performing an analysis of the current scenario compared with the original design flood and analysis under climate change. It is expected to find a relationship between the current and projected data with the original design flood to understand the bias between the hydrological series. This study will provide a global view of the drivers that affect the risk of dams due to overtopping in a current and climate change scenario.		
Signature of Student		Date:	11/11/2019.
Signature of Mentor		Date:	11/11/2019
Signature of Supervisor		Date:	11-11-2019

1.2 Screening checklist

These are common activities that may result in ethical issues. If not of them apply to your research, submit Part 1 of the application to IHE RECO. If one or more of the items apply to your research, you need to complete parts 1 and 2 and submit the application with the required documentation.

Answer yes or no to the questions that apply to your research.	**Yes**	**No**
Collecting personal information		
Will your research involve collecting, processing and/or reporting personal data obtained from primary or secondary sources?	☐	☒
Will you obtain information from individuals or groups of individuals through questionnaires, interviews, focus groups or other methods?	☐	☒
Debriefing and consent process		
Will you obtain information from individuals or groups through questionnaires, interviews, focus groups or other methods?	☐	☒
Will your research involve individuals or groups who need to give their voluntary consent to participate?	☐	☒
Will the participants include individuals belonging to groups that require special considerations, e.g. people under legal age of consent, immigrants, refugees, disable people, or other vulnerable groups in the country of the research?	☐	☒
Will your research involve participants for whom voluntary and informed consent may require special attention (e.g. children (under 18s), people with learning disabilities, undocumented migrants, patients, prisoners)?	☐	☒
Will your research include observation of individuals or groups of people without their explicit consent or knowledge?	☐	☒
Will your research require withholding information about the project or misleading participants?		
Will your research use the cooperation of a person or organization of influence or power (gatekeeper) in a community, organization, or other, to involve individuals or groups in your research?	☐	☒
Will you require the help of a translator to collect, process and/or report information from participants?	☐	☒
Will you use animals in your research?	☐	☒
Benefits and risks to participants and researchers		
Could the participation in the research, or the dissemination of its results cause -directly or indirectly- psychological stress, anxiety, harm or other negative consequences for participants or the researcher?	☐	☒
Could the involvement in the research contribute to any risk for participants or researchers because of the situation in the country or specific locations in which the research will take place?	☐	☒
Will you provide or offer any financial, material or other incentives for people to participate in your research?	☐	☒
Could any aspects of the research, or the communications related to, be perceived as inappropriate in the context of the culture, beliefs or practices of individuals or groups of informants, e.g. ethnic or religious groups, or could interfere with their culture, beliefs or practices?	☐	☒

For comments or questions about this form, write to a.mendoza@un-ihe.org.

Answer yes or no to the questions that apply to your research.	Yes	No
Research context		
Will your research also require any research permits or ethical approval from national or local institutions or organizations?	☐	☒
Could any factors of the research - including design, funding, dissemination of results, or other - be associated to potential conflict of interest that would put at risk its integrity?	☐	☒

If you are a student and answered *No* to all items, fill-in the declaration and submit it to your Program' Secretary and MSc Coordinators. Keep a copy for your records. Part 1, including the written personal declaration must be included in Annex 1 of the MSc. Thesis submitted for defence. Staff should contact RECO directly.

If you answered *Yes* to any of the questions, in addition to submitting the check list and declaration, you also need to answer the applicable questions in Part 2. Submit this part together with the check list and the declaration to your Program' Secretary and MSc Coordinators. They will submit it to the Research Ethics Committee. Staff should contact RECO directly.

Declaration

Check what applies to your research

☒ I Nathalia Silva Cancino have read the Netherlands Code of Conduct for Research Integrity and IHE guidelines for Research Ethics.

☒ My research does not have any ethical implications because of the use of personal data or involvement of humans or animals as research subjects. I understand the Principles of Research Integrity and the Standards of Good Research Practices, and have considered them for my research in the following way:

[Write a short description, minimum 1,000 words, of how you have or will consider in your research the Principles and the Standards mentioned above]

☐ My research involves the collection of personal data and/or the involvement of human or animal subjects. I understand the principles that guide the use of personal data and/or involvement of human subjects or animals and have considered the ethical issues that may arise from my research. I have incorporated measures to prevent harm and/or ethical repercussions for research subjects (humans and/or animals), and the institutions or groups involved in the research and elaborate on them in the attached form (Part 2) that I submit for ethical clearance.

Signatures

Student/Researcher	Mentor
Signature Name: Nathalia Silva Cancino Date: 11/11/2019.	Signature Name: Daniel Valero Huerta Date; 11/11/2019
Supervisor Signature Name: Michael Werner Date: 11-11-2019	

For comments or questions about this form, write to a.mendoza@un-ihe.org.